[American Journal of Science, Vol. 277, May, 1977, P. 513-584]

American Journal of Science

MAY 1977

MAGNETOSTRATIGRAPHY OF EASTERN ICELAND

N. D. WATKINS* and G. P. L. WALKER**

ABSTRACT. Two oriented samples have been taken from each of over 700 successive lavas in eastern Iceland. The section extends from about t = 13.6 to 2.0 m.y. and as sampled is 9 km thick. Down-dip thickening of lavas, characteristic of eastern Iceland, causes measured thicknesses to depend on distance from extrusive sources. The section thickness is therefore standardized to a depth corresponding to the top of the analcite zeolite zone and is then computed to be 7 km. At least fifty successive geomagnetic polarity changes, four of which have not been previously detected, are recorded in the sequence, which is firmly correlated to the known and predicted polarity time scale. The average period separating successive polarity reversals for the past 13.6 m.y. is shown to be between 145,000 and 190,000 yrs. A series of stratigraphically valuable mapping units are defined, with potential for extension to other parts of Iceland. On average, one lava was extruded each 16,000 yrs, and the long-term volcanic production rate varies by no more than a factor of four, appearing to be constant for up to 6 m.y. Three separate volcanic episodes can be characterized by differing volcanic production rates. The major increase in activity occurs at about t = 7.3 m.y., shortly before a substantial increase in volcanic activity occurred during formation of the Reykjanes Ridge, immediately south of Iceland.

Zeolite zones facilitate recognition of the varying depth of burial. The results of the survey demonstrate that the intensity of magnetization of basalts decreases with depth of burial.

Geomagnetic secular variation was virtually constant throughout the period represented, whether the data are analyzed in groups of equal lava numbers or equal group thicknesses. It is concluded that the average non-dipole to dipole field ratio has not changed appreciably and that the ratio of the drifting to standing non-dipole fields has similarly not changed over the long term in Iceland between t = 13 and 2 m.y. Evidence exists for complete cancellation of non-dipole field effects when the data are averaged over the entire period. For shorter periods, there is some evidence to show independence of non-dipole and dipole fields. Comparison of paleomagnetic data for abyssal igneous cores obtained during the Deep Sea Drilling Project with the results from the eastern Iceland lavas suggests that the shallow remanent magnetism inclinations frequently encountered in the former materials most probably are because of local tectonic effects and not geomagnetic field behavior.

INTRODUCTION

Iceland is geologically unique in several ways. It is the World's largest mid-oceanic island and is the only segment of the mid-oceanic ridge system that is well exposed and clearly and actively spreading (fig. 1). While islands must in general be atypical of sea floor, the igneous relationships in eastern Iceland are nevertheless sufficiently clear to have enabled Bodvarsson and Walker (1964) to postulate a mechanism of growth involving dike injection which closely resembles that currently accepted for sea-floor genesis. As an extension of this, Walker (1975) has employed the igneous intrusive relationships in southeastern Iceland to suggest a model for the development of Layer 3.

* Graduate School of Oceanography, University of Rhode Island, Kingston, Rhode Island 02881

** Department of Geology, Imperial College, London SW7, England

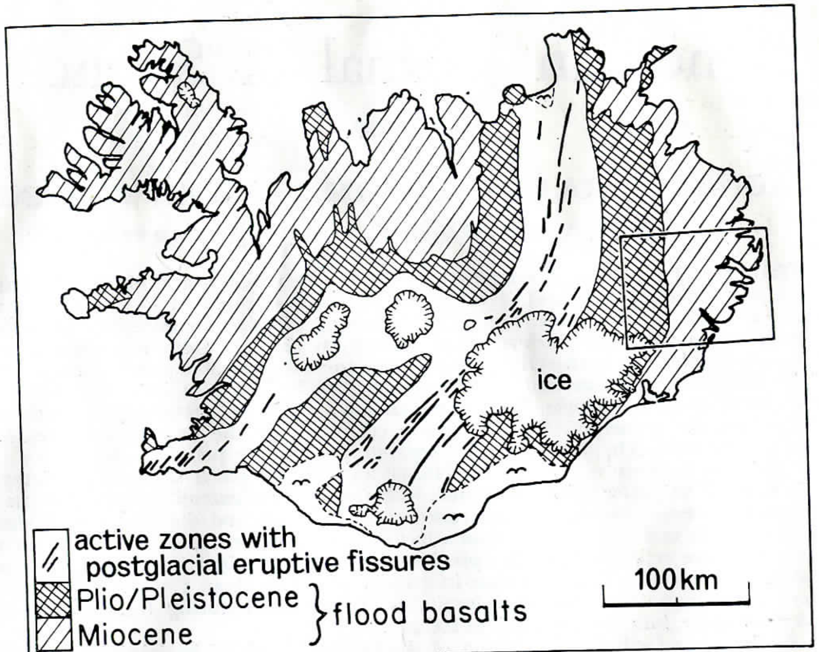

Fig. 1. Map of Iceland showing the location and geologic setting of the area in eastern Iceland that is the subject of this paper. Block corresponds to limits of map shown in figure 2.

Despite its geological significance and reasonably simple basic structure, Iceland nevertheless presents great difficulty to the stratigrapher, because of the almost complete absence of fossiliferous sediments and a limited petrological range within the overwhelmingly dominant basaltic rocks. Stratigraphic mapping requires techniques ideally capable of yielding chronological units. Trausti Einarsson recognized the problem more than two decades ago and employed the Earth's changing magnetic polarity (as is readily recorded by the remanent magnetism of lavas) for his local stratigraphic index, to provide the first magnetostratigraphic map, for a lava sequence northeast of Reykjavik (Einarsson, 1957). He mapped twelve successive changes of polarity using a Brunton compass as the simple mapping tool. These polarity changes are now understood to occur on average once every 0.45 m.y. or less during the Upper Cenozoic (Heirtzler and others, 1968; Cox, 1975) and are globally synchronous. Unless some independent control is available, magnetostratigraphy cannot be employed as a dating tool. While the geomagnetic polarity history is well known for the past 5 m.y. (Cox, 1969), the earlier polarity time scale becomes increasingly less well defined with increasing age, since it is based on the time scale derived from marine magnetic anomalies, assuming constant sea-floor spreading rates (Heirtzler and others, 1968; Talwani, Windisch, and Langseth, 1971). McDougall and others (1976) have shown that this predicted scale is precise, however, for the last 10 m.y. Extrapolation of the anomaly time scale by a factor of only 1.6 from this datum provides a polarity history that can be used for an entire stratigraphic map of Iceland, since the oldest rocks exposed on the island are only 16 m.y. old (Moorbath, Sigurdsson, and Goodwin, 1968). In principle, therefore, given some degree of K:Ar age control, the magnetostratigraphy of one of the uniquely thick sections exposed in Iceland can provide a type section in true time units for a complete geological map of the island.

This paper presents the magnetostratigraphy of a 9000 m thick sequence of lava flows in eastern Iceland. The availability of four sets of K:Ar data for lavas in the same sequence (Moorbath, Sigurdsson, and Goodwin, 1968; McDougall and others, 1976; McDougall, Watkins, and Kristjansson, 1976; Ross and Mussett, 1976) provides an opportunity to tie the sequence to this polarity time scale. It follows that the volcanic history can be defined in detail. Conversely, the paleomagnetic data for such a thick sequence provide means to examine past geomagnetic field behavior.

GEOLOGICAL BACKGROUND AND FIELD METHODS

The early geological studies of eastern Iceland by Thorodssen (1906) and Hawkes (1924, and other papers) have been summarized by Walker (1964). The basaltic lavas that dominate the region have an exposed volume of more than 10,000 km^3, are deeply dissected by glacial erosion, and outcrop in vertical sequences of up to 1000 m and more. A gentle westerly dip of the lavas mirrors the easterly dip of many western Iceland sequences and diminishes upward. This dip facilitates examination of an outcrop of lavas totalling over 9 km thick between the oldest units at Gerpir (fig. 2 sec. G) and the edge of the actively spreading central part of Iceland. Walker and his coworkers began the geological investigation of eastern Iceland in 1955. This includes the mapping in 1964 and 1965 of a complete 9000 m thick succession (excluding overlaps) containing a total of about 700 lava flows. To accomplish this, 21 separate profiles were employed. These are labelled A to V in figure 2. The details of each section location are given in figure 3 (A to C), and the corresponding stratigraphic sketches of all 21 sections are included in app I. A number was painted on each sampled lava, and most of these are still clearly legible. The numbers are indicated in the detailed stratigraphic sketches (app I). In addition to conventional stratigraphic notations, the distribution of zeolites was mapped. Walker (1960) and others have demonstrated that the temperatures reached by lava flows on burial after initial emplacement can be diagnosed by zeolite mineralogy. The resulting zeolite zones do not follow any structural features but are diachronous, simply reflecting paleogeoisotherms, parallel to the original pre-erosion surface.

Continuous profiles more than 1000 m thick are easily located, but there are three complications to mapping the whole pile. The first arises

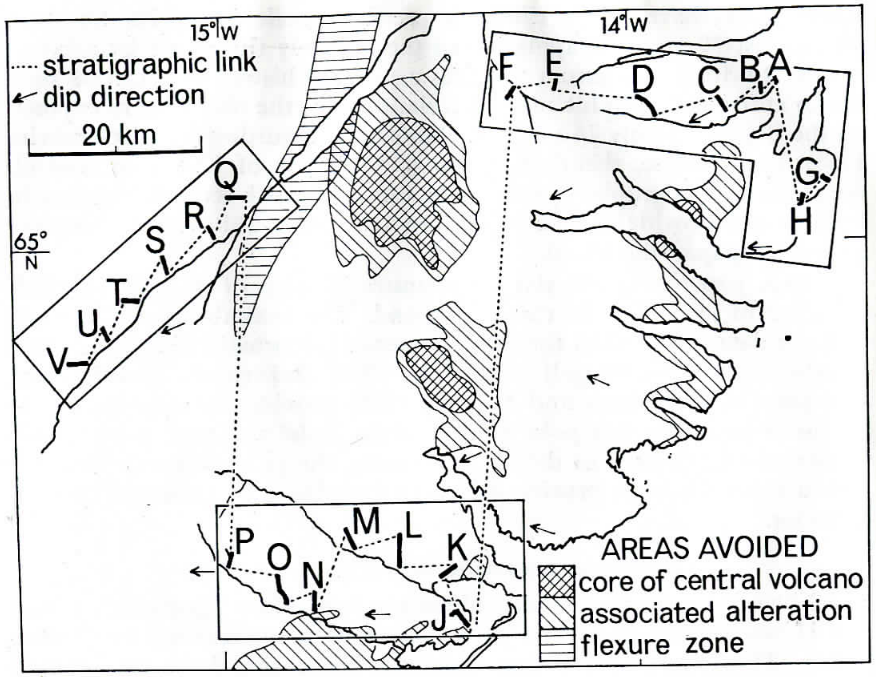

Fig. 2. The east Iceland area, showing locations of the 21 profiles from which samples were collected for magnetic study and the areas that were avoided for reasons discussed in the text. The three blocks indicated correspond to limits of maps given in figure 3.

because the pile contains silicic volcanic centers (central volcanoes in fig. 2) within which a wide range of rock types besides basalt occurs. Each center is roughly lenticular in form but interfingers with the surrounding flood basalts. It was judged advisable to avoid these centers because of the stratigraphic and structural complications that exist within them, uncertainty of the extent to which often high dips are original depositional slopes and not due to subsequent tilting, and the existence of pervasive aureoles of hydrothermal alteration in and around each center.

The second complication is that a prominent flexure zone occurs along Fljótsdalur (fig. 2, northeast from secs. V through Q) in which many faults occur and unconformities might possibly also exist. This is called the Lagarfljót Flexure Zone. Flexuring, which imparts to the lavas a tilt commonly of 5 to 10 degrees, is a normal accompaniment of volcanism in Iceland, but the Lagarfljót Flexure Zone is different in that dips much steeper than normal occur in it, and although the main flexure is monoclinal, the zone includes synclines arranged en-echelon having narrow limbs in which the dip direction is reversed (Walker, 1974). The zeolite zones in the lavas east of the flexure appear moreover to be down-flexed which implies that the flexuring took place in part sub-

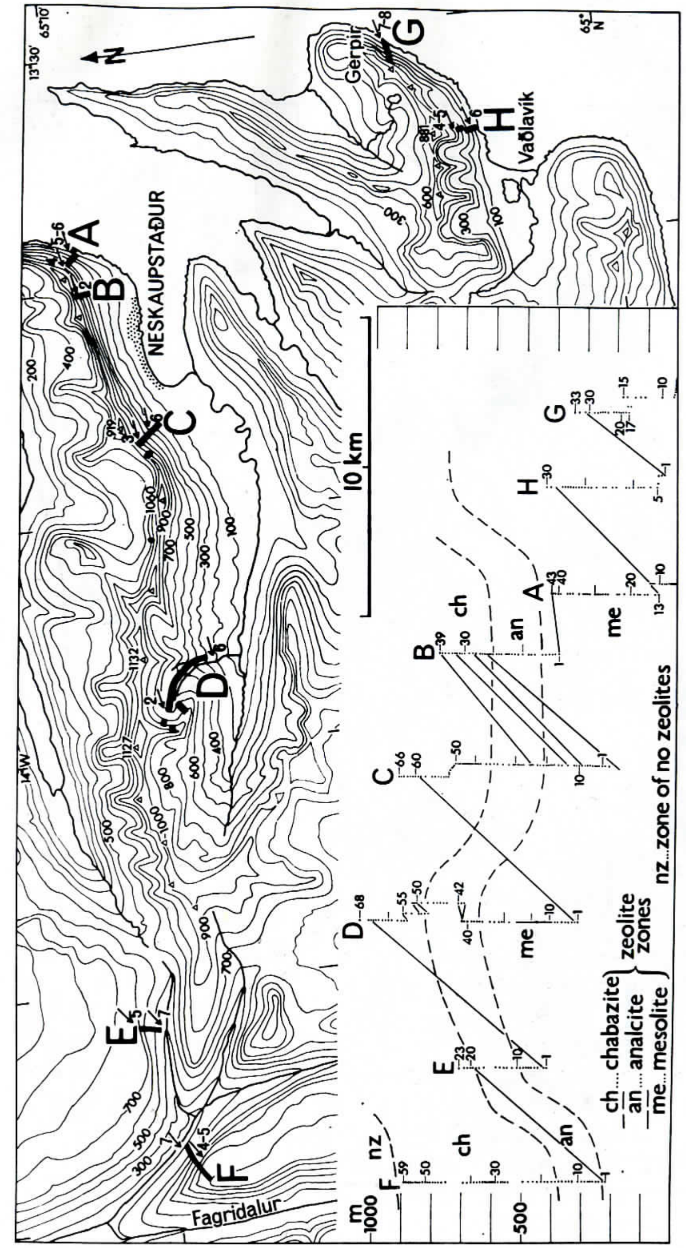

A.

Fig. 3. Maps showing detailed locations, vertical extent, and zeolite zones for (A) sections A to G, (B) J to P, and (C) Q to V. Each diagram shows between-section correlation lines. Numbers adjacent to vertical sequences are original field numbers of each lava, corresponding to the numbers used in the detailed stratigraphic sketches, data tables, and polarity logs in app I. In (C) the shaded zone indicates the occurrence of tillites.

Fig. 3

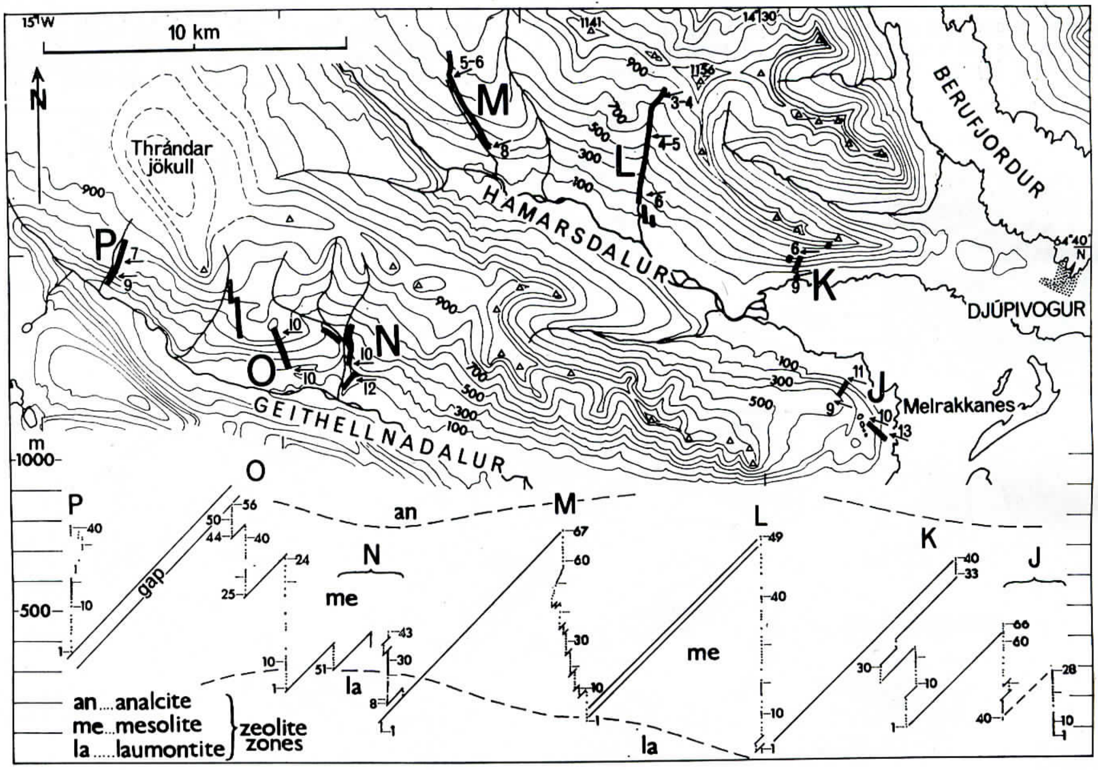
15°W
10 km
N
Thrándar jökull
HAMARSDALUR
GEITHELLNADALUR
BERUFJORDUR
DJÚPIVOGUR
Melrakkanes
64°40' N
P
O
N
M
L
K
J
m
1000
500
an
me
la
gap
an....analcite
me...mesolite
la.....laumontite
zeolite zones

B.

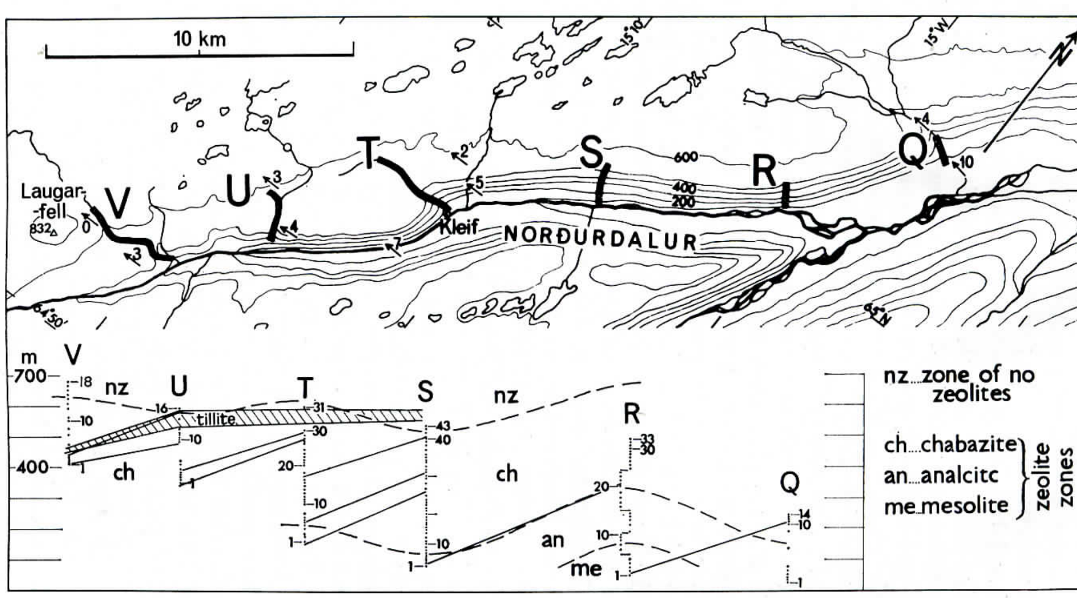
10 km
15°10'
15°W
N
Laugar-fell
832
V
U
T
S
R
Q
Kleif
NORÐURDALUR
64°50' N
m
700
400
nz
ch
an
me
tillite
nz...zone of no zeolites
ch...chabazite
an...analcitc
me...mesolite
zeolite zones

C.

sequent to, rather than synchronous with, the eruption of these lavas. The real difficulty of coping with the Lagarfljót Flexure Zone is that the topography is too subdued to enable stratigraphic mapping to be carried out across the folds and faults and hence for the rocks on one side of the zone to be correlated with those on the other.

To avoid the flexure zone and volcanic centers, the middle part of the sampled succession (profiles J to P in fig. 2) was sited in Hamarsdalur and Geithellnadalur, 50 km south of the lower and upper parts.

The third complication is that the basaltic outpouring of the upper third of the succession coincided with a change to a cold climate, with the possible existence of erosional breaks caused by early glaciations. This climatic change is evidenced by abundant gray- or buff-colored tuffaceous and sedimentary beds occurring between these lavas. Some of these beds are palagonite tuffs and associated sediments transported and deposited by sheet floods originating probably from intraglacial eruptions outside the sampled area. Some are solifluxion sheets, veins from which commonly penetrate down into the bedrock and into which blocks of floor have been upheaved, as a result of contemporary frost action. Some thick clastic deposits in profile Q are hyaloclastites containing pillow-like basalt due to eruption probably into a shallow temporary lake. A few are mudflows, implying the existence of a mountainous topography in adjacent areas. A few are tillites and rest on an eroded surface, and one (that resting on lavas T30, U14, and V6, fig. 3C) has been found to contain striated cobbles.

Cold-climate deposits are prevalent throughout profiles P to V and are particularly thick in P, Q, and T. Such deposits characterize all sections through the Quaternary and Upper Pliocene of Iceland. Moberg mountains produced by intraglacial eruptions and now buried in the associated interglacial flood basalts are also commonly found, for instance in the Jökulsá á Brú valley near Adaból, and they produce angular disconformities. Profiles P to V however lack such moberg mountains, which tends to indicate that periglacial rather than strictly glacial conditions prevailed: these profiles contain predominantly well-stratified successions of flood basalt lavas without any apparent angular disconformities apart from that which may occur at the tillite on lavas T30, U14, and V6.

The upper part of the highest profile, V, terminates at a glaciated surface. The uppermost lava flow (V18) was erupted at some time within the Pliocene Ice Age, but there is no purely geological method of assessing the length of time that has since elapsed. The fact that the lavas at the top of V are nearly horizontal and occur well up in the zone of no zeolites suggests however that the amount of erosion has been small. Moberg mountains formed by eruptions within an ice sheet rest on this erosion surface near the top of V and include Laugarfell.

Immediately following the mapping of each section, at least two cores were taken from each numbered lava, using a gasoline-powered portable drill (Doell and Cox, 1964). Thirteen cores were apparently lost either in the field or laboratory, and so in thirteen cases, data from only a single specimen was available from the lavas involved. Cores, of 2.5 cm diam and average length 10 cm, were geographically oriented while still attached to outcrop. In this way, over 2000 separate oriented cores were obtained. A small number of additional oriented samples was collected from critical parts of the sequence in 1973 and 1974.

LABORATORY METHODS

Each core was sliced into several specimens for various purposes, including transmitted and reflected light petrographic work and geochemical and isotopic analyses. A specimen of 2.2 cm length was sliced from the deepest, least weathered, part of each core, for paleomagnetic studies.

The direction and intensity of the natural remanent magnetism (NRM) of each specimen was measured using astatic magnetometers. Unstable components of remanent magnetism were then minimized by treatment in up to ten successively higher alternating magnetic fields (having peak values ranging from 50-660 oersteds) with remeasurement of the direction and intensity of remanent magnetism taking place after each treatment. The vast majority of samples was subjected to treatment in only three or four successively higher alternating magnetic fields, ranging from 125 to 400 oersteds. All the original paleomagnetic data were obtained at the University of Liverpool and were made available by the Science Institute of the University of Iceland. The final best direction of remanent magnetism for each lava was computed on a minimum scatter basis: here, data obtained (following any of the demagnetizing treatments) for each of the two specimens are combined to provide maximum precision in the final mean direction. The rationale for this computational system is that variations in magnetic stability within single lavas are often sufficiently large to require drastically different peak demagnetizing fields for removal of unstable components (Watkins and Haggerty, 1967; Wilson, Haggerty, and Watkins, 1968). Hence the mean direction of the two specimens is in effect weighted accordingly, toward that in the more stable specimen (Watkins and Richardson, 1968). The reader is cautioned that other methods of computing the mean direction are possible. No doubt the simplest is to select the data following demagnetization treatment of the entire collection at a single optimum alternating magnetic field value, since it could be argued that the minimum scatter method is vulnerable to the production of mean directions which in part are artifacts of imperfect demagnetizing systems or are the result of very low stabilities in all cores from a given unit. For reasons summarized elsewhere (Watkins and Richardson, 1968) we nevertheless prefer the minimum scatter system. As we shall show, the method of computation is, in any case, not critical in our results and interpretation. The final mean direction of remanent magnetism of each lava was corrected for the observed post-emplacement dip of the lavas, which were assumed to be originally flat. Virtual geomagnetic pole positions are then computed from the mean direction, for each lava.

The polarity of each unit is designated normal if the virtual geomagnetic pole is in northern latitudes and reversed if the virtual geomagnetic pole is in southern latitudes. Because of the fact that with only few exceptions two cores were taken from each lava, data reliability cannot be expressed using conventional statistical methods (Fisher, 1953). It appears reasonable to define as unsatisfactory the data for those lavas where the resultant vector (R) is <1.6. For this value of R, the direction of remanent magnetism in each specimen is 37° from the mean. This figure drops to 32° for $R = 1.7$, to 26° for $R = 1.8$, and to 18° for $R = 1.9$. More cores per lava are obviously statistically desirable, but the sampling density employed is far superior to that employed in some other magnetostratigraphic methods. For example, all abyssal piston core studies have used only one specimen per horizon, which is also the case for a recent highly successful magnetostratigraphic study of the Cretaceous-Paleocene boundary in Italy (Alvarez and others, 1977).

RESULTS

Correlations between profiles.—The correlation between one profile and another inevitably poses problems. It is normally not possible to identify a lava flow in one profile with what is unquestionably the same lava flow in another profile several kilometers away. Indeed because of the rapid thinning of the lava pile due to the termination of many lavas up-dip, it is thought that normally only one in every two or three lava flows at the base of one profile actually exists at the top of the next profile in the up-dip direction. The best that can normally be done is to correlate lava flows in one profile with those occupying an equivalent stratigraphic position in another.

Acid tuffs are particularly useful for such correlation. An example is the group of six tuffs at the top of profile C (the Seldalur Tuffs of Walker, 1959) which is the stratigraphic equivalent of the thick tuffs at the base of D (lava flows C62 and D2 are thus in equivalent positions).

Lava groups of contrasted lithologies such as were used for the original stratigraphic mapping of the Reydarfjördur area provide the other main basis for correlation. The distinctive feldspar-porphyritic basalts of the Gerpir Porphyritic Group enable profile H (lavas H29 and H30) to be correlated with A (A13 and A14), and the equally distinctive Graenavatn Porphyritic Group (see map, Walker 1963, fig. 4) allows F (F33 to F36) to be correlated with J (J1 to J5).

The greatest uncertainty lies in correlating profiles Q and P, which are 40 km apart. The several thick clastic beds in Q are believed to correlate broadly with those in P. The main group in Q has been traced nearly half the distance from Q to P, but the remainder of this distance is a relatively inaccessible plateau in which stratigraphic mapping is difficult because of the subdued relief. Precise correlation between Q and P has thus not been achieved.

The Lagarfljót Flexure Zone does not appear to persist as far south as profile P. In Q, the lavas lying between the several clastic beds have slightly different dips which suggest that flexuring proceeded intermittently during deposition, and angular unconformities possibly exist. In P the lavas have a normal dip, and the rate of upward decrease in dip is normal so that there is no reason to suspect the existence of angular unconformities.

The between-section correlations are given in figure 3. It should be emphasized that they are based on purely geological observations, and their limitations are clear. Considerable overlaps were incorporated between some profiles (for example, between F and J) to allow for palaeomagnetic verification.

Geological notes.—The stratigraphic sketches (included in app I) provide all essential details about each section. Some generalities about the local geological circumstances cannot be readily derived from diagrams and are therefore given below.

Many of the lava flows and particularly those of pahoehoe type are compound, that is, they are divisible into flow units. Their significance is that whereas separate lava flows may be erupted at intervals commonly of hundreds or thousands of years, all flow units of a compound flow are products of the same eruption and were emplaced over at most a few years. Flow units can be ideally distinguished from separate flows because of the absence of red dust beds between units and the close lithological similarity of the units to one another. In our study, each flow unit in a compound lava flow was given the same serial number, with the suffix A, B . . . ; thus J40A, J40B . . . are flow units of the same compound flow (J40). There are many examples where the status of individual lava sheets was uncertain; in cases of doubt such sheets were regarded as separate lava flows and were given separate serial numbers. The flow units sampled are all clearly identified in the stratigraphic sketches (app I). The median thickness of the basaltic lava flows is 5.3 m.

A small number of salic lava flows also occur in the profiles, notably several andesite/dacite flows from the Gerpir silicic volcanic center in section G (G9, 10, 12, and 13), and a few probably andesitic lava flows also occur elsewhere (D60, L22, N100, and O23).

Interbasaltic clastic beds constitute about 10 percent of the volcanic succession; it could be more than 10 percent because some of the non-exposed parts, which account for 5 percent of the succession, probably conceal such beds. The interbasaltic beds include many red dust layers. They are individually usually less than 1 m thick and are interpreted as wind-blown volcanic dust deposits. In profiles A to O they have an aggregate thickness of 270 m. Other clastic deposits total a further 450 m in the same profiles. They include acid tuffs, some of which (for example, in profile O) are welded ignimbrites. Profile A includes palagonite tuffs between lavas A21 and A22 and between A38 and A39 that probably resulted from basaltic eruptions into temporary shallow lakes. The various kinds of detrital beds (including cold-climate deposits) in profiles P to V amount to 570 m in total thickness and are noteworthy for the almost complete absence of acid tuffs.

Zeolite zones.—The zeolite zones are included in figure 3. These vary from the zone of no zeolites in the uppermost parts of sections F, S, and V to the laumontite zone, which is indicative of a burial metamorphism to between 180° and 300°C (Ade-Hall and others, 1971) in sections M, N, and O. The bulk of the sections lies in the mesolite zone, consistent with heating to no more than 180°C. As summarized by McDougall, Watkins, and Kristjansson (1976) and McDougall and others (1977), the mild hydrothermal activity that has led to the creation of the zeolite zones has been a major cause of difficulty in obtaining reliable K:Ar ages of Icelandic rocks.

Paleomagnetic results.—Mean directions of remanent magnetism, plus the resultant vector length (applying unit vector per specimen) from which all conventional statistical parameters can be derived, are given for each lava and flow unit as tables in app I. Copies of all data, for the NRM and following each demagnetizing treatment, are available on request. We urge any reader with interest in the fine details to take this opportunity. The data copies include intensity of magnetization (J) results. In app I, results in the tables are arranged in stratigraphic order and are given adjacent to the corresponding stratigraphic sketch, for ease of inspection. The VGP position for each lava is added to the tables, and a diagram of the variation of VGP latitude as a function of stratigraphic position, together with the resultant polarity log, is presented next to the table. The polarity logs in app I are for *all* data including overlaps between sections and are plotted without any data rejection criteria being applied. Roman numerals are used to indicate stratigraphic correlation horizons on each log. By exclusion, these also provide the number of lavas representing overlap between sections. For those who do not favor the minimum scatter method of computing mean directions of remanent magnetism in each lava, we include as app II data for all those lavas demagnetized at a single peak alternating magnetic field of 250 oersteds. In this case, we provide only the data for lavas that make up the final complete stratigraphic sequence: overlaps are excluded. Also excluded from app II are data for lavas in which all cores were not demagnetized at 250 oersteds and for lavas in which only a single specimen was available.

The mean directions of remanent magnetism for each of the 21 sections and conventional associated statistical and other parameters are given in table 1. Data for flow units (lettered suffixes in app) were added to those of the base unit to provide a single vector, except for two cases (K31 and R9) where the flow unit possessed a polarity that was reversed compared to the base unit (so that the assumption of a single point in time for base unit plus flow units was obviously incorrect). The initial survey indicated that the same problem was encountered in flow C52 (of reversed polarity) and flow unit C52A (of normal polarity). Additional sampling of flow C52, made in 1975 because of its possible relevance to polarity time scale fine structure, has cast some doubt on the reversed polarity first indicated, and so although the final average result for C52 is included in app I, the data are excluded from further consideration. While not presented here, J and magnetic stability are very commonly variable between specimens within the same lava. This is not surprising, in view of the very large variations of J and stability demonstrated to exist throughout lavas south and north of Djúpivógur by Watkins and Haggerty (1967) and Wilson, Haggerty, and Watkins (1968), respectively. These variations, which most frequently reflect variations

Table 1
Eastern Iceland
Mean paleomagnetic data for all sections

The data are in two groups. The upper part is for all data, and the lower results for sets that exclude data from lavas with virtual geomagnetic poles (VGP) latitudes lower than 45°. Section identification number: see figures 2 and 3 and app I. N = number of separate lavas. D and I = mean declination and inclination of remanent magnetism, in degrees east of north, and below the horizontal, respectively. R = resultant vector, applying unit vector per lava. K = N-1/N-R. Φ' and θ' = longitude and latitude of mean VGP in degrees east of Greenwich and north, respectively. $\alpha 95$ = semi-vertical angle of 95 percent confidence cone. S_F = angular standard deviation of VGP for each lava. Su and Si = upper and lower 95 percent confidence levels of S_F. All reversed polarity data are transported to the northern hemisphere. Data for each lava were derived using minimum scatter computations (see text).

(i) All Units

Section	N	D°	I°	R	K	ϕ'	θ'	$\alpha 95$	S_F	S_u	S_i
V	18	24.6	82.8	17.37914	27.4	10.5	76.5	6.7	20.2	26.2	16.5
U	15	6.9	75.4	13.80205	11.7	110.4	86.1	11.7	27.0	35.8	21.7
T	30	346.2	76.7	27.01511	9.7	259.6	84.1	8.9	33.8	40.5	29.0
S	43	11.3	80.3	40.32800	15.7	13.7	82.5	5.7	32.1	37.3	28.1
R	33	351.1	83.4	30.66591	13.7	341.9	77.8	7.0	34.9	41.5	30.1
Q	14	37.5	80.8	12.32866	7.8	30.9	74.9	15.2	37.0	49.5	29.6
P	35	356.3	77.0	30.94702	8.4	279.0	88.3	8.9	38.3	45.3	33.2
O	56	4.7	74.8	51.05623	11.1	128.9	86.2	6.0	35.9	42.1	31.8
N	58	16.2	67.5	53.80858	13.6	126.6	73.4	5.3	30.9	36.3	27.4
M	64	20.5	76.8	59.38722	13.7	64.7	81.3	5.0	31.4	36.1	28.0
L	54	16.9	65.8	46.74828	7.3	128.5	71.1	7.7	36.1	42.2	31.9
K	41	6.5	76.3	36.88728	9.7	82.5	87.1	7.6	34.0	39.8	29.8
J	55	351.4	75.1	49.35695	9.6	226.4	85.4	6.5	33.7	39.4	29.8
F	58	1.8	74.7	55.32141	21.3	153.1	86.2	4.1	26.2	30.8	23.2
E	22	14.2	77.2	21.15329	24.8	65.0	84.1	6.4	20.5	25.7	17.0
D	66	10.8	66.3	57.94872	8.1	141.6	72.6	6.6	37.4	43.1	33.4
C	65	10.4	68.2	56.10085	7.2	139.8	75.3	7.1	31.9	36.7	28.4
B	39	355.3	66.8	30.86945	4.7	177.5	74.2	11.9	42.9	50.3	37.5
A	40	21.3	71.3	33.69255	6.2	107.9	76.1	9.9	41.0	48.0	35.8
H	30	15.0	78.0	25.10599	5.9	51.5	83.6	11.8	43.8	52.5	37.6
G	33.	23.6	70.0	29.06224	8.1	107.4	73.8	9.4	30.1	35.8	26.0

(ii) Excluding Units with θ' <45°

Section	N	D°	I°	R	K	ϕ'	θ'	$\alpha 95$	S_F	S_u	S_i
V	16	17.6	79.9	15.76858	64.8	27.0	81.4	4.6	16.5	21.7	13.4
U	12	359.8	78.7	11.90713	118.4	343.6	86.6	4.0	13.2	18.1	10.4
T	26	355.8	77.6	25.23927	32.9	293.1	87.8	5.0	23.1	28.0	19.7
S	37	2.6	77.8	35.86436	31.7	16.0	88.0	4.2	24.1	28.4	21.2
R	25	19.8	78.2	24.26598	32.7	49.6	81.7	5.1	23.6	28.8	20.1
Q	11	37.1	81.6	10.72911	36.9	25.1	74.7	7.6	22.7	31.6	17.8
P	26	0.2	74.6	25.05714	26.5	163.7	86.6	5.6	24.0	29.1	20.4
O	43	2.7	70.7	41.18010	23.1	155.8	80.3	4.6	25.1	29.2	22.0
N	49	12.9	69.1	46.99733	24.0	130.3	76.3	4.2	24.9	28.8	22.0
M	50	16.9	75.0	48.57437	34.4	88.0	81.9	3.5	20.3	23.5	17.8
L	39	9.9	70.0	37.69676	29.2	135.5	78.3	4.3	20.7	24.3	18.1
K	32	17.7	74.1	31.06078	33.0	94.5	80.8	4.5	22.4	26.7	19.3
J	44	3.1	73.1	42.73213	33.9	149.6	84.0	3.7	21.6	25.1	19.0
F	54	4.5	74.2	52.22101	29.8	139.9	84.9	3.6	22.6	26.4	20.0
E	20	3.7	77.0	19.41403	32.4	70.3	88.4	5.8	16.6	21.2	13.7
D	51	15.8	68.0	48.64462	21.2	128.2	73.8	4.4	26.4	30.7	23.2
C	52	7.6	73.6	50.52361	34.5	130.7	83.4	3.4	19.4	22.6	17.1
B	23	355.5	73.1	22.20915	27.8	186.9	83.3	5.8	22.9	28.6	19.1
A	27	15.1	71.8	25.67947	19.7	118.4	78.8	6.4	24.8	30.0	21.2
H	19	338.4	73.9	18.28671	25.2	238.6	78.9	6.8	25.3	32.4	20.8
G	26	22.0	73.7	25.13335	28.8	93.0	78.5	5.4	22.7	27.5	19.3

in the high temperature titanomagnetite oxidation state and maghemitization resulting from weathering, do not prevent reliable polarity measurements being derived for the vast majority of the lavas (where R > 1.6 in tables of data in app I).

EARLIER AND INDEPENDENT RESULTS FROM STUDY OF THE COLLECTION

As described above, the initial field studies were begun in 1955, and the paleomagnetic survey was completed in 1965. Despite a lack of any published details involving geological control, a substantial number of publications based on various analyses of the samples have already appeared. Some of these are relevant to the interpretation of the data presented in this paper.

Dagley and others (1967) published the preliminary results in the form of a polarity log for the entire sequence. They concluded that at least 60 successive changes of polarity were recorded, and that two long periods of normal polarity (involving secs. E, F, and J, and secs. M and N) were indicated. Because of difficulties in K:Ar dating of the samples, they were unable to determine the age range of the sequence, except to the extent that the age of the base was probably no more than 20 m.y. It must be stressed, however, that prior estimates of the age of the Gerpir lavas (sec. G in fig. 2) which have the oldest units in eastern Iceland, ranged back to Cretaceous, on the basis of palynological data (summarized by Einarsson, 1963). An incidental result of the Dagley and others (1967) analysis was the demonstration that about 7 percent of the lavas sampled possessed VGP latitudes lower than 44°. They categorized the lava polarities into 551 normal, 406 reversed, 73 'anomalous' (with directions > 40° from the axial dipole direction), and 43 'discordant' (with inconsistent within-lava directions). Overlaps were obviously included in this summary.

Wilson (1970, 1971) incorporated the paleomagnetic data for the entire survey into an analysis of global geomagnetic variations for the Upper Cenozoic but in doing so only presented mean data sets for groups of 100 successive lavas. Dagley and Wilson (1971) later used the same data to show a direct relationship between mean intensity of magnetization (J) and VGP latitudes, suggesting that the geomagnetic field intensity decreases when the VGP latitude is low. Dagley and Lawley (1974) made detailed analyses of the longitudinal paths swept out by the VGP during periods of transition between opposite polarity and showed that, contrary to earlier speculations, no preferred "corridor" is present, indicating the presence of randomly occurring non-dipole fields during the transition period.

Wilson and McElhinny (1974) presented the mean VGP of each of the 21 sections in an analysis of the data in terms of the offset dipole model for the geomagnetic field. This was developed in response to the fact that Upper Cenozoic VGP's lie beyond the geographic pole from the sample site, whatever site longitudes are involved. These "far side" poles can be explained by the axial dipole being displaced northward along the spin axis of the Earth, so that the magnetic inclinations at the surface become shallower than those for an axial geocentric dipole. Because of this, application of the conventional centered dipole equation to computation of the VGP at any site then provides magnetic colatitudes greater than the geographic colatitudes or "far side" VGP's. In their paper, Wilson and McElhinny (1974) first analyzed all available Upper Cenozoic paleomagnetic data to show an apparent decrease in the northward offset between early Miocene and Pleistocene times. This conclusion was then used to interpret a problem in the eastern Iceland sequences. Here, the youngest 6 sections (Q to V in fig. 2) contrast with the older 15 sections in possessing *near*-sided VGP's (or inclinations *steeper* than that required by an axial geocentric dipole). If the axial dipole were apparently migrating southward along the spin axis between Miocene and Pleistocene times, a corresponding gradual increase in geomagnetic inclination would occur at the surface. The observed inclination discontinuity between the group of sections A to P and the group of sections Q to V could therefore be due to a break in volcanic activity of several million years duration between the respective groups, during which time the inclination change was progressing. Wilson and McElhinny suggested that a break between t = 7 and 4 m.y., similar to that proposed by Saemundsson (1974) on totally different grounds involving tectonic arguments, could account for the observed inclination contrasts. Saemundsson (1974) had compared the Dagley and others (1967) polarity log to the polarity time scale predicted by Talwani, Windisch, and Langseth (1971), in suggesting a period of volcanic quiescence between t = 8 and 4 m.y. A significant difference between the mean J for the two groups of sections was interpreted by Wilson and McElhinny (1974) to represent different magma chambers, which could be also consistent with the existence of a hiatus.

Piper (1973) used the data of Dagley and others (1967) to speculate on the magnetostratigraphy of eastern Iceland. The map he produced is by necessity of very small scale and contains no fine detail, perhaps because the relevant data and stratigraphic details were not published at that time.

It was not until 1968 that the first apparently reliable K:Ar ages for the area were published. Moorbath, Sigurdsson, and Goodwin (1968) showed that the lavas of Gerpir (sec. G, fig. 1) were extruded between t = 13.0 and 12.4 m.y. McDougall and others (1976) mentioned confirmation of these results, and the data are here published for the first time, courtesy of Dr. Ian McDougall, as table 2. Because of its key stratigraphic position in the ideas involving a hiatus in volcanic activity, section Q was sampled for K:Ar analyses by McDougall, Watkins, and Kristjansson (1976). The sequence examined also includes 32 lavas above the original sampled sequence (app I), so that equivalents of sections R and S were collected. Because of their importance to the present study, the data are reproduced in figure 4. The results show clearly that polarity epochs 6 and 5 and the

TABLE 2

Potassium-argon ages on whole rock samples of lavas from the Gerpir (G) Section

Field no.	Lab. no.	K (wt. %)	Rad. ^{40}Ar (10^{-11} mol/g)	100 Rad. ^{40}Ar / Total ^{40}Ar	Calculated age (m.y. ± 1 s.d.
G10	74-504	2.923,2.913	6.462	94.7	12.40 ± 0.15
G9B	74-503	0.928,0.927	2.094	87.4	12.64 ± 0.15
G9A	74-502	0.942,0.943	2.150	69.9	12.77 ± 0.15
G8	74.501	1.140,1.136	2.616	86.9	12.87 ± 0.15
G6	74-499	0.637,0.636	1.397	81.6	12.29 ± 0.15

$\lambda_e = 0.585 \times 10^{-10} y^{-1}$ $\lambda_\beta = 4.72 \times 10^{-10} y^{-1}$ $^{40}K/K = 1.19 \times 10^{-2}$ atom %

For location of section G see figures 2 and 3A. For sample field numbers, see app I. Data are published courtesy of Dr. Ian McDougall (Australian National University). See McDougall, Watkins, and Kristjansson (1976) and McDougall and others (1976) for full details of experimental methods. The results confirm those by Moorbath, Sigurdsson, and Goodwin (1968) for the same section.

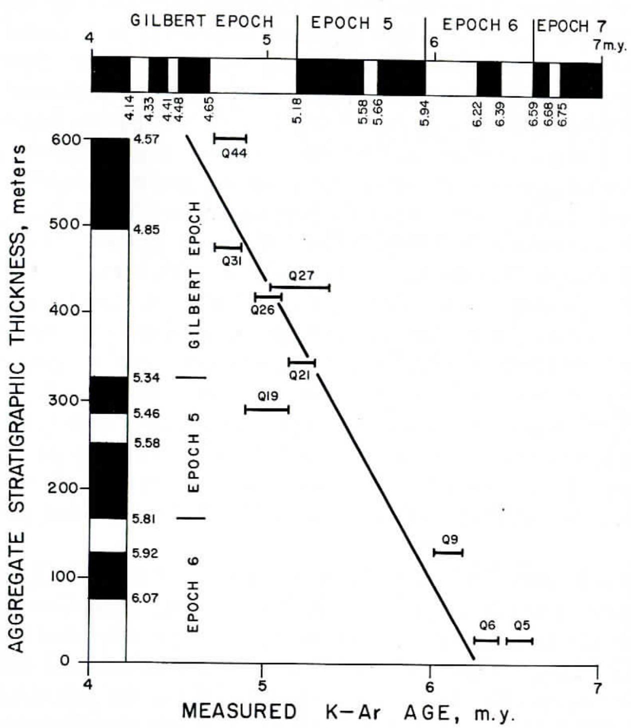

Fig. 4. K:Ar and paleomagnetic results for a sequence of 46 successive lavas in Fljótsdalur (fig. 2), from McDougall, Watkins, and Kristjansson (1976, fig. 4). K:Ar results are plotted as confidence limits at the height of the lavas measured. The linear regression line (relating age to height) is used to assign ages to the polarity boundaries in the section. Height above an arbitrary base is given on left. The polarity log is black = normal polarity, clear = reversed polarity. Known and predicted history at the top of the diagram. The lower 14 lavas comprise section Q of figures 2 and 3C, and the upper 32 lavas are equivalent to sections R, S, and part of T. The diagram shows that the Gilbert and polarity epochs 5 and 6 are represented in the section.

Gilbert epoch are represented in the sequence, and that the hiatus proposed by Saemundsson (1974) and Wilson and McElhinny (1974) either does not exist in the area or occurred prior to t = 6.5 m.y. The long sequence of normal polarity lavas in sections E, F, and J led McDougall and others (1976) to suspect that "Anomaly 5", which is an important time unit identified in marine magnetic anomaly analyses, might be recorded by the lavas, as suggested by Piper (1973). The results (reproduced in fig. 5) show clearly that the age of the period of normal polarity (predicted to have begun at t = 10.21 m.y. by Blakely, 1974, using the lower age limit of 8.71 m.y. proposed by Talwani, Windisch, and Langseth, 1971) is that represented by the lavas. Ross and Mussett (1976) have recently presented a series of $^{40}Ar/^{39}Ar$ ages for the entire sequence (A to V) which they used to show that all the lavas were erupted from an axial zone that has not shifted appreciably, and that the inferred spreading rate is very similar to that independently derived for the Mid-Atlantic ridge to the south. The confidence limits on the data reach greater than

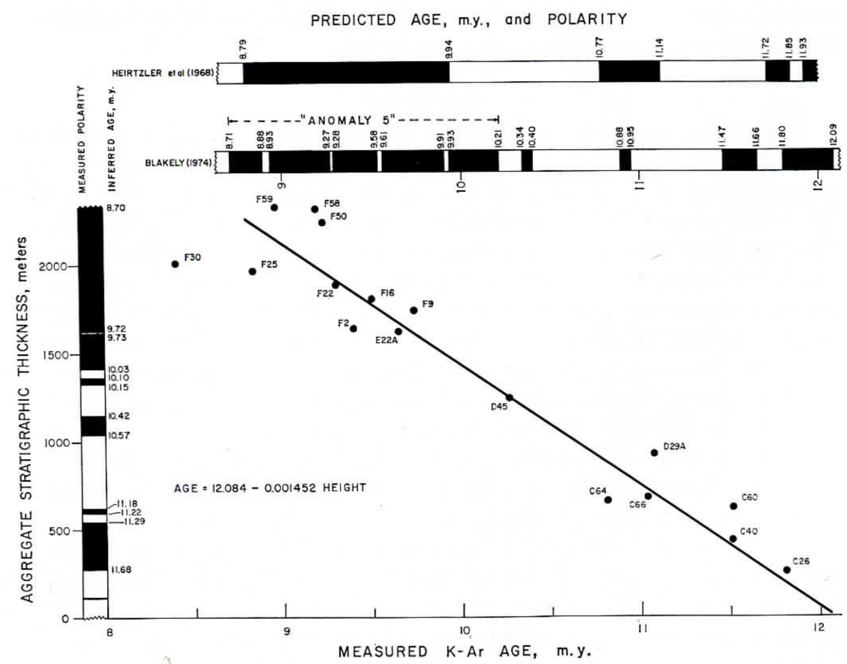

Fig. 5. K:Ar and paleomagnetic results for sections C, D, E, and F from McDougall and others (1976). Height above an arbitrary base is given on left, measured polarity log (black = normal, clear = reversed), and K:Ar results plotted at the height of the lavas involved. The regression line (eq given) facilitates estimates of the ages of the polarity boundaries. The predicted polarity time scales, after Heirtzler and others (1968) and Blakely (1974) are given at the top of the diagram. The long period of normal polarity corresponding to "Anomaly 5" in marine magnetic anomaly terms is presented in the section.

± 20 percent, but the results show that the sequence extends from about 13 to 2 m.y. ago.

Other studies of the eastern Iceland collection include rare earth analyses by Wood, Gibson, and Thompson (1976) who show an apparent decrease in the Lanthanium to Samarium ratio with decreasing age. Schilling and Noe-Nygaard (1974) have also noticed this relationship. Wood, Gibson, and Thompson (1976) favor an interpretation for their observation involving hydrothermal effects, since the youngest lavas occur highest in the zeolite zones (fig. 3). Ade-Hall, Palmer, and Hubbard (1971) have used samples from the "Eastern Iceland Collection" to evaluate the role of mild hydrothermal activity in the development of ferrirutile "granulation" on titanomagnetites. They concluded that a temperature of 150°C was essential for the development of this specific type of mineralogical overprint.

Because of its size and the stratigraphic control represented by the collection, it can be anticipated that additional use will be made of the data. One motive for publishing this highly detailed report is indeed to encourage such developments, although the primary intention is to provide a series of mappable time units and in doing so to examine the details of the regional volcanological history.

DISCUSSION

Effect of computation method.—Comparisons of app I and II provide a means to evaluate the relative merits of the minimum scatter computational procedure and the single demagnetizing field method. Only 6 out of over 700 lavas which comprise the section yield contrasting polarities, between the two computational methods. Lavas C8 and J6 produce VGP latitudes of 5.6°N and 17.1°S using the minimum scatter system, in comparison with 0.4°S and 43.7°N using the single field method. Both lavas produce apparent reversals of polarity (polarity events) within the respective sections in logs computed using the minimum scatter system throughout. On the other hand, the opposite situation occurs for the other 4 lavas (B7, D40, M6, and N43): here the polarity events are evident when the logs are compiled using the single demagnetizing field system but are not present with the other method. So if any selection were to be made on the basis of any arguments involving polarity coherence in the section, the single field method would be unacceptable, since it yields a larger number of polarity events based on single lavas. This could explain, at least in part, the fact that the initial data analysis, which did not employ minimum scatter techniques (Dagley and others, 1967) reported "at least 61" polarity changes, which (as we shall show) is larger than the minimum number of polarity changes we believe to exist in the section. In all 6 of the conflicting cases, the VGP latitudes are low, whatever computational system is used. It is clear that doubt exists about the polarities of these 6 lavas, and this will be considered in the discussion which follows. The fact that only 6 out of over 700 lavas are so affected provides

confidence in our preferred computational system, which is now adopted for the remainder of this paper.

Data rejection criteria—Within the sequence that excludes overlaps and that therefore comprises the section to be discussed, the resultant vector R is < 1.6 for only 16 lavas, and these are rejected from further consideration. In only 25 cases is $R < 1.8$. The section is obviously made up of a series of lavas that on the whole have produced remarkable within-body agreement of results and must therefore be accepted as highly suitable for the compilation of a polarity history for the period represented.

Polarity log.—Because of the availability of sets of K:Ar data from three parts of the section (figs. 4 and 5; table 2) a magnetostratigraphic sequence can be proposed that can be correlated unambiguously with the known and predicted polarity time scale. This is presented in figure 6. We have adopted the following methods in compiling the polarity log in figure 6: (A) Slight adjustments of the original geologically-based correlations between sections have been made, to render complete compatibility between polarity signatures in those sequences that overlap. The exact tie points between each section are indicated by arrows and roman numerals on the polarity logs of app I. (B) The polarity log has been compiled by correlating between the youngest unit in any section with whatever lava is considered equivalent in the section immediately overlying. Other methods could be used to compile the final polarity log (and these are readily possible, given the data in the appendices), but our preferred system has minimum subjectivity. The vertical extent of each of the 21 sections is added to figure 6. Correlation to the known and predicted polarity time scale for the period $t = 13$ to 2 m.y. is based on the three ties provided by K:Ar data for the sequences in sections G, C through F, and Q through S and is displayed in figure 6. The correlation lines between the K:Ar control points are based on simple comparison with the polarity time scale: this is straightforward for the oldest 60 percent of the section (sec. G through M in fig. 6) but is less clear for sections O, T, U, and V, although the $^{40}Ar/^{39}Ar$ results by Ross and Mussett (1976) are consistent with the interpretation shown. It is doubtful if any drastic error (in excess of 0.5 m.y.) is possible in the correlations shown in figure 6.

Volcanic episodes.—The rate of accumulation of the Icelandic lava pile is likely to be intimately associated with the processes involved in creation of the North Atlantic sea floor, as continental drift continues. The accumulation rates will be excess to that accomplished by simple sea-floor spreading in the region. Pitman and Talwani (1972) have proposed a comprehensive history of sea-floor spreading for the North Atlantic. They show that an increase in the rate of sea-floor spreading took place about 9 m.y. ago, over much of the Atlantic. Perhaps of greater relevance to the eastern Iceland study is the analysis by Vogt (1971) of the marine magnetic anomalies and morphology of the Reykjanes Ridge. He shows that

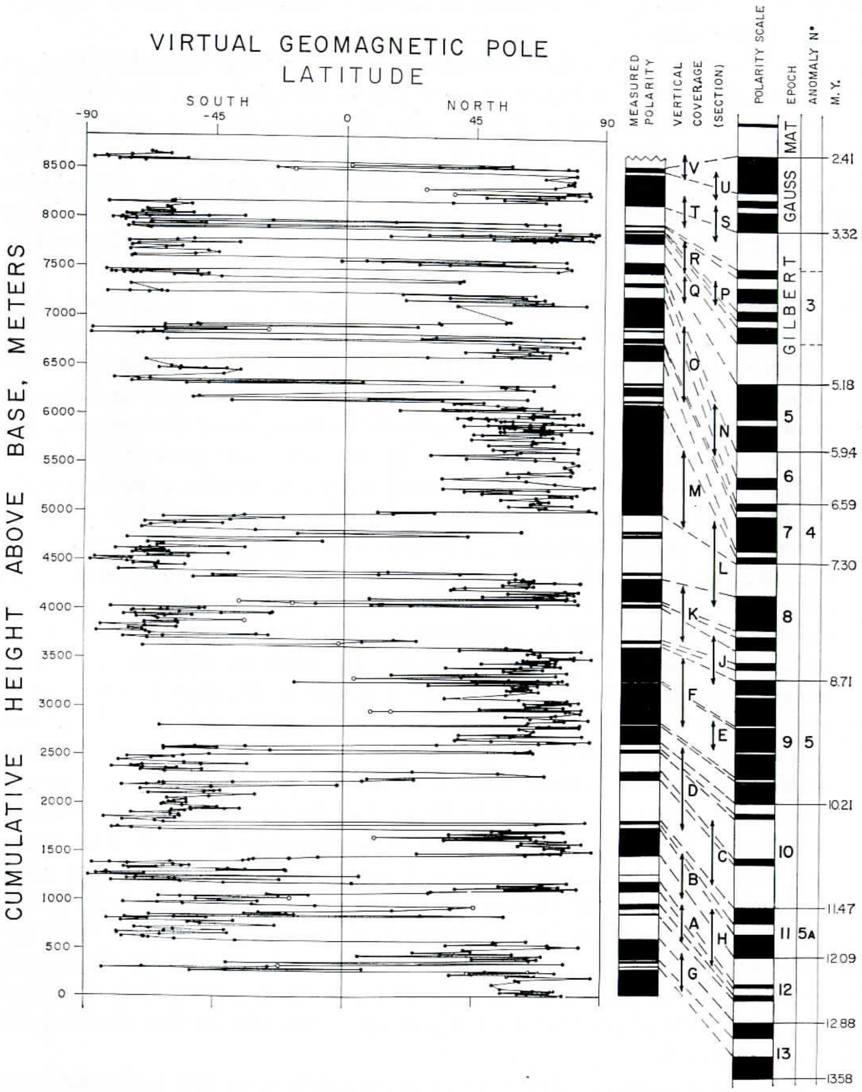

Fig. 6. The polarity log for eastern Iceland. Vertical extent of the 21 sections (figs. 2 and 3) shown, after the correlation shown in figure 3. The latitude of the virtual geomagnetic pole (VGP) for each lava is plotted against height above the base of the sequence. Data points with low reliability (resultant vector less than 1.6 when applying unit vector to each of two separate specimens per lava) plotted as open circles. Polarity log resulting from VGP plot is black = normal (VGP in northern hemisphere), clear = reversed (VGP in southern hemisphere). The independently known and predicted polarity history, after Cox (1969), Talwani, Windisch, and Langseth (1971), and Blakely (1974), shown at right, with terminology for polarity epochs and "anomaly numbers" added. The K:Ar data for section G (Moorbath, Sigurdsson, and Goodwin, 1968), sections C, D, E, and F (fig. 5) from McDougall and others (1976), and sections Q, R, S, and perhaps T (fig. 4) from McDougall, Watkins, and Kristjansson (1976) facilitate the correlation (dashed lines) between the measured polarity and established polarity history. For the paleomagnetic data for each lava, by section, see app I.

beginning 7 m.y. ago, the ridge morphology changed to reflect a greater volcanic production rate which has persisted since that time. Vogt (1974) also draws attention to a similar increase in volcanic production rate which occurred on the Ridge about 16 m.y. ago. This is the time when the oldest known lavas in Iceland were extruded (Moorbath, Sigurdsson, and Goodwin, 1968). Relative configuration of the magnetic isochrons (anomalies) and the ridge bathymetry can be explained by a southward migration of mantle "plume" activity, or a thermal front, at a rate of about 20 cm yr^{-1}. The data in figure 6 is now examined to see if corresponding changes in volcanic production rates can be identified in eastern Iceland.

The measured and inferred ages of the sequence illustrated in figure 6 are plotted against height in figure 7. Linear regression analysis yields an average lava accumulation rate of 860 m/m.y., but it is clear that at least three different episodes or rates of volcanic activity (V1, V2, and V3 in fig. 7) occurred. The respective volcanic production rates involved (which vary by a factor of over seven) are summarized in table 3.

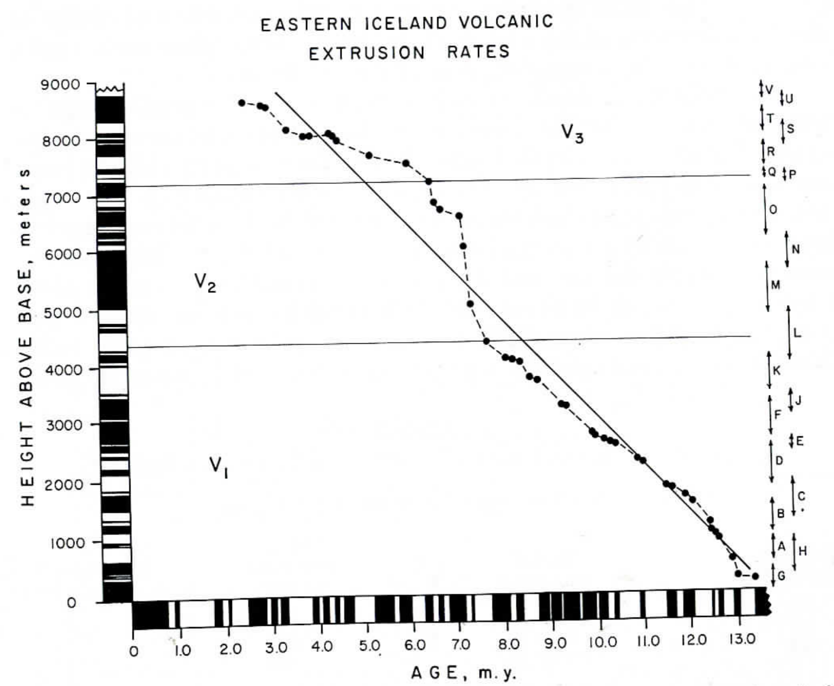

Fig. 7. Age versus height for the east Iceland sequence. The measured polarity log and height for the sequence (fig. 6) is the vertical axis, and the age and polarity of the known and predicted polarity history is the horizontal axis. Data points are derived from figure 6 (opposite ends of the dashed correlation lines). Linear regression line added. Vertical extent of the 21 separate sections (figs. 2 and 3) added on right. The discontinuities in the plot represent three different volcanic production rates V1, V2, and V3 (table 3A).

McDougall and others (1976) have shown that 13,000 yrs is the average time between successive extrusions in sections C, D, E, and F. The major discontinuity in extrusion rates apparently occurred at about t = 7.3 m.y. It is tempting to suggest that this discontinuity may be related to the drastic increase in volcanic production rates that Vogt (1971) has proposed for the Reykjanes Ridge, beginning about 7 m.y. ago. Before considering this possibility, it is necessary however to examine sources of error in the timing and magnitude of the apparent volcanic episodes shown in figure 7. This problem is considered below.

Corrected extrusion rates.—The measured rate of lava accumulation will almost certainly be a function of distance from the extrusion center in Iceland, because as Walker (1964) has demonstrated, most lava sequences are characterized by rapid downdip thickening. Thus for any given period, the apparent volume of lava extruded could vary substantially, depending on the location of the measured profiles. The factor of two to seven variation between episodes V1, V2, and V3 may thus not be a true reflection of variations in regional volcanic activity. It therefore becomes necessary to derive means to normalize lava thickness to that at a fixed distance from the extrusion centers. The definition of zeolite zones and measurements of dip and thickness of the lavas allow such a normalizing process to be accomplished as explained below.

In figure 8 the depth of each section below the original surface as deduced from the zeolite zonation is given. Since the measured dip increases linearly with depth below the original surface, the thickness of any lava group likewise increases linearly with depth (fig. 9A), and the best way to compare thicknesses on the same basis is to transform them into thicknesses at a standard depth. The top of the analcite zone is the most convenient datum, and the resulting normalizing factor is given as a function of depth in figure 9B: all lava thicknesses are divided by this factor, so that the normalized thickness of units deeper and shallower than the top of the analcite zone becomes less and greater, respectively.

TABLE 3

Inferred rates of volcanic production in eastern Iceland

Volcanic episode	Period (m.y.b.p.)	Rate of extrusion (m/m.y.)	Normalized rate of extrusion
A. Uncorrected for downdip thickening			
V1	13.4 to 7.6	720	2.0
V2	7.6 to 6.5	2600	7.3
V3	6.5 to 2.3	360	1
B. Corrected for downdip thickening			
V1	13.4 to 7.2	560	1.2
V2	7.2 to 6.4	1900	4.1
V3	6.4 to 2.3	460	1

See figure 7 for source of data in A and figures 8 to 11 for explanation and source of data for B. Normalized rate of extrusion based on unity for episode V3.

This computation has been applied to all lava thicknesses in the section. The resultant polarity log is given in figure 10.

Comparison of the polarity logs in figures 6 and 10 provides several conclusions. The normalized sequence in figure 10 is, of course, thinner (since most of the sections are below the analcite zone). When the age and depth relationship are replotted using the normalized thickness data (fig. 11), the three volcanic episodes derived from the original data (fig. 7) are still apparent, but the relative magnitudes of the volcanic production rates are drastically reduced, as summarized in table 3B, to a maximum variation by a factor of 4.1 as opposed to 7.3. Linear regression analysis of the normalized data provides an average volcanic production rate of 620 m/m.y., which is about 25 percent less than the uncorrected value, but more significant is the increased linearity of net extrusion rate

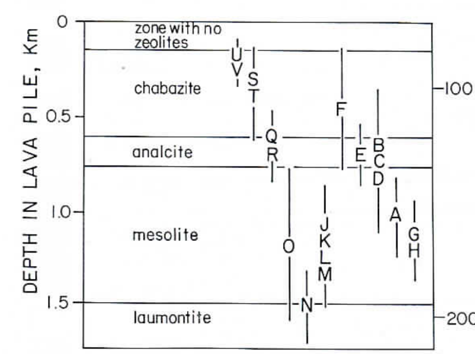

Fig. 8. Distribution of zeolite zones between the sections, compiled from figure 3. Depth in km beneath the original surface and the probable temperature involved in the consequent hydrothermal metamorphism leading to the respective zeolites (as summarized by Ade-Hall and others, 1971) added on left and right, respectively.

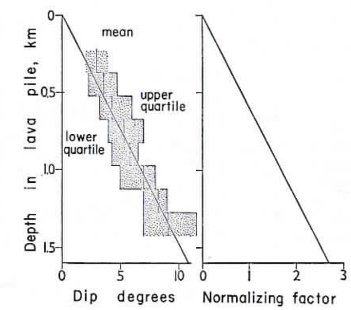

Fig. 9. A. Relationship between depth beneath the original surface (deduced from zeolite zones in fig. 8) and dip angle of the lavas, based on several hundred measurements. Upper and lower quartile limits are shown. The diagram shows the clear increase in dip with depth beneath the original surface.

B. "Normalizing factor", by which lava thicknesses are divided to obtain thicknesses at a standard depth (taken as the top of the analcite zone, 0.6 km deep). This normalizing procedure is necessitated by the rapid downdip thickening of the lavas.

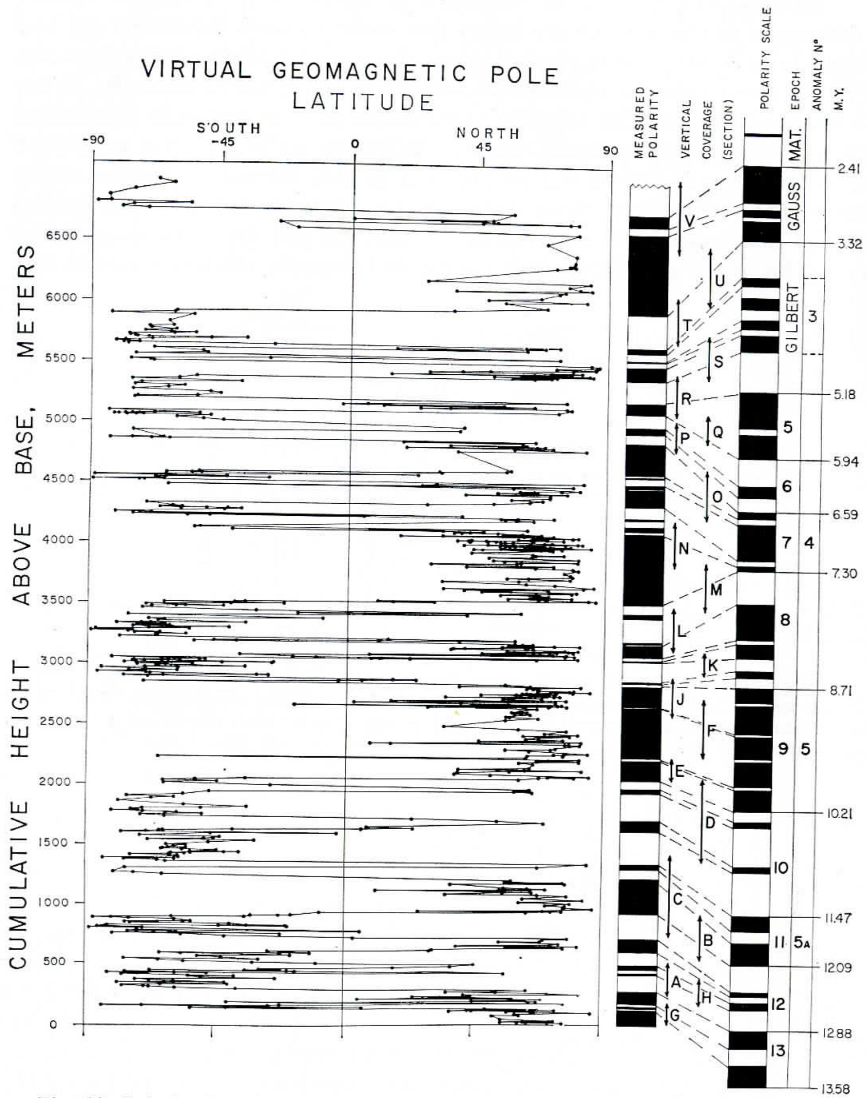

Fig. 10. Polarity log for the east Iceland sequence as in figure 6 but following normalizing of each component lava thickness for downdip thickening, to that thickness expected at the top of the analcite zone (see text for explanation).

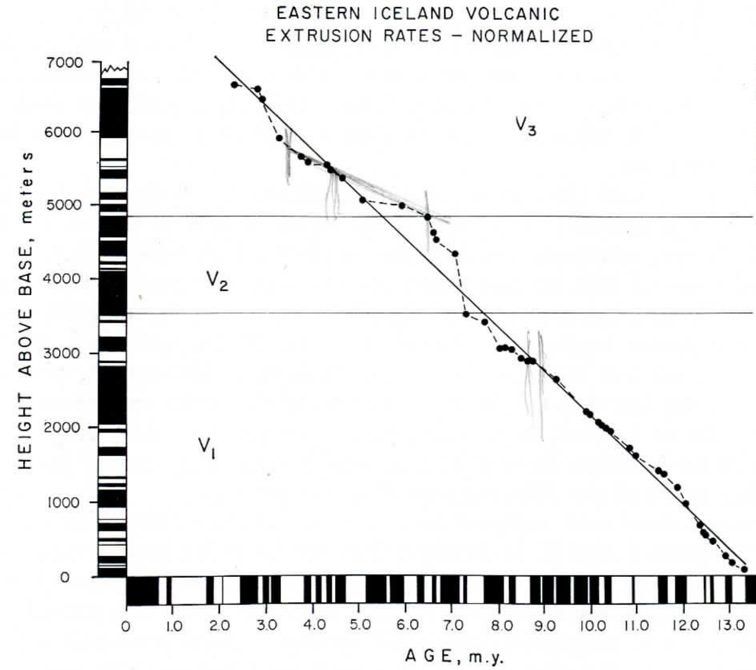

Fig. 11. Age versus height for the east Iceland sequence, as in figure 7, following normalizing of each component lava thickness for downdip thickening, to that thickness expected at the top of the analcite zone, corresponding to figure 9.

accomplished by the normalization process: f values for the height to age linear regression increase from 799 to 2265. This strongly suggests that the normalizing procedure has been successful.

The normalizing procedure has not removed the three-fold volcanic periodicity from the sequence, and so episode V_2 is considered to be a real volcanic maximum, when the lava production rate, which has previously remained virtually constant for a period of at least 6 m.y. increased suddenly by a factor of about 4 (fig. 11 and table 3). The normalizing process has resulted in the initiation of this increase in volcanic activity being dated at $t = 7.3$ m.y. (fig. 11), and this is virtually indistinguishable from the timing of the proposed sudden increase in volcanic activity on the Reykjanes Ridge (Vogt, 1971). Episode V_2 ceases in eastern Iceland at $t = 6.4$ m.y., however, in contrast to the increased level of activity on the Reykjanes Ridge, which according to Vogt's analysis has persisted with accompanied southward migration until the present. If the eastern Iceland and Reykjanes Ridge volcanic activity were related, this would require the drastic increase in volcanic activity to have begun almost simultaneously in eastern Iceland and the Reykjanes Ridge but to have ended in the former area less than 1 m.y. later, to return to levels closely comparable to those of earlier periods. Meanwhile the volcanism has tended to expand southward along the Ridge at about 20 cm per yr. While these independently derived observations on the island and on the ridge to the south are quite consistent with a southward migrating "plume" edge, they do not by any means constitute proof of such a mechanism, which would require further independent testing, possibly by chemical means.

It is in any case clear that volcanic productivity in eastern Iceland varied over a period of 11 m.y. by a factor of up to four or so (table 3B), although it was relatively constant for periods of at least 6 m.y. The measured rates of lava accumulation are between 620 and 860 m/m.y., which closely matches that defined by McDougall and others (1977) for the Borgarfjördur region of western Iceland. McDougall and others (1976) have, on the basis of data from sections C through F, already pointed out the fact that similar volcanic production rates were occurring on both sides of Iceland, so that a symmetry in processes with respect to the Mid-Atlantic ridge, as required by simple crustal spreading models, existed for much of the Miocene and Pliocene periods.

Nomenclature and regional stratigraphic units.—The polarity log shown in figures 6 and 10 is clearly a data set far more stratigraphically definitive than any petrographic observations. It thus becomes inevitable that local stratigraphic terms will emerge from the data. The growth of the application of magnetostratigraphic methods has necessitated a parallel development of a stratigraphic nomenclatural system. This need led to the formation of the Polarity Time Scale Subcommission of the International Commission on Stratigraphy, within the International Union of Geological Sciences. The subcommission has also been recognized by the International Association of Geomagnetism and Aeronomy, which is part of the International Union of Geodesy and Geophysics. Thus the subcommission acquires the international contribution to its deliberations, which is so clearly desirable in the formulation of a globally-applicable set of magnetostratigraphic terms. The philosophy behind the subcommission's work is the development of a nomenclature that would be in least conflict with the long-established conventional stratigraphic terminology. Three series of recommendations have been published.[1] The main set of magnetostratigraphic terms and some of the rationale involved are reproduced in table 4. Two special properties of magnetostratigraphic methods and the associated nomenclature are worthy of stress:

1. The three-fold nomenclatural system of suffixes (table 4) is designed to accommodate progress from the simple naming of a local magnetozone (the polarity zone or subzone) without any implication of time element being involved, to a more definite time element, which is likely to result as the regional extent of any magnetozone becomes apparent, so that a polarity subinterval or interval is defined. Ultimately, local stratigraphic terms may become so well defined that they can be related to the established polarity time scale, in which case chronologic units (polarity events and polarity epochs) can be applied.
2. Because the known and predicted polarity time scale has been developed (as summarized by Watkins, 1972) using three diverse methods (K:Ar dating and paleomagnetic studies of igneous rocks; paleomagnetic studies of deep-sea sedimentary cores micropaleontologically dated; and analysis of marine magnetic anomalies using crustal spreading models), it was recommended by the Polarity Time Scale Subcommission (footnote 1, refs. 5 and 6) that three sets of nomenclature be allowed: polarity epochs and events that are *named,* following the proposals of Cox, Doell, and Dalrymple (1964) as summarized by Cox (1969), when the K:Ar and paleomagnetic methods were employed; a simple numbering of epochs and events, when the definition results from deep-

[1] Publications involving proceedings of Polarity Time Scale Subcommission of the International Commission on Stratigraphy are:
1. Magnetic polarity time scale: Geotimes, 1973, v. 18, May, p. 21-22.
2. Subcommission on the magnetic polarity time scale: Geol. Soc. Japan Jour., 1973, v. 79, p. 319-322.
3. Editorial comment: Nature Phys. Sci., 1973, v. 242, p. 65.
4. Magnetostratigraphic nomenclature I – Terminology, Comments on the Earth Sciences: Geophysics, 1973, v. 3, p. 55-58.
5. Correlating stratigraphic zones and magnetic polarities: Geotimes, 1975, v. 20, June, p. 26-27.
6. Magnetostratigraphy: data acceptability criteria and definition of polarity "excursions": Geotimes, 1976, v. 21, April, p. 18-20.
7. On the second meeting of the IUGS Subcommission On The Magnetic Polarity Time Scale: Geol. Soc. Japan Jour., 1976, v. 81, p. 211-212.

TABLE 4

Summary of terms recommended for use in magnetostratigraphy by IUGS Polarity Time Scale Subcommission of the International Commission on Stratigraphy

Magnetostratigraphic units	Approximate duration in yrs	Chronostratigraphic units	Chronologic units
polarity subzone	10^4—10^5	polarity subinterval	polarity event
polarity zone	10^5—10^6	polarity interval	polarity epoch
polarity superzone	10^6—10^7	polarity superinterval	polarity period
polarity hyperzone	10^7—10^8	polarity hyperinterval	polarity era

Notes accompanying this recommended system included the following:
1. A magnetostratigraphic unit may be defined as a local body of rock strata unified by its magnetic polarity and thus differentiated from adjacent strata.
2. The basic local magnetostratigraphic unit is the magnetozone, but the term "zone" may be used without the prefix when the usage is clear.
3. Each local magnetozone should be designated in such a way that it can be referred to readily in discussion. (This could be by letter, or by letter and number within a group or formation, or by name.) At this time, the use of new stratigraphic names should be discouraged to avoid proliferation of terms.
4. It is strongly recommended that the magnetostratigraphic units must be initially local ("provincial") or informal units until wide, preferably global, correlations and therefore polarity history (formal units) can be recognized. The time-representative component inherent in chronostratigraphic terms will permit their use in a time sense pending the adoption of internationally approved chronological terms.

sea sedimentary core studies; and the use of the well-established "anomaly number" system for those parts of the polarity time scale derived from marine magnetic anomaly analysis. Thus an ultimate goal of magnetostratigraphic systems will be to enable the stratigrapher to state that "polarity epoch X is equivalent to polarity epoch number Y in deep-sea sediments, which occurs as anomaly number Z in marine magnetic anomalies."

In table 5 we propose a series of local magnetostratigraphic terms for eastern Iceland and show their relationships to global chronologic magnetostratigraphic units. As discussed by McDougall and others (1977) in their magnetostratigraphic study of the Borgarfjördur region of western Iceland, we are reluctant to suggest a series of names for those polarity epochs and events preceding the Gilbert epoch based on local Icelandic geographic terms, merely because of the simplicity of the numbering system that has evolved in marine sediment studies (Opdyke, 1972). It is nevertheless clear that ambiguities concerning the correlation of specific local polarity events (in particular) with the predicted polarity time scale are such that local terms are best employed, and to avoid any confusion with global units, it is therefore recommended that, until definite corre-

TABLE 5

Summary of recommended and established magnetostratigraphic terms for eastern Iceland lavas

The table contains from left to right: height above base (meters); vertical coverage of respective sections (from figs. 3 and 6); measured polarity (from fig. 6 and app I), proposed magnetosubzones (local terms for thin segments of single polarity; N = normal polarity. R = reversed polarity); proposed chronostratigraphic units (terms for the local magnetozones which probably have more than local significance, but which are not uniquely defined chronologically), odd numbers are for short periods of reversed polarity within dominantly normal polarity segment, and even numbers are for short periods of normal polarity within reversed polarity segment, with lettered suffix going down alphabet with increasing age (note question marks, explained below); magnetic anomaly number (from marine magnetic anomaly time scale, for example, Talwani, Windisch, and Langseth, 1971; Blakely, 1974); chronological units (true time units, divided into polarity epochs and events, depending on relative duration. Epoch numbers after Opdyke, 1972; event numbers after Hays and Opdyke, 1967, except for the named units younger than 5.18 m.y. (Cox, 1969; McDougall and others, 1977). Age in m.y., from Cox (1969); Talwani, Windisch, and Langseth, (1971) and Blakely (1974). See table 3 for definition and discussion of magnetostratigraphic nomenclature and app I for details of constituent paleomagnetic data for the sections. An example of the use of this nomenclature is as follows: the upper set of normal polarity lavas in section L would be locally termed the Langagil upper normal polarity magnetozone; polarity subinterval 8a (if shown to be regionally applicable); and if of known age, of an appropriate globally applicable term at the polarity event level. In marine magnetic anomalies, it should be found immediately adjacent to anomaly 4. As discussed in the text, the number of polarity subintervals for the period shown may be less than indicated, for one of three reasons: the data representing the polarity change may be of low precision (for example, polarity subintervals 12d and 12a); the data representing the polarity change may not represent a full polarity reversal, but rather a field excursion (for example, polarity subintervals, 9a, 8f, and 7g); or the data representing pairs of polarity subintervals may result from a possible field excursion between what would otherwise be a single polarity subinterval (for example, polarity subinterval pairs 13c and 13b; 8e and 8d; 8b and 8a; 7f and 7e; 7b and 7a. Polarity subintervals 12a and 9a are also of dubious reality because of possible computational ambiguities (see text). See app I for details of polarity subinterval data.

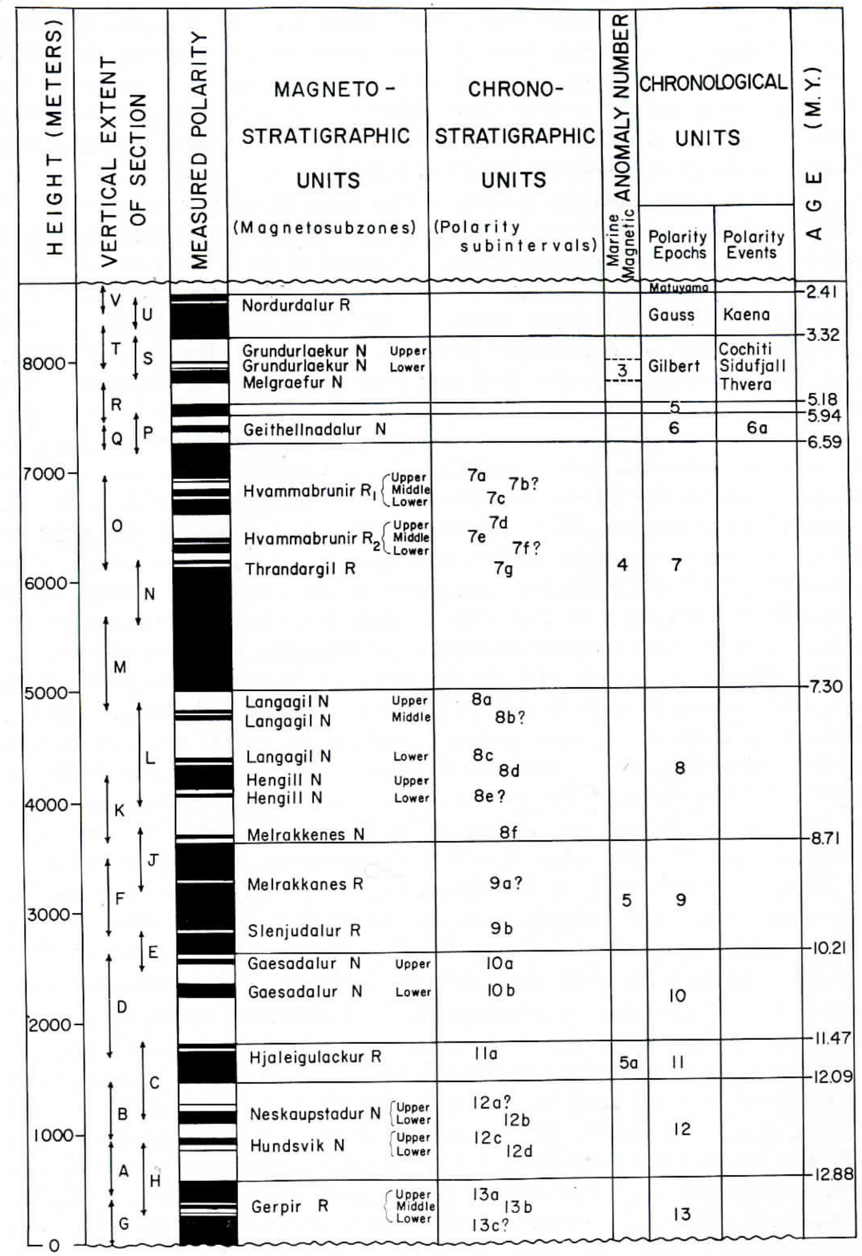

lation *is* accomplished, local terms be employed in several cases (table 5). We have added the chronostratigraphic unit numbers of table 5 to the polarity logs given in app I, so that the exact data source for the units can be readily examined. As will be discussed later, in some cases the data do not provide totally clear detection of true polarity reversals which might be otherwise inferred from table 5: the reader's attention is drawn to the seven question marks in table 5.

Geomagnetic polarity history.—The data in figures 6 and 10 are relevant to the problem of finer definitions of the geomagnetic polarity history for the Miocene and Pliocene. Because of the impressive precision of the K:Ar data for section G by Moorbath, Sigurdsson, and Goodwin (1968) and their subsequent confirmation by McDougall (table 2), and the publications by McDougall and others (1976), McDougall, Watkins, and Kristjansson (1976), and Ross and Mussett (1976), the section is confidently interpreted to extend from epoch 13 to the lowest part of the Matuyama epoch, at about t = 2.0 m.y. When the most refined analysis of relevant paleomagnetic data (Cox, 1969; Opdyke, 1972) and marine magnetic anomalies (Talwani, Windisch, and Langseth, 1971; Klitgord, Mudie, and Normark, 1972; Blakely, 1974) are employed, the polarity history shown on the right hand side of figures 6 and 10 materializes. This provides a total of 57 polarity changes or an average of one change every 195,000 yrs, between t = 13.5 and 2.4 m.y. This is a more frequent reversal than provided by early estimates (for example, Heirtzler and others, 1968), because of the recent development of "stacking" techniques in magnetic anomaly analysis (Blakely, 1974; Cande and Labreque, 1974), whereby periods of a single polarity as short as 10,000 yrs may be detected. Previously, Vine (1966), for example, suggested that this detection limit would be about 25,000 yrs. In the eastern Iceland sequence, as many as 71 polarity changes would appear to be present (table 5). But close inspection of the data (app I, where the polarity subinterval numbers of table 5 are indicated on the detailed polarity logs) shows that not all the changes of VGP latitude from one hemisphere to the other can be relied upon to represent definite polarity changes. Two of the possible polarity subintervals (12d and 12a) are identified using paleomagnetic data with low precision; a geomagnetic field excursion rather than a full polarity change may be the cause of polarity subintervals 9a, 8f, and 7g; and, finally, single polarity subintervals may have been split into apparent subinterval pairs by field excursions in the cases of subintervals 13c and 13b, 8e and 8d, 8b and 8a, 7f and 7e, and 7b and 7a. Polarity subintervals 12a and 9a are doubly dubious because of the conflicts in results of different computational procedures, as discussed above. If all these ambiguities are eliminated from consideration as true polarity changes, then the figure of 71 changes would be reduced to 51. This range of from 51 to 71 reversals compares with the figure of "at least 60" suggested by Dagley and others (1967) for the first examination of these data. Our figure of 51 is certain to be a too conservative result, if for no other

reason than the fact that definite polarity subintervals, such as the Kaena event and event 6a, are not represented in the sequence of high latitude VGP positions, and, indeed, known events such as the Mammoth are not represented at all. While it is therefore certain that the lava sequence has not recorded an absolutely complete polarity history, the record is unlikely to be substantially deficient, since the average interval between successive eruptions is only about 16,000 yrs. Major possible additions to the polarity history are summarized in table 6. Given the fact that volcanic extrusions may, over a short period, have very variable intermissions, we believe that we cannot propose any specific times for the additional events within the polarity epochs involved, but we can state with some certainty that evidence for at least 2 hitherto undetected polarity events is contained in the eastern Iceland sequence. One of these would be within polarity epoch 7, and the other in polarity epoch 13. As table 6 shows, 17 events are now predicted for epochs 5 through 13 by the most recent magnetic anomaly analyses. A maximum of only 11 have been detected for the same period in deep-sea sediments, while at least 16 (but possibly several more) have been apparently recorded by the eastern Iceland lavas. By combining the results of anomaly analyses and the data from this study (table 6) it appears that at least 20 events have actually occurred within epochs 5 to 13, inclusive. If the ambiguous paleomagnetic data, which were discussed earlier, are all assumed to represent true polarity changes, an upper figure of 30 events would be arrived at. Thus, including the known polarity history for the Gauss, Gilbert, and more recent epochs, a total of between 70 and 92 changes of polarity are indicated since t = 13.58 m.y. Alternatively stated, an average of

TABLE 6

Comparison of the number of polarity events in polarity epochs 5 to 13 according to three different recording systems

Polarity Epoch	Boundary Ages (m.y.)	Number of Polarity Events		
		Anomaly analysis*	Sediment cores**	This study***
5	5.18 – 5.94	1	1	0 (0)
6	5.94 – 6.59	1	1	1 (1)
7	6.59 – 7.30	2	3	7 (4)
8	7.30 – 8.71	3	2	6 (3)
9	8.71 – 10.21	4	0	2 (1)
10	10.21 – 11.47	2	1	2 (2)
11	11.47 – 12.09	1	1	1 (1)
12	12.09 – 12.88	2	2	4 (2)
13	12.88 – 13.58	1	0	3 (2)
	Total Events	17	11	26 (16)

* From analysis of Talwani, Windisch, and Langseth, (1971) and Blakely (1974).
** From either Theyer and Hammond (1974) or Opdyke, Burckle, and Todd, (1974). The number given represents the maximum number of events detected in either publication for the given polarity epoch.
*** See figures 6 and 10, and table 5. The number in brackets results if all possible ambiguities (such as polarity events identified from low precision data or polarity events representing possible polarity excursions) are removed from consideration.

between 145,000 and 190,000 yrs elapsed between each polarity change during the last 13.6 m.y. This is about half the average duration of periods of single polarity, suspected by some investigators, but approaches the 0.1 m.y. interval proposed by Harrison (1969) on purely statistical grounds. Knowing the rate of polarity reversals for parts of geological time has much significance, being relevant to such problems as an understanding of geomagnetic field origins (Cox, 1968), to the confidence limits that can be placed on estimates of the thickness of the sea-floor magnetic layer, from analyses of magnetic anomaly profiles (Harrison, 1976). Because our estimate of the average time between polarity changes is derived to a large extent from paleomagnetic data on basaltic lavas, it must be considered to have substantial validity, in comparison with data from deep-sea sedimentary cores, the paleomagnetic properties of which are dubious in terms of short period polarity changes because of bioturbation and other sources of signal distortion (Watkins, 1968) and because the data are usually derived from only one specimen per horizon. It will be instructive to see if the other relevant analytical methods, which employ deep sea sediments and marine magnetic anomalies (and reasonable assumptions of constant sedimentation rates, or sea-floor spreading rates, respectively, for limited periods) can ultimately facilitate not only confirmation but also dating of the fine structure we believe is recorded in the eastern Iceland lavas.

Deep Sea Drilling Project: paleomagnetic inclination distortion.—Efforts to core several hundred meters into the igneous and metamorphic basement of the sea floor during the current phase of the Deep Sea Dilling Project (which is called the International Phase of Ocean Drilling) have been generally successful. As summarized by Hall (1976) and several others in the August 1976 special issue of the *Journal of Geophysical Research,* one of the major problems paleomagnetic studies of the cores have apparently produced involves the mean inclination of remanent magnetism in the cores. More often than not, the inclination is shallower (and frequently much shallower) than would be expected from axial dipole considerations and more variable than reasonable geomagnetic secular variations would allow. Whether or not this is a surprising result is certainly debatable: Watkins (1973, 1975) has argued, for example, that the lack of sampling control inherent in drilling is likely to yield incoherent data, due to the highly localized tectonic effects that are conventionally avoided in outcrop and due to other effects such as rotation of large blocks on shallow magma chambers, a conclusion favored by James (1966) to explain discordant stable remanent magnetism of basaltic bodies in the caldera of Mt. Lassen, Calif. In any case, it is appropriate to examine the eastern Iceland paleomagnetic data in terms of shallow inclination possibilities the geomagnetic field could be expected to provide, in order to provide a sound statistical basis for any resort to geomagnetic field behavior, when attempting to explain the available and future paleomagnetic data from abyssal igneous cores. In figure 12

we present prelimary results of the consideration of this problem, in the form of a simple relevant function: ΔI is the amount in degrees by which the mean inclination of remanent magnetism in the entire section is less than the inclination that can be expected according to the axial dipole field in Iceland. This has been computed for both the eastern Iceland section and for the western Iceland study of Watkins, McDougall, and Kristjansson (1977). The similar distributions of ΔI provide much confidence in the validity of the data as a whole. ΔI is expressed in figure 12 as a percentage of the entire data set, exclusive of overlaps. Since the lava production rate is generally linear (fig. 11) the relationship indicated in figure 12 can be used as a good approximation of the percentage probability that a given value of ΔI can be expected to be encountered during random drilling of undisturbed abyssal igneous rock of age between 13 and 2 m.y. While models such as those involv-

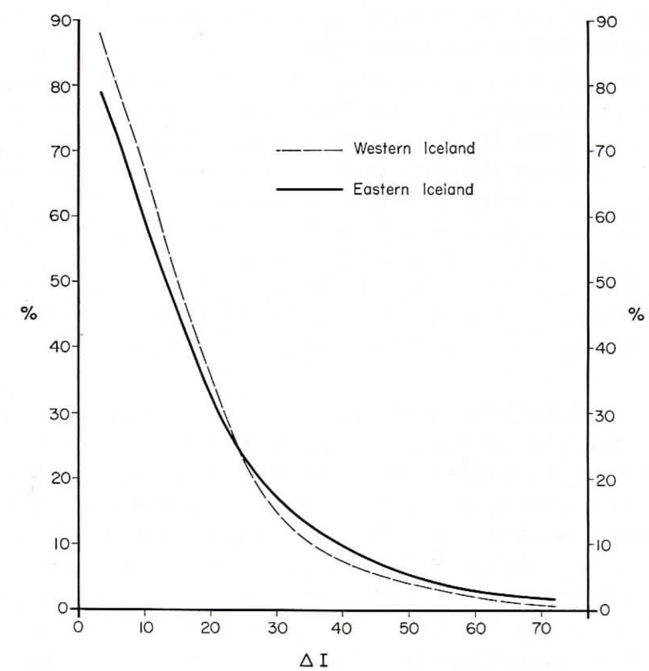

Fig. 12. Distribution of the difference (ΔI) in degrees between the paleomagnetic inclination observed in the eastern Iceland sequence and that expected for an axial dipole, expressed as a percentage of the total number of observations. ΔI is negative; that is, the figures between 0° and 70° are the amount by which the data are *less* than the axial dipole inclination. The curve is cumulative, to be used as follows: a ΔI of 50° or more occurs only 5 percent of the time, a ΔI of 30° occurs only 18 percent of the time, and a ΔI of 20° occurs only 33 percent of the time, et cetera. The data for a sequence of 351 lavas ranging from 7 to 2 m.y. in western Iceland (McDougall and others, 1977; Watkins, McDougall, and Kristjansson, 1977) are added to the diagram, which is used to show the low probability of obtaining high ΔI values in abyssal igneous cores collected during the Deep Sea Drilling Project, unless causes other than geomagnetic field behavior are involved in causing the high ΔI.

ing geomagnetic secular variation (McElhinny and Merrill, 1975) can also lead to similar probability estimates and are therefore of value, they are nevertheless not based primarily on data, especially a set with such few time gaps as that used to compile figure 12. From the curves, one can deduce that, for example, a ΔI of 40° occurred less than 10 percent of the time; that a ΔI of 30° occurred less than 20 percent of the time; that a ΔI of 20° occurred less than 40 percent of the time; and so on. When the high latitudes involved are considered, it would appear that frequent large ΔI observations in abyssal basalt core will be difficult to accept as indications of geomagnetic field behavior, and so other causes should be favored to explain such results. It follows that any use of remanent magnetism inclination differences between segments of abyssal igneous core to infer minimum time differences between the respective segments should be highly qualified. Harrison and Watkins (1976) have made further statistical analyses of the data in the above context, which allow our conclusions to be expanded with some confidence to abyssal drill sites at lower latitudes.

Possible undetected geological complexities.—A major danger in the interpretation of magnetostratigraphic data in volcanic piles is the degree of freedom available, by the possible forcing of an agreement between the predicted polarity time scale and any measured magnetostratigraphic sequence, merely by varying the extrusion rate, or by invoking repetitions of section through hypothetical faulting. Given such degrees of freedom, any polarity scale can be fitted to any set of polarity data. The availability of three sets of K:Ar results in well-separated parts of the eastern Iceland sequence fortunately provides strong and critical restrictions to any interpretation, but several possible problems are still evident, as discussed below.

The K:Ar data show unambiguously that sections E, F, and J represent the time of "Anomaly 5" or epoch 9 (fig. 6) while the base of section Q is epoch 6 (fig. 5). This forces the polarity variation in sections K and L to represent epoch 8, so that by elimination, sections M, N, O, and P must represent epoch 7 (fig. 6). While the measured polarities are consistent with this possibility, somewhat larger fractions of reversed polarity and more polarity changes are evident than might be reasonably expected to exist within epoch 7 (table 5). Therefore one might surmise that the correlation between sections M and N and the amount of section omitted between sections O and P might be in error. If, for example, section P overlapped substantially with section M, then the volcanic episode V2 (fig. 11) which is *apparently* about 4 times as productive as V1 and V3 might in fact be an artifact of errors in mapping. Similarly, the apparently long normal polarity sequence contained between sections T, U, and V might conceivably be the result of repetition of section by undetectable faults in the sections, so that within the volcanic episode V3 less variability of extrusion rate would be evident.

At the time of writing, we cannot be absolutely certain if our mapping of the head of Geithellnadalur and Nordurdalur (fig. 3B, C) completely eliminates the possible ambiguities discussed above, although sections J through O (fig. 3B) have all possible appearances of being clearly and accurately correlated. We, therefore, place some limitation on the reliability of our interpretations of the magnetostratigraphy in sections S to V but place confidence on the stratigraphy of the rest of the sequence. The strong agreement between the independently defined polarity time scale and the magnetostratigraphy of the eastern Iceland sequence is gratifying and adds confidence to prospects for extending the mappable units so defined laterally to other parts of Iceland.

Magnetic properties and zeolitization.—The very large volume of paleomagnetic data together with the zeolite mapping facilitate examination of the possibility that the intensity of magnetization (J) is affected by low temperature metamorphism, as suspected by several authors (Akimoto and Kushiro, 1960; Watkins, 1967; and others). This is relevant to such problems as the decrease in magnetic anomaly amplitude with distance from mid-oceanic ridge and more directly to the proposed contrast in magma sources between the younger and older parts of the entire eastern Iceland section, because of a corresponding contrast in J, as discussed earlier (Wilson and McElhinny, 1974).

Figure 13 shows the variation of mean J as a function of zeolite zone, for both the natural remanent magnetism (NRM) and for the remanent magnetism following treatment in peak alternating magnetic fields of 100 or 125 oersteds. A decrease of J with increasing metamorphic grade is apparent. Variation of J with titanomagnetite oxidation state and with age as the result of simple spontaneous demagnetization (Banerjee, 1971) is likely to mask to some extent exact determinations of the effect of hydrothermal overprinting, but the results shown in figure 13 provide an alternative interpretation to that of Wilson and McElhinny (1974). The mean J values for each section, which are summarized in their figure 6, can be readily divided into two fields: the ten sections H, B, and J through Q with lower intensities, and the remaining 11 sections with higher intensities. When it is seen that 9 of the 10 sections in the former group are confined to the higher grade mesolite or laumontite zones (fig. 8), and that 9 of the 11 sections in the latter group are overwhelmingly in the lower grade analcite or chabazite zones, then it would appear that low temperature metamorphism is by far the dominant factor in the variation of intensity of magnetization in the lavas, and for the age range involved any age effect is therefore secondary. Piper (1973, p. 176) did not detect any change in low field magnetic susceptibility of basalt with distance from the present volcanic zone in Ireland, and so this would argue for differential effects of low temperature metamorphism on remanent and induced intensity of magnetization.

Geomagnetic field models.—Our final analysis of the data involves the problem of geomagnetic secular variation. McElhinny and Merrill

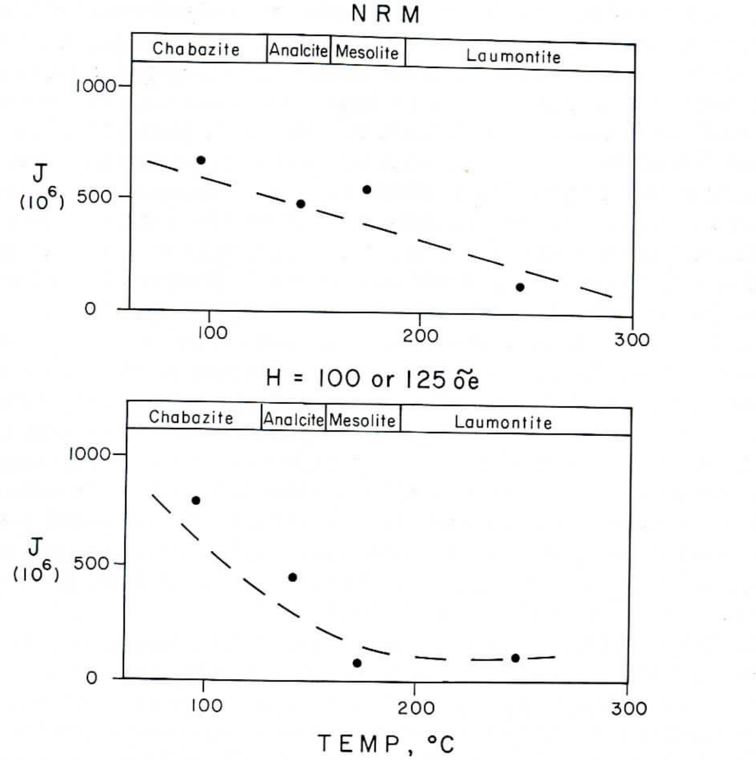

Fig. 13. Mean intensity of magnetization (J) in emu gm^{-1} as a function of zeolite zones, for (upper) natural remanent magnetism and (lower) remanent magnetism after demagnetization in alternating magnetic fields of 100 or 125 oersteds. The temperature profile represented by the zeolite zones (summary by Ade-Hall and others, 1972) is added to each diagram. The reason two different demagnetization fields are involved is that no single field was applied to all specimens.

(1975) recently provided a convenient summary of the various geomagnetic field models and the methods and limitations of their testing by paleomagnetic data. All these models involve analysis of the variation of S_F (which is the angular standard deviation of VGP from data sets at a given site) as a function of site latitude. The Upper Cenozoic geomagnetic field is thought to be best represented as a geocentric dipole (which wobbles between 9° and 11° around the spin axis) upon which is superimposed a non-dipole field which may have separate standing and drifting components. The resultant of the dipole and non-dipole components is, for all acceptable models as well as the present field, a marked latitudinal increase in S_F. A new model, which McElhinny and Merrill (1975) introduced, stresses the role of standing and drifting non-dipole fields, which occasionally combine to become a large fraction of the total field, yielding very high S_F values at high latitudes. As they show, this concept, if valid, would also require S_F to fluctuate substantially in a given site, over any

extended period. In some contrast, Cox (1975) has recently proposed the existence of long-term secular variation foci for restricted latitudinal but complete longitudinal ranges, so that time-averaged distortions of inclination away from that of a centered dipole would occur, with results similar to that of Wilson's (1971) offset dipole model, mentioned earlier. Watkins and Richardson (1975) have also proposed means to match the similar inclination distortion required by all Brunhes Epoch ($t = 0.69$ to 0 m.y.) paleomagnetic data but instead employ a system of minor dipoles on the spin axis at the core-mantle boundary, superimposed on a major dipole offset to the north. In all paleomagnetic testing of geomagnetic field models a major obstacle is the requirement of an adequate time range in the data. For example, if a very rapid extrusion rate has occurred, then an insufficient sampling of geomagnetic variations is likely to result in any paleomagnetic survey. Aziz-Ur-Rahman and McDougall (1973) believe that very small S_F values in their survey of Norfolk Island volcanics is the result of this problem, with perhaps only tens or hundreds of years being the average time between eruptions. The eastern Iceland sequence does not present this difficulty, with an average of about 16,000 yrs between eruptions and long periods of extraordinarily linear accumulation rates (fig. 11). In principle, of course, should there exist periods when large segments of the section accumulated rapidly, then low S_F values would be expected, assuming that the geomagnetic secular variation did not vary greatly. It is stressed that according to Doell and Cox (1963) six or even more separate cores per lava are ideally required for computation of S_F, since the within-lava precision parameter of the remanent magnetism directions (K_W) is involved in computation of S_F, and precise estimation of K_W cannot be obtained with only two cores per lava. On the other hand, Ellwood and others (1973) have shown using paleomagnetic data from lava flows collected in the Azores that between two and four cores per lava can be adequate for the definition of S_F, within a 95 percent confidence parameter. While the absolute value of S_F may be affected by the use of only two cores per lava, the between-group variation should be real. We have computed S_F for successive groups of twenty lavas and for successive groups of an equal thickness of 200 m. The results are illustrated in figure 14, which includes plots of several other data: mean declination (D) and inclination (I) of remanent magnetism for each data group, and the within-lava precision parameter (K_W) for each group. We have computed the same series of variables using the data based on a single demagnetizing field treatment (app II) and find no significant difference in the results derived from minimum scatter computation, as discussed earlier.

For all four parameters (D, I, S_F, and K_W) the results are shown for situations where all data are used (solid circles), and where data from lavas with VGP latitudes less than 45° are rejected (open circles). The latter use of a VGP latitude cutoff of about 45° is a convention employed widely in paleomagnetic secular variation studies, in order to discriminate

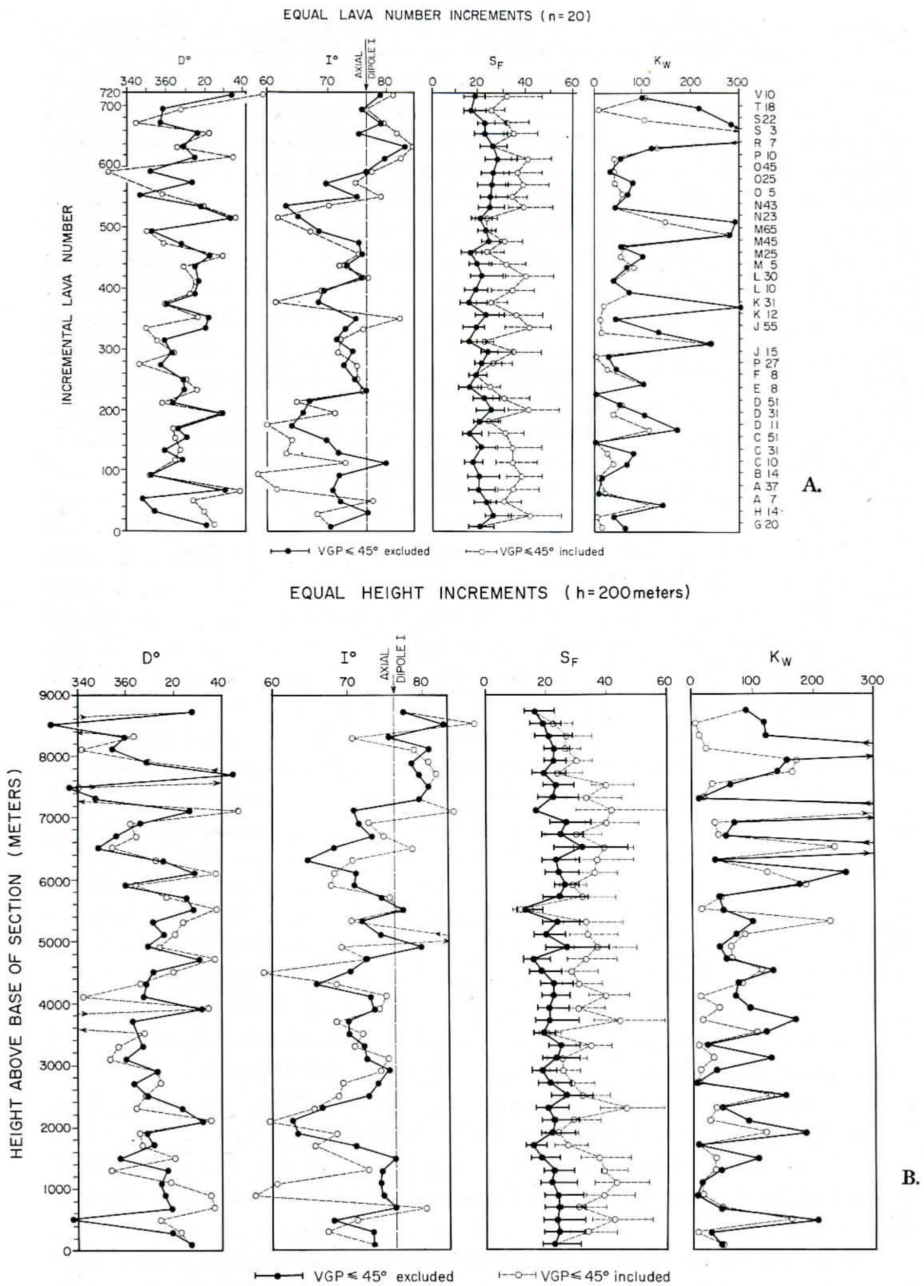

Fig. 14. Mean paleomagnetic results for (A) increments of 20 successive lavas and (B) increments of 200 m thickness, for the east Iceland sequence. D = declination in degrees east of geographic north, I = inclination in degrees below the horizontal (inclination for axial dipole field indicated), S_F = angular standard deviation of virtual geomagnetic poles in degrees: kw = within-lava precision parameter (see Ellwood, and others, 1973, for summary of methods used to compute S_F and kw). Solid circles are results from data sets that exclude lavas with virtual geomagnetic poles <45°. At right: lava number at boundary of groups. All reversed polarity data are transposed to the northern hemisphere for those computations.

against the use of data which may result from anomalous geomagnetic field behavior, not reflecting normal axial dipole and non-dipole field results. Such would be the case, for example, during the period of transition between opposite polarities. McElhinny and Merrill (1975) and Watkins, McDougall, and Kristjansson (1977) have discussed the significance of the approx 45° VGP latitude data cutoff: the convention may eliminate prospects for discovery of real long-term secular variation maxima.

Inspection of figure 14 shows the following: mean D is generally consistent with a "right handed" (or easterly) declination as pointed out by Wilson (1970) for much other Upper Cenozoic data. There continues to be no satisfactory explanation of this fact. As stressed by Wilson and McElhinny (1974) the mean inclination in the eastern Iceland sections changes from less than, to greater than, the axial dipole value (fig. 14). As discussed earlier in detail, this translates into a change from "far side" to "near side" VGP position. Particularly since Watkins, McDougall, and Kristjansson (1977) have shown that the same behavior does *not* occur in lava sequences of the same age in western Iceland, and since no acceptable tectonic explanation for this regional difference is even remotely possible, the cause of the steepening inclination in sections Q through V remains enigmatic. As Watkins, McDougall, and Kristjansson (1977) point out, explanations appear to require a mechanism that diminishes the vertical component or increases the horizontal component of stable remanent magnetism upon burial (since sections Q through V are less zeolitized than the older sections), and no such anisotropic overprinting system is known. In contrast with the earlier interpretation of the inclination change in the eastern Iceland sections (which utilized a hypothetical hiatus in volcanic activity during which the axial dipole migrated from northern to very little offset), the change is sudden, with steep inclinations being characteristic of section P and those that are younger. It is not a function of the within-lava scatter of directions being systematically related to I as figure 14 shows.

S_F is remarkably constant throughout the eastern Iceland sequence and is at that value (≈20°) which is characteristic of the latitudes involved for several geomagnetic field models. This consistency of S_F has three main implications:

1. There is no period of rapid lava extrusion indicated, since high S_F values are not found anywhere in the sequence.

2. There is no contrast in S_F between the older sections characterized by "far-sided" VGP's and the younger sections with "near sided" VGP's. Thus whatever the cause of the change in paleomagnetic inclination, it is not associated with any change whatsoever in short-term geomagnetic secular variation rate and by further inference, ratio of non-dipole to dipole field activity. If an anisotropic effect (such as an increase in the horizontal component of remanent magnetism in association with zeolitization) were the cause of the inclination contrast, then a change in S_F would also be

expected, because the between-lava variation of remanent magnetism directions would decrease, but such is not the case. The cause of the inclination change to higher values in the youngest part of the section remains a problem.

3. The consistency of S_F is evidence against any substantial fluctuation in ratio of standing to drifting non-dipole component or in the ratio of non-dipole to main dipole components during the entire 11 m.y. period represented. Thus Cox's (1975) proposed model of a quasi-permanent component in the non-dipole field in mid- to high-latitudes which reduces the geomagnetic inclination is more consistent with the observed S_F values, at least between t = 13.0 and 6.6 m.y. The same conclusions are reached if the data groups are doubled in size, or if the grouping is based on equal thickness of lavas (fig. 14B), which was attempted in order to detect possible effects of extrusive rate variation. To what extent the data rejection system (exclusion of data from lavas with VGP latitudes $<45°$) has contributed to the consistency of S_F in figure 14 may be critical: might a true variation in S_F be conceivably masked by the application of this conventional analytical method? Figure 14 includes S_F values computed without any data rejection (open circles). The difference between the results of these two computational methods (ΔS_F) is summarized in figure 15 for the actual height and the height compiled from the lava thicknesses normalized for fixed distances from the source (fig. 10). Close inspection of figure 6 and comparison with figure 15 reveal clearly that ΔS_F fluctuations are to a large extent a function of the number of polarity changes recorded in the sequence, and the fluctuations of ΔS_F cannot therefore be unambiguously interpreted to represent any long term fluctuations in the magnitude of geomagnetic secular variation. It is interesting to realize that if the collection were from a series of lavas without the unusually detailed stratigraphic control and regular extrusion rates of the eastern Iceland section, then it would be highly probable that directions transitional between opposite polarities would be sampled without being certainly identified as such, since they cannot be distinguished from excursions in isolated examples. Irving and Pullaiah (1976) have recently noticed that paleosecular variation throughout the Phanerozoic appears to be greater during intervals when the polarity reversal frequency is higher, from which they conclude that the balance of non-dipole and dipole field controls the rate of polarity reversals. While this may be true, it would appear that apparently higher paleosecular variation of the geomagnetic field would inevitably result from paleomagnetic surveys that cannot identify and therefore reject data from polarity reversal transitions. It follows that the relationship that Irving and Pullaiah (1976) have observed between paleosecular variation and polarity reversal frequency could to some extent at least be a sampling artifact or deficiency, rather a cause and effect relationship. The problem, of course, is to some extent alleviated by the application of the rejected criterion. It is clear that the conventional computational systems may to some

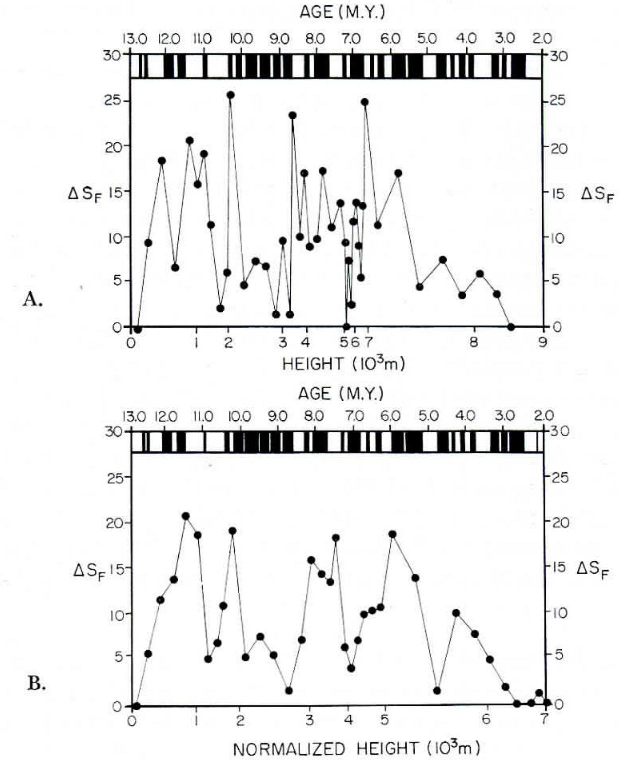

Fig. 15. ΔS_F as a function of age for equal height increments for (upper) the east Iceland section and (lower) the east Iceland section following normalizing of each lava thickness for downdip variation, to that expected at the top of the analcite zone (see figs. 8 through 10 for further explanation). ΔS_F is the difference between the two S_F curves in figure 14 (lower); that is, the amount by which S_F increases when conventional exclusion of data from lavas with virtual geomagnetic pole latitudes $<45°$ is not followed. The diagram shows that secular variation of the geomagnetic field apparently fluctuates in a possibly systematic way, but the inclusion of directions transitional between opposite polarities may be the cause of the observation.

extent preclude the emergence of information about long term secular variation fluctuations. Unless a sequence of paleomagnetic data can be obtained from a similar sequence of lavas in lower latitudes, no definitive test can be made of secular variation models (McElhinny and Merrill, 1975) using the data. Variation of the "goodness of fit" of the data to Fisherian distribution (Fisher, 1953) can in principle be used to estimate variations of non-dipole to dipole fields at a single site, but results for such an analysis of the data have proved inconclusive.

The unambiguous chronology of the section provides the opportunity to attempt detection of apparent polar wander between t = 13 and 2 m.y. Compiling a curve from the mean VGP for each section given in table 1 shows that no discernable systematic polar wander path is evident: a large number of the sections have overlapping 95 percent confidence ovals.

The correlation of the sequence to the polarity time scale also provides the opportunity to search for any differences between the geomagnetic field during reversed and normal polarity epochs. Table 7 shows mean VGP for the Gauss and Gilbert epochs and for polarity epochs 5 through 13, when data for the opposite polarity events and excursions within each epoch have been removed. Reversed polarity epochs have VGP's between longitudes 27° and 126° east, whereas normal polarity epoch VGP's are between 120° and 323° east. According to Cox (1975) this could mean that during the periods involved the non-dipole field has not reversed completely with the dipole field, but the differences in VGP position are partially obscured by the magnitude of the secular variation or confidence oval, so that this interpretation is not made with confidence. As shown in table 7, the mean pole position for all reversed polarity and all normal polarity lavas are quite similar. The simplest, if not the only interpretation of this would be that the non-dipole field has well and truly averaged out over the 11 m.y. period. Therefore, a quasi-permanent non-dipole field, such as that envisaged by Cox (1975) for Iceland would be, if valid, of shorter term than 10 m.y.

CONCLUSIONS

An eastern Iceland volcanic sequence over 9000 m thick with a total of 709 separate lavas extends from about t = 13.5 to about 2.0 m.y. and possesses a polarity variation which together with four sets of K:Ar data

TABLE 7

Mean virtual geomagnetic poles in eastern Iceland for the Gauss and Gilbert epochs, and polarity epochs 5 through 13

Polarity Epoch	Polarity	No.	Mean virtual geomagnetic pole: Longitude (°E)	Latitude (°N)	α_{95}°
Gauss	N	21	323	87	8.7
Gilbert	R	31	35	81	8.4
5	N	5	250	79	21.7
6	R	12	27	74	13.5
7	N	122	120	81	3.9
8	R	53	96	80	5.7
9	N	82	132	85	4.5
10	R	44	126	75	7.5
11	N	22	170	82	8.6
12	R	41	74	83	6.4
13	N	33	144	84	8.6
All R lavas	R	205	106	80	2.0
All N lavas	N	352	133	83	1.4

For age range of epochs see table 5. Polarity N = normal, R = reversed. No. = number of separate lavas in epoch (excludes data for polarity events within epoch; data for lavas with VGP latitudes less than 45°; and data for lavas where R, which is resultant vector using unit vector for each of the two cores, is less than 1.6).

has facilitated unambiguous correlation to the established and predicted polarity time scale. Stratigraphic terms have been suggested for the resulting magnetostratigraphic sequence and can in principle form a series of mappable units that can be used to construct a geological map of much of the island.

Volcanism was virtually continuous. When the lava thicknesses are normalized to a standard datum level, equivalent to the top of the analcite zeolite zone, the sequence is computed to span about 7000 m. The average rate of production is then 640 m per m.y., or one lava extruded on average every 16,000 yrs. The production rate was constant for up to 6 m.y., but three different episodes can be identified. The major increase in volcanic production rate occurred at about t = 7.3 m.y., shortly before an independently proposed increase in volcanism on the Reykjanes Ridge. This can be interpreted to represent mantle plume activity initiated at 7.3 m.y. and a subsequent southward migration.

Geomagnetic secular variation, computed using conventional methods, was remarkably constant for the 11 m.y. period, so that the ratio of non-dipole to axial dipole components does not appear to have been variable, but the exclusion of data from lavas with lower latitude VGP's prohibits complete confidence in this interpretation. A previously detected change of mean inclination of the geomagnetic field from less than to steeper than the axial dipole field at about t = 6.6 m.y. cannot be explained but can be disassociated from any change in short-term geomagnetic secular variation.

During the 11 m.y. period, the average time separating polarity reversals was between 145,000 and 190,000 yrs. The section provides a more finely detailed polarity history than can be derived for much of the period from analyses of marine magnetic anomalies and sedimentary cores, but possible short-term variations in volcanic extrusion rates prevent the obtaining of exact dates for the fine structure by extrapolation between major polarity boundaries. Nevertheless at least two hitherto unrecognized polarity events have been identified in the sequence. Verification in other sequences of Icelandic lavas is likely to materialize, as magnetostratigraphic mapping of the island continues.

ACKNOWLEDGMENTS

The paleomagnetic survey was carried out under the direction of Dr. R. L. Wilson in 1964 and 1965. Persons participating included P. Dagley, S. Edwards, N. Watkins. S. Haggerty, P. Smith, L. Kristjansson, and Th. Sigurgeirsson. The geological mapping was carried out by G. P. L. Walker. Support was provided by the Department of Industrial and Scientific Research and the Icelandic Research Council. The paleomagnetic data were obtained at the subdepartment of geophysics of the University of Liverpool and made available by the Science Institute of the University of Iceland. Support for further computation was provided by the University of Rhode Island, where much invaluable assistance was provided by

Miss Linda Steere. The manuscript was typed by Mrs. Susan Keany. The drafting and photography of illustrations and tables were carried out by Mrs. Rosemarie Raymond and Mr. Dennis Cassidy of Florida State University. Early versions of this paper benefitted from review by Dr. Leo Kristjansson (University of Iceland) and by Dr. R. L. Wilson (University of Liverpool). The authors are, however, solely responsible for the contents.

Appendix I

Stratigraphic and paleomagnetic details for each section

For each section (A through V in figs 2, 3, 6, 7, 8, 10, and 11, and tables 1 and 5) the following are given:

Upper diagram. Detailed stratigraphic section, redrawn from the original field diagram of GPLW. Heights of each unit are given in meters and feet above sea level. Number is the original number of each lava. A suffix denotes a flow unit; thus 16A is a flow unit of a compound lava of which the lowest unit is 16. R.B. = red bed. For exact locations, see figure 3.

Lower left (table). Mean paleomagnetic data for each lava flow and flow unit. No. = the lava number; N = number of separate cores; D and I = mean declination and inclination of remanent magnetism, in degrees east, and with respect to the horizontal (− = upward; no sign = downward), respectively. R = resultant vector, applying unit vector per specimen. θ' and Φ' = latitude and longitude of virtual geomagnetic pole, in degrees north (no sign) or south (negative), and in degrees east of Greenwich, respectively. All data result from minimum scatter computation (see text for explanation). When only one specimen was available, N and R columns are blank.

Lower right diagram. Polarity log. The latitude of the virtual geomagnetic pole is plotted for the lavas arranged in stratigraphic sequence. Arrows and roman numerals indicate the top and bottom lava of the segment of each section used to compile the complete sequence (see correlation lines in fig. 3). The roman numerals increase with decreasing age, odd numbers of one section indicating the lava that overlies the even number of the immediately older section. For compound lavas the data for all the flow units are averaged to produce a single data point, unless a polarity change occurs. The polarity log on the right is constructed using the simple interpretation of black = normal polarity (VGP in northern hemisphere), clear = reversed (VGP in southern hemisphere). Numbers and letters to the right of the polarity log refer to the polarity epoch (or interval) number, and polarity event (or subinterval) respectively, as finally compiled in table 5. Only the data for the events are identified. For sections R to U, the established names are used for the polarity events. Note that the polarity log contains *all* data, and is not directly comparable to the final compiled log for the entire sequence (in figs. 6 and 10), where rejection criteria (see text) have been applied.

PROFILE G

GERPIR

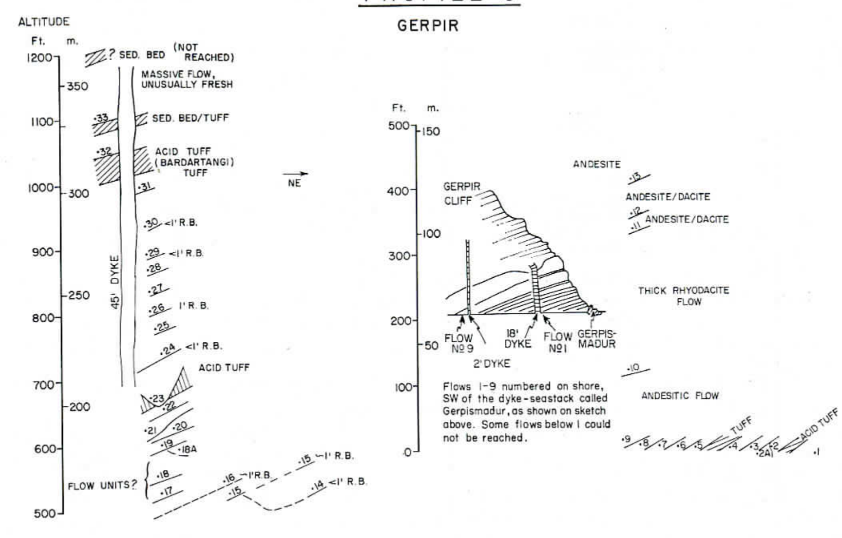

G GERPIR

NO	N	D	I	R	θ'	φ'
EG 33-	4	68.8	74.7	3.9810	60.3	50.0
EG 32-	3	58.5	58.8	2.9841	48.3	83.7
EG 31-		303.1	-72.8		-40.5	200.8
EG 30-	2	355.1	69.1	1.9992	77.3	179.0
EG 29-	2	217.8	-6.6	0.5976	-22.7	303.8
EG 28-	2	166.0	-3.7	1.6767	-26.0	1.0
EG 27-	2	165.0	-64.7	1.9916	-69.9	16.6
EG 26-	2	180.3	-80.3	1.9998	-83.9	166.2
EG 25-	2	354.4	-33.4	1.6760	6.6	170.7
EG 24-	2	352.9	-77.2	1.9991	-40.7	169.2
EG 23-	2	64.0	-80.3	1.9154	-53.0	136.6
EG 22-	2	54.8	58.8	1.9888	49.9	87.3
EG 21-	2	272.3	89.0	1.9982	65.0	340.9
EG 20-	2	32.9	68.1	1.9943	68.3	98.7
EG 19-	2	126.6	75.6	1.5669	43.7	15.9
EG 18A	2	24.1	70.6	1.9820	74.4	104.4
EG 18-	2	62.5	57.3	1.9759	45.3	81.1
EG 17-	2	50.2	40.8	1.9885	37.4	102.8
EG 16-	2	40.2	68.8	1.9986	66.1	88.3
EG 15-		14.7	62.2		67.0	137.3
EG 14-	2	341.7	54.0	1.9981	57.6	194.2
EG 13-	2	7.1	77.1	1.9981	87.0	65.8
EG 12-	2	351.5	55.4	1.9981	60.5	179.4
EG 11-	2	57.1	71.6	1.9926	61.9	65.6
EG 10-	2	259.4	77.1	1.9993	52.4	303.4
EG 9-	3	52.3	63.4	2.9984	55.4	84.9
EG 8-	2	54.6	75.6	1.9995	66.6	55.2
EG 7-	2	36.9	76.0	1.9996	74.1	64.0
EG 6-	2	35.6	73.6	2.0000	72.8	77.4
EG 5-	2	272.8	84.6	1.9385	63.4	320.7
EG 4-	2	45.2	60.5	1.9974	55.4	95.8
EG 3-	2	24.6	68.8	1.9953	72.2	109.2
EG 2A	2	46.5	66.8	1.9983	61.3	85.6
EG 2-	2	41.2	67.8	1.9885	64.6	89.4
EG 1-	2	342.8	70.8	1.9996	77.0	214.2

G GERPIR

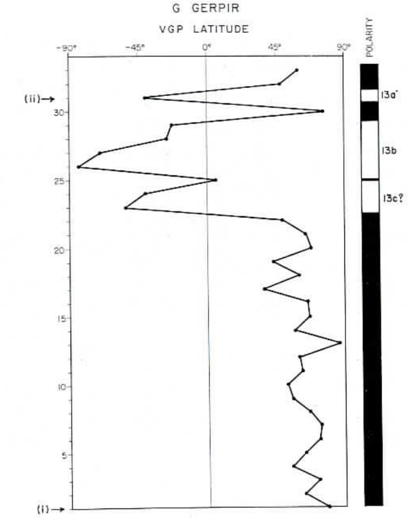

PROFILE H

VAÐLAVÍK

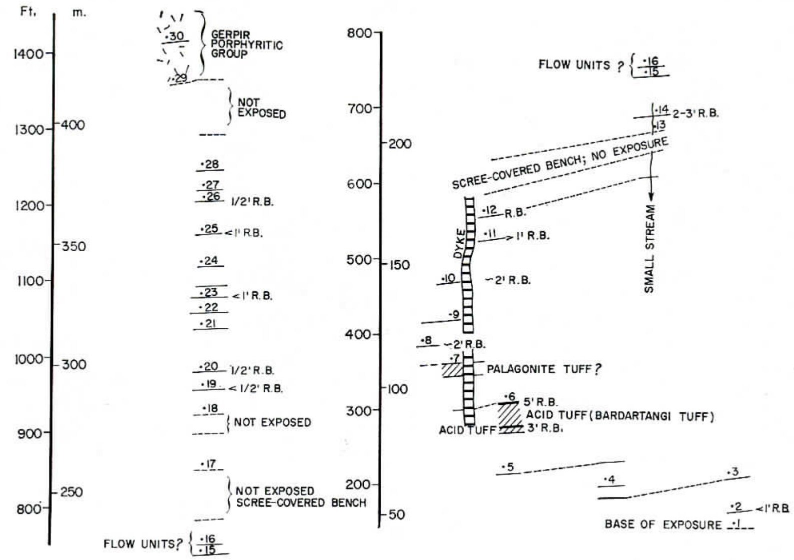

H VAÐLAVÍK

NO	N	D	I	R	θ'	φ'
EH 30-	2	150.8	-79.9	1.9819	-77.8	114.3
EH 29-	2	112.0	-83.8	1.9990	-66.8	135.5
EH 28-	2	50.1	48.4	1.6282	42.9	99.5
EH 27-	2	184.0	-84.3	1.9972	-76.2	168.6
EH 26-	2	127.5	-37.0	1.9362	-34.1	49.0
EH 25-	2	74.2	-26.8	1.6758	-6.3	95.6
EH 24-	2	334.4	62.3	1.9953	64.2	211.5
EH 23-	2	344.3	48.0	1.9995	52.7	188.3
EH 22-	2	340.6	48.7	1.9998	52.6	193.7
EH 21-	2	300.8	64.6	2.0000	53.7	254.0
EH 20-	2	94.7	61.6	1.9935	36.2	50.4
EH 19-	2	325.7	71.9	1.9992	71.8	245.2
EH 18-	2	324.7	72.4	1.9980	71.9	248.3
EH 17-	2	350.1	73.5	1.9995	82.7	209.4
EH 16-	2	83.5	63.3	1.9999	42.3	57.7
EH 15-	2	81.7	65.1	1.9899	44.8	57.2
EH 14-	2	158.3	65.9	1.9962	24.5	1.1
EH 13-		47.2	34.4		34.4	108.1
EH 12-	2	48.1	65.4	1.9989	59.2	86.3
EH 11-	2	65.2	-11.0	1.9682	5.1	100.3
EH 10-	2	9.1	63.5	1.9980	69.4	146.9
EH 9-	2	331.3	63.2	1.9983	64.4	217.3
EH 8-	2	263.8	70.4	1.9948	45.4	290.3
EH 7-	2	332.2	66.1	1.9921	67.9	220.6
EH 6-	2	69.3	80.6	1.9913	65.2	29.6
EH 5-	2	280.7	-79.5	1.9828	-55.4	202.2
EH 4-	2	309.0	-42.1	1.6276	-7.5	210.9
EH 3-	2	308.6	-32.8	1.4975	-1.5	213.4
EH 2-	2	90.2	-74.9	1.9999	-53.0	113.4

H VAÐLAVÍK

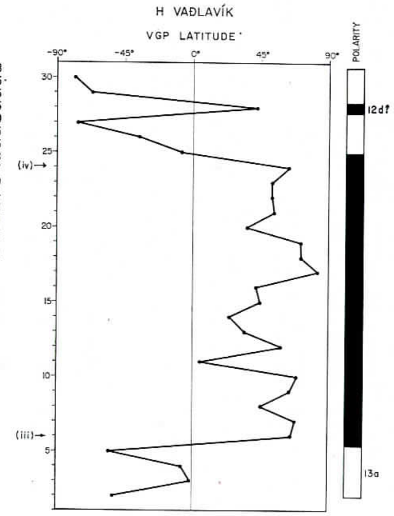

PROFILE A

HUNDSVÍK

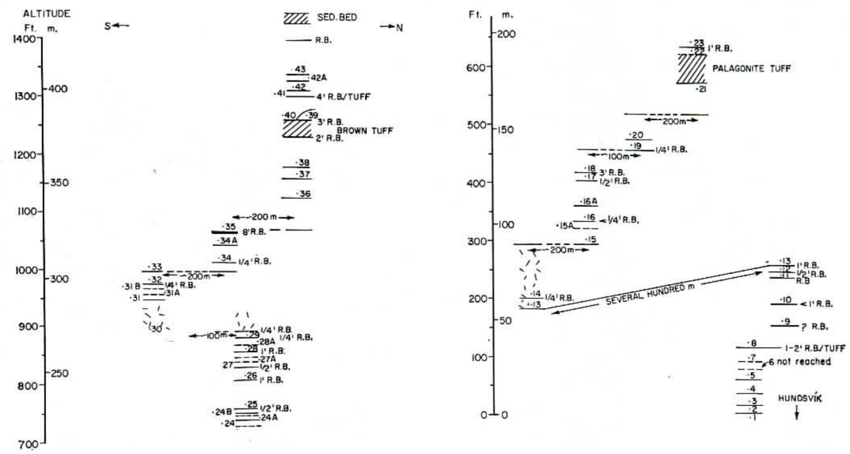

A HUNDSVÍK

NO	N	D	I	R	θ'	φ'
EA 43-	3	149.6	-50.5	2.9727	-51.4	30.1
EA 42A	2	151.7	-54.5	1.9990	-55.5	29.5
EA 42-	2	179.6	-13.5	1.9554	-31.7	346.8
EA 41A	2	188.2	-55.1	1.9951	-60.1	332.8
EA 40-	2	324.6	68.6	1.9808	67.7	237.0
EA 38-	2	99.1	71.5	1.0366	45.8	38.2
EA 37-	2	11.5	25.4	1.9996	37.6	152.2
EA 35-	2	310.0	3.6	1.9908	17.4	219.6
EA 34A	2	250.0	-40.6	1.9998	-29.3	264.1
EA 34-	2	247.5	-25.9	1.9999	-21.8	271.1
EA 33-	3	263.7	-54.8	2.9027	-34.2	245.0
EA 32-	2	246.2	-20.6	1.9999	-19.5	273.7
EA 31B	2	250.8	-19.1	1.8717	-16.9	269.7
EA 31A	2	113.5	-84.8	1.9859	-67.3	141.2
EA 30A	2	46.3	21.0	1.9998	27.2	113.3
EA 29-	2	33.0	56.9	2.0000	56.3	115.1
EA 28A	2	203.1	-71.6	1.9921	-75.8	283.6
EA 28-	2	225.2	-63.7	1.9863	-58.6	273.0
EA 27A	2	307.2	-78.1	1.9943	-47.4	193.5
EA 27-	2	199.1	-76.9	1.9943	-82.0	247.7
EA 26-	2	239.9	-80.3	1.9998	-67.9	214.5
EA 25-	2	191.7	-65.5	1.9993	-71.5	320.8
EA 24B	2	205.4	-73.6	1.9966	-77.1	269.8
EA 24-	2	210.8	-31.9	1.9988	-38.0	307.9
EA 23-	2	215.3	-55.0	1.9992	-53.8	293.6
EA 22-	2	208.6	-47.7	1.9994	-49.5	306.0
EA 21-	2	31.4	-64.2	1.9888	-23.7	142.9
EA 20-	2	136.8	-83.4	1.9993	-72.3	135.7
EA 19-	2	131.5	-73.4	1.9995	-67.3	84.4
EA 18-	2	264.2	-78.5	1.9999	-58.9	212.8
EA 17-	2	312.5	-74.7	1.9952	-41.2	194.4
EA 16A	2	287.9	-86.3	1.9406	-62.0	181.4
EA 16-	2	161.4	-82.2	1.9959	-78.6	140.8
EA 15A	2	164.8	-82.6	1.9921	-78.5	147.1
EA 15-	2	281.0	-67.4	1.9986	-40.2	221.6
EA 14-	3	245.2	-76.6	2.9915	-63.5	227.3
EA 13-	3	158.1	-83.0	2.9921	-76.9	143.2
EA 12-	2	234.4	-85.0	1.9983	-69.3	189.7
EA 11-	2	228.5	-75.6	1.9996	-69.1	239.8
EA 10-	2	184.5	-61.6	1.9811	-67.5	337.6
EA 9-	2	186.5	-53.3	1.9998	-58.5	335.9
EA 8-	2	307.2	-71.2	1.9913	-37.3	200.6
EA 7-	2	325.6	7.6	1.3348	24.0	204.3
EA 5-	2	257.9	64.2	1.9997	36.2	288.8
EA 4-	2	336.3	65.7	1.9992	68.6	214.1
EA 3-	3	333.8	66.8	2.9939	69.1	220.1
EA 2-	2	336.7	69.4	1.9999	73.2	221.7
EA 1-	2	224.3	33.9	1.1650	0.2	304.8

A HUNDSVÍK

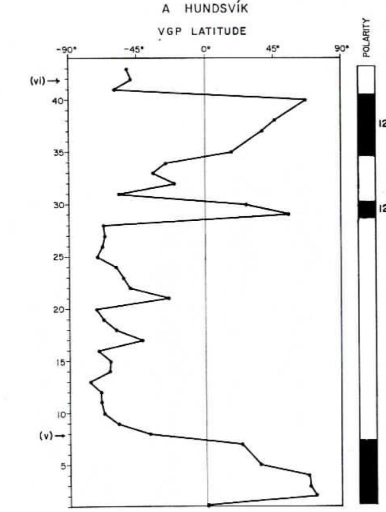

PROFILE B

NESKAUPSTAÐUR

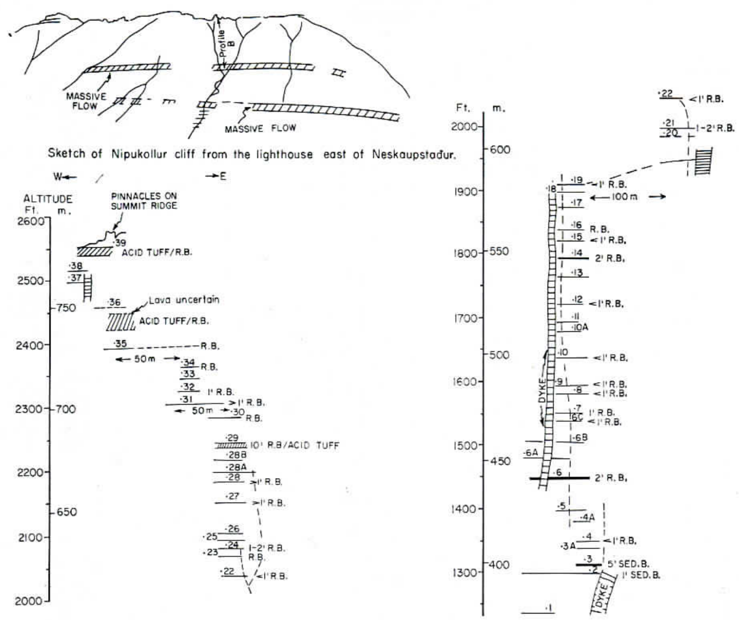

B NESKAUPSTAÐUR

NO	N	D	I	R	θ'	φ'
EB 39-	2	185.5	-77.5	1.9996	-87.5	230.3
EB 38-	2	303.1	-74.0	1.9890	-42.3	200.5
EB 37-	2	96.2	-74.4	1.9944	-28.2	83.8
EB 36-	2	100.9	-50.2	1.9993	-32.3	81.0
EB 35-	2	284.2	-45.1	1.9997	-18.3	232.2
EB 34-	2	162.7	-44.1	1.9981	-49.2	10.5
EB 33-	2	167.9	-65.4	1.9984	-71.3	12.4
EB 32-	2	155.3	-69.2	1.9940	-72.5	43.6
EB 31-	2	170.1	-70.1	1.9997	-77.9	15.0
EB 30-	2	220.4	-44.3	1.9993	-43.3	293.1
EB 29-	2	228.2	-70.8	1.9996	-64.8	256.4
EB 28B	2	185.4	-53.8	1.9769	-59.1	337.5
EB 28A	2	207.7	-62.3	1.9814	-63.6	297.2
EB 28-	2	225.1	-62.2	1.9996	-57.2	275.1
EB 27-	2	155.2	-79.0	2.0000	-79.7	108.6
EB 26-	2	130.2	-68.0	1.9987	-61.2	71.5
EB 25-	2	112.1	-61.6	1.9992	-47.1	79.3
EB 24-	2	99.6	-21.4	1.9953	-14.1	72.3
EB 23-	2	59.2	-19.3	1.9973	3.2	108.3
EB 22-	2	349.5	83.0	1.9999	78.4	333.7
EB 21-	2	309.5	77.7	1.9994	69.8	283.0
EB 20-	2	37.5	70.5	1.9976	69.0	87.7
EB 19-	2	67.3	68.6	1.9988	54.5	64.8
EB 17-	2	323.2	79.6	2.0000	75.4	291.0
EB 16-	2	343.2	67.3	1.9989	72.6	204.6
EB 15-	2	152.1	75.5	1.8414	39.4	2.4
EB 14-	2	346.6	80.6	1.9874	81.8	315.8
EB 13-	2	349.5	52.0	1.9993	56.9	182.6
EB 12-	2	8.9	83.8	1.7101	77.0	354.7
EB 11-	2	326.7	20.7	1.9978	30.9	205.3
EB 10-	2	322.1	21.5	1.9989	30.1	210.4
EB 9-	2	183.5	-2.8	1.9923	-26.3	342.4
EB 8-	2	174.8	24.8	1.9759	-11.8	351.4
EB 7-	2	43.2	-60.9	1.9986	-22.2	132.9
EB 6C	2	212.2	-64.1	1.9993	-64.0	288.4
EB 6B	2	210.2	-56.1	1.9965	-56.4	299.3
EB 6-	2	214.8	3.4	1.0116	-18.6	309.3
EB 5-	2	266.7	-72.1	1.9836	-50.8	225.3
EB 4-	2	273.6	-67.2	1.9813	-42.6	227.1
EB 3-	2	175.2	-9.8	1.9959	-29.7	351.8
EB 2-	3	177.7	-68.3	3.0000	-76.3	352.3
EB 1-	2	157.7	-61.5	1.9968	-64.3	26.3

B NESKAUPSTAÐUR

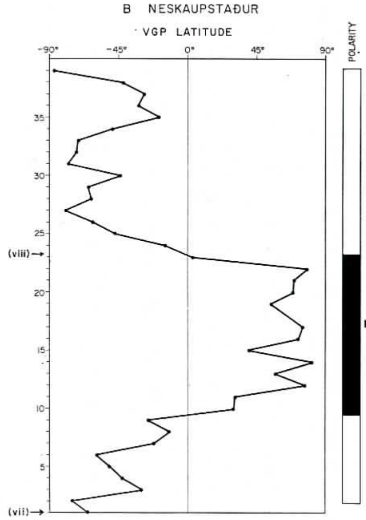

PROFILE C

HJÁLEIGULÆKUR (ORMSTAÐAÁ)

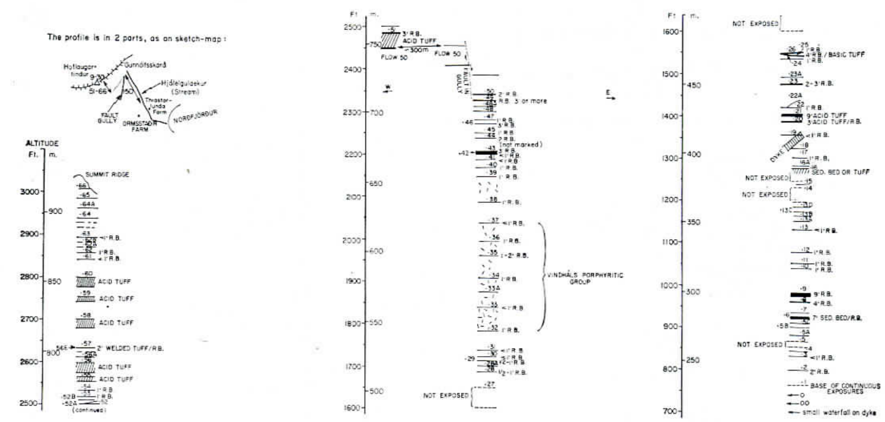

C HJÁLEIGULAEKUR

NO	N	D	I	R	θ'	φ'
EC 66-	2	198.9	-72.1	1.9098	-76.0	288.5
EC 65-	2	221.1	-65.3	1.9997	-61.9	275.1
EC 64A	2	173.3	-58.1	1.9999	-63.3	357.9
EC 64-	2	166.0	-57.7	1.8746	-62.0	10.0
EC 63-	3	144.0	-74.1	2.9412	-73.1	76.7
EC 62B	2	125.4	-81.6	1.9999	-69.9	124.0
EC 62A	2	206.4	-75.7	1.9986	-78.3	254.6
EC 62-	2	163.9	-65.9	1.9999	-71.0	20.9
EC 61-	2	202.1	-68.5	1.9907	-72.6	295.2
EC 60-	4	236.1	-65.5	3.9838	-56.0	259.1
EC 59-	2	9.0	79.2	1.9995	84.7	23.7
EC 58-	4	340.3	63.7	3.9982	67.5	204.4
EC 57-	2	188.6	-68.7	1.9989	-76.2	323.4
EC 56B	2	202.9	-76.4	1.9974	-80.2	250.7
EC 56A	2	223.3	-79.7	1.9890	-73.2	220.0
EC 55-	2	232.6	-71.3	1.9996	-63.4	251.0
EC 54-	2	94.0	80.5	0.7334	58.3	23.1
EC 53-	3	8.4	53.1	2.7563	58.1	152.9
EC 52B	2	344.2	70.0	1.9974	76.4	208.9
EC 52-	3	16.8	10.7	2.6734	29.1	147.0
EC 51-	2	347.9	69.8	1.9998	77.1	199.8
EC 50-	4	300.8	45.6	3.2207	37.2	240.0
EC 49-	2	296.3	68.3	1.9994	55.7	264.2
EC 48A	2	0.2	58.3	1.9968	64.0	165.9
EC 48-	2	9.0	64.2	1.9838	70.3	147.3
EC 47-	2	41.6	57.8	1.9307	54.2	103.6
EC 46-	2	37.7	67.0	1.9999	65.1	96.2
EC 45-	2	45.3	-12.9	1.4837	11.0	120.2
EC 44-	2	77.8	85.4	1.9989	65.5	8.0
EC 41-	2	347.4	50.6	2.0000	55.4	185.2
EC 40-	2	352.2	20.7	1.9912	35.4	175.6
EC 39-		16.7	63.2		67.6	133.8
EC 38-	2	348.7	70.2	1.9885	77.8	199.0
EC 37-	2	21.8	59.6	1.9972	62.4	128.5
EC 36-	2	10.5	79.8	1.9999	83.5	19.4
EC 35-	2	334.0	59.6	1.9984	61.2	210.1
EC 34-	2	349.4	82.6	1.9999	79.1	332.1
EC 33A	2	343.3	65.5	1.9994	70.4	201.3
EC 33-	2	347.5	70.1	1.9999	77.3	201.4
EC 32-		350.4	69.2		76.8	192.3
EC 31-	2	353.2	77.4	1.9979	87.0	277.1
EC 30-	2	305.2	80.8	1.9972	69.7	299.6
EC 29-	2	264.5	50.7	1.7190	26.0	275.2
EC 28A	2	15.1	86.1	1.9855	72.5	352.9
EC 28-	2	28.1	82.6	1.9999	76.2	16.0
EC 27-	2	15.5	59.5	1.9952	63.7	138.8
EC 26-	2	229.0	15.7	1.9701	-8.5	297.1
EC 25-	2	213.7	4.1	1.9997	-18.5	310.4
EC 24-	2	210.7	-3.3	1.9031	-22.8	312.6
EC 23A	2	236.8	-37.4	1.9698	-32.6	278.0
EC 23-	2	241.2	-43.1	1.9991	-34.6	271.5
EC 22A	2	277.8	-82.7	1.9976	-59.8	195.6
EC 22-	2	188.9	-81.7	1.9997	-80.8	181.9
EC 21-	2	186.9	-76.9	1.9966	-87.1	254.4
EC 20-	2	202.4	-70.4	1.9911	-74.7	289.1
EC 19-	2	287.9	-74.2	2.0000	-46.5	209.1
EC 18-	2	165.7	-54.6	1.9960	-58.9	9.1
EC 17-	2	169.8	-47.8	1.9099	-53.2	1.2
EC 16A	2	211.0	-55.8	1.9166	-55.9	298.4
EC 16-	2	206.5	-73.0	1.9992	-76.0	271.4
EC 15-	2	113.5	-78.7	1.9998	-64.8	113.2
EC 14-	2	141.1	-77.7	1.9998	-74.2	98.4
EC 13D	2	103.9	-57.7	1.9621	-39.9	82.9
EC 13C	2	128.2	-36.4	1.9964	-33.9	48.9
EC 13B	2	111.9	-23.4	1.9997	-20.2	61.3
EC 13A	2	109.9	-58.7	1.9804	-43.4	78.4
EC 13-	2	111.4	-22.9	1.9999	-19.7	61.5
EC 12-	3	161.1	-77.4	2.9930	-82.1	90.3
EC 11-	2	170.1	-76.3	2.0000	-85.6	65.4
EC 10-	2	211.0	-68.1	1.9963	-68.9	282.3
EC 9-	2	183.6	-76.7	1.9992	-88.4	270.0
EC 8-	2	6.9	-34.8	1.7955	5.6	159.6
EC 7-	2	218.5	-73.9	1.9999	-71.8	254.5
EC 6-	2	227.1	-79.3	1.9997	-71.8	221.7
EC 5C	2	218.0	-79.9	1.9995	-75.0	218.7
EC 5B	2	214.6	-66.7	1.9991	-65.9	280.6
EC 5A	2	238.4	-70.5	1.9982	-60.2	248.2
EC 5-	2	246.8	-71.9	1.9994	-58.3	238.7
EC 4-	2	263.2	-38.0	1.9660	-22.1	252.8
EC 3-	2	157.0	-78.8	1.9995	-80.4	106.1
EC 2-	2	86.7	-78.8	1.9353	-56.5	124.3
EC 0C	2	319.6	-75.9	1.9843	-41.9	189.1
EC 0B	3	203.9	-68.4	2.9908	-71.9	292.3
EC 0A	3	211.9	-62.9	2.9907	-62.9	290.3

C HJÁLEIGULÆKUR

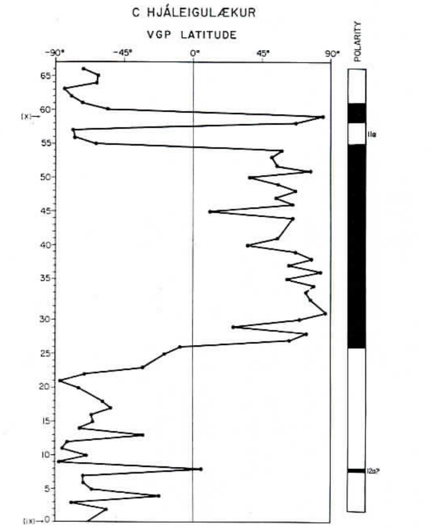

PROFILE D
GÆSADALUR

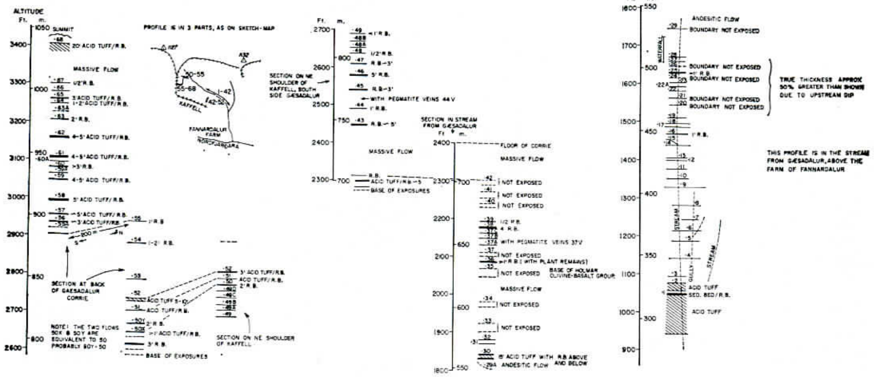

D GAESADALUR

NO	N	D	I	R	θ'	φ'
ED 68-	3	174.4	-79.2	2.9999	-85.4	140.2
ED 67-	2	263.3	72.3	1.9965	47.6	293.7
ED 66-	2	257.7	-57.3	1.9999	29.1	284.1
ED 65-	2	258.8	-52.0	1.9719	-33.9	250.6
ED 64-	2	200.7	-47.6	1.9986	-51.3	316.2
ED 63A	2	72.1	-86.8	2.0000	-62.4	152.6
ED 63-	2	345.8	-78.8	1.9738	-43.8	173.3
ED 62-	2	236.1	-71.5	2.0000	-62.2	247.6
ED 61-	2	136.9	-15.4	1.9999	-25.3	34.6
ED 60A	2	65.3	78.8	2.0000	65.2	39.1
ED 60-	2	47.2	70.3	1.9972	64.7	78.3
ED 59A	2	11.0	55.2	1.9999	59.9	148.0
ED 59-	2	14.9	61.7	1.9980	66.2	138.3
ED 58-	2	228.4	-51.9	1.9965	-46.4	280.1
ED 57-	2	171.3	-50.1	1.9999	-55.4	359.3
ED 56-	2	164.0	-68.9	1.9975	-74.9	26.3
ED 55-	2	213.6	-59.4	1.9969	-58.6	291.8
ED 54-	2	168.4	-61.4	1.9911	-66.4	7.9
ED 53-	2	205.5	-74.6	1.9937	-77.9	263.5
ED 52-	4	115.0	-68.3	3.9876	-55.1	85.2
ED 51-	4	235.6	-37.8	3.9383	-33.4	279.0
ED 50-	2	121.9	-59.5	2.0000	-49.2	67.9
ED 49C	2	235.2	-80.5	1.9999	-69.5	214.1
ED 49B	2	181.5	-85.8	1.9999	-73.4	166.9
ED 49A	2	136.6	-85.4	2.0000	-70.8	146.8
ED 49-	2	184.4	-82.2	1.9885	-80.2	172.9
ED 48B	2	178.1	-63.0	1.9999	-69.3	350.0
ED 48A	2	194.2	-53.3	1.9934	-57.6	323.8
ED 48-	2	204.3	-59.3	2.0000	-61.4	305.0
ED 47-	2	258.1	-67.5	1.9999	-48.9	237.9
ED 46-	2	174.7	-63.8	1.9967	-70.1	357.0
ED 45-	2	187.5	-56.6	1.9915	-61.7	333.4
ED 44-		345.3	0.6		24.3	182.3
ED 43-	2	26.2	52.3	1.9998	54.1	126.8
ED 42-	4	328.4	69.5	3.8917	70.3	234.4
ED 41-	2	263.4	23.8	1.9996	8.5	267.3
ED 40-	2	287.7	34.7	1.8979	24.7	248.3
ED 39-	2	277.5	7.8	1.9233	6.7	250.9
ED 38-	2	252.5	-54.0	1.8926	-38.2	255.0
ED 37V	6	232.9	-66.4	5.9531	-58.2	260.8
ED 37C	2	226.7	-67.7	1.9991	-62.2	264.7
ED 37B	2	225.4	-68.5	1.9999	-63.6	264.3
ED 37A	6	230.2	-68.9	5.9893	-62.0	258.5
ED 37-	2	219.2	-70.3	1.9986	-68.0	266.4
ED 36-	2	158.3	-71.9	1.9951	-76.7	47.7
ED 35-	2	310.7	-34.5	1.9702	-2.0	211.9
ED 34-	2	216.9	-46.0	1.9943	-45.7	296.2
ED 33-	2	210.8	-69.1	1.9983	-70.2	279.9
ED 32-	2	253.1	-59.3	1.9997	-42.7	250.6
ED 31-	2	250.9	-60.6	1.9990	-44.8	251.4
ED 30-	2	232.0	-55.6	1.9710	-48.1	273.6
ED 29A	2	114.4	-85.4	1.9986	-67.4	143.9
ED 29-	3	42.8	-68.0	2.5794	-30.7	136.3
ED 28-	2	278.4	-71.8	1.9865	-46.4	218.0
ED 27-	3	226.7	-66.4	2.9972	-60.9	266.8
ED 25-	2	218.3	-56.7	1.9887	-54.3	288.3
ED 24-	3	206.8	-57.1	2.9995	-58.4	303.1
ED 23-	2	189.4	-55.4	1.9947	-60.4	330.5
ED 22A	2	195.4	-49.8	1.9997	-54.2	323.0
ED 22-	2	209.2	-61.3	1.9891	-62.1	295.8
ED 21-	2	201.6	-60.0	1.9985	-62.8	308.5
ED 20-	2	186.6	-50.2	1.9922	-55.6	336.0
ED 19-	2	175.9	-34.3	1.9936	-43.7	351.5
ED 18-	2	183.9	-46.8	1.9986	-52.8	340.3
ED 17-	2	164.3	-23.4	1.9192	-36.0	5.1
ED 16-	2	190.9	-31.0	1.9990	-41.1	332.1
ED 15-		207.7	-51.1		-52.6	305.5
ED 14-	2	205.2	-57.5	1.9966	-59.3	305.1
ED 13-	2	214.2	-55.6	1.9938	-54.7	294.2
ED 11-	2	183.1	-54.5	1.9984	-59.8	341.0
ED 10-	2	187.4	-66.6	1.9994	-73.5	328.7
ED 9-	2	201.7	-57.1	1.9999	-59.8	310.5
ED 8-	2	150.5	-56.4	1.9987	-57.0	32.2
ED 7-	2	132.7	-62.7	1.9912	-56.7	60.2
ED 6-	2	163.8	-78.5	1.9990	-83.0	107.2
ED 5-	2	251.8	-73.8	1.9999	-58.2	231.2
ED 4-	2	203.3	-72.2	1.9917	-76.5	280.0
ED 3-	2	177.1	-59.5	1.9950	-65.1	351.2
ED 2-	2	212.3	-62.5	1.9892	-62.2	290.2
ED 1-	3	210.6	-71.4	2.9951	-72.7	273.0

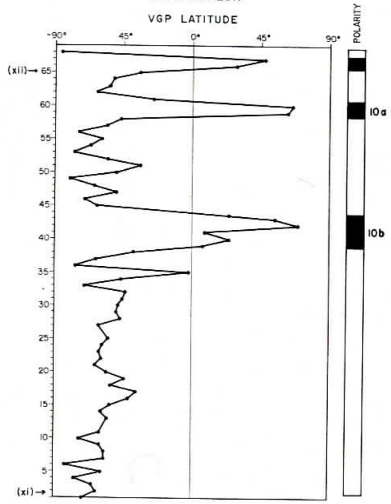

PROFILE E
SLENJUDALUR

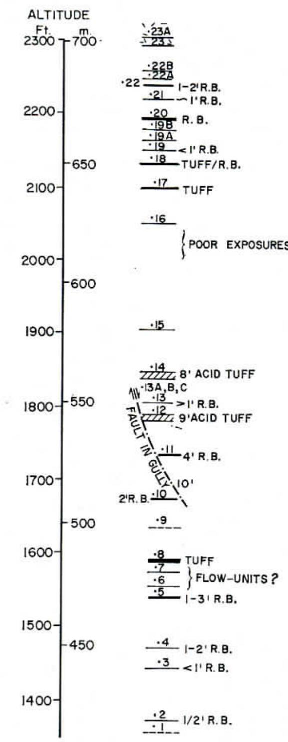

E SLENJUDALUR

NO	N	D	I	R	θ'	φ'
EE 23A	2	7.7	81.0	1.9999	82.2	3.1
EE 23-	2	8.6	79.4	1.9999	84.6	19.7
EE 22B	2	242.2	77.8	1.9996	49.0	313.5
EE 22A	2	272.1	79.0	1.9999	58.3	302.3
EE 21-	2	328.4	81.4	1.9893	76.4	305.9
EE 20-	5	140.2	-67.0	4.9580	-64.2	85.3
EE 19B	2	15.3	75.0	1.9993	82.5	94.3
EE 19A	2	14.7	66.2	1.9980	71.8	133.6
EE 19-	2	22.5	65.2	1.9897	68.4	120.8
EE 18	2	61.3	86.2	1.8761	67.8	3.4
EE 17-	2	358.5	72.4	1.9977	82.4	172.0
EE 15-	2	19.1	58.1	1.9796	61.4	133.6
EE 14D	2	309.2	73.7	2.0000	66.5	266.4
EE 14-	2	49.2	71.6	1.9994	65.1	72.9
EE 13C	2	331.9	34.7	1.8905	40.4	201.6
EE 13B	2	346.0	49.5	1.9999	54.2	186.8
EE 13A	2	342.3	55.8	2.0000	59.4	195.6
EE 13-	2	347.9	58.9	1.9992	63.6	187.2
EE 12-	2	2.2	73.0	1.9875	83.3	156.0
EE 11-	2	84.6	78.0	1.9986	58.2	33.7
EE 10-	2	58.4	49.1	1.9206	40.1	91.1
EE 9-	2	118.4	70.8	1.9999	39.0	26.2
EE 8-	2	271.5	73.4	1.9999	51.7	290.2
EE 7-	2	9.6	77.5	1.9984	85.9	56.6
EE 6-	2	46.0	78.1	1.9983	71.7	48.6
EE 5-	2	20.5	75.6	1.9998	80.8	80.5
EE 4-	2	51.2	75.9	1.9996	68.3	56.6
EE 3-	6	269.1	83.0	3.6363	61.6	316.0
EE 2-	4	212.7	63.3	3.9623	-63.0	288.3
EE 1-	4	201.0	-62.8	3.9602	-66.1	306.6

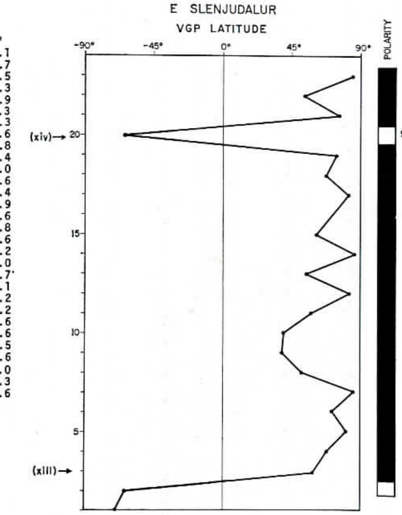

PROFILE F
SKAGAFELL

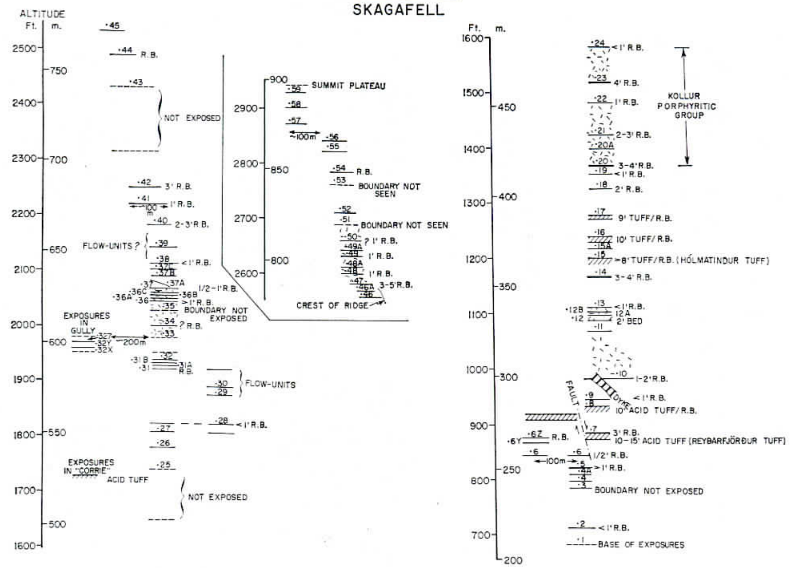

F SKAGAFELL

NO	N	D	I	R	θ'	φ'
EF 59-	2	351.3	46.0	1.9999	51.9	178.3
EF 58-	2	207.7	83.7	1.9999	53.7	336.0
EF 57-	2	234.3	84.0	1.9730	56.7	327.9
EF 56-	2	30.9	88.5	1.9997	67.6	349.9
EF 55-	2	313.8	66.1	1.9959	60.7	243.9
EF 54-	2	351.3	78.9	1.9982	85.1	305.5
EF 52-	2	290.1	77.4	1.9962	62.6	289.8
EF 50-	2	19.0	45.8	1.9556	50.2	138.8
EF 49A	2	7.8	62.6	1.9908	68.5	150.3
EF 49-	2	331.8	64.2	1.9995	65.5	218.2
EF 48A	2	88.4	66.5	1.9998	43.8	51.1
EF 48-	2	74.4	72.6	1.9996	56.0	51.8
EF 47-	2	182.6	86.6	1.9744	58.4	345.2
EF 46A	2	82.1	67.5	1.9949	47.3	54.6
EF 46-	2	343.2	62.7	1.7750	67.0	197.9
EF 45-	2	24.3	78.1	1.9972	80.0	52.9
EF 44-	2	149.1	67.7	1.9989	28.1	7.4
EF 43-	2	21.3	72.4	1.9984	77.4	102.4
EF 42-	2	10.9	75.1	1.9999	84.2	103.9
EF 41-	2	11.3	86.6	1.9992	71.8	350.1
EF 40-	2	353.3	75.5	1.9930	86.1	218.9
EF 39-	2	16.6	75.9	1.9992	82.6	82.3
EF 38-	2	34.1	81.1	1.9981	75.9	29.0
EF 37B	2	307.7	63.4	1.9964	55.4	246.2
EF 37A	2	341.1	70.8	1.8952	76.4	217.9
EF 37-	2	315.5	59.7	1.9990	54.8	233.5
EF 36C	2	301.8	76.1	1.9997	65.7	279.5
EF 36B	2	304.3	78.4	1.9964	68.3	287.5
EF 36A	2	318.0	75.9	1.9991	72.0	269.3
EF 36-	2	320.1	73.9	1.9869	71.3	259.0
EF 35-	2	54.6	79.2	1.9999	69.1	40.5
EF 34-	2	86.3	62.1	1.9999	40.0	57.0
EF 33-		288.6	41.8		29.5	249.7
EF 32-	2	350.7	62.0	1.9982	67.6	183.6
EF 31B	2	359.4	56.1	1.9979	61.6	166.8
EF 31A	2	3.6	57.0	1.9999	62.4	159.6
EF 31-	2	4.1	53.4	1.9998	58.8	159.1
EF 30-	2	12.4	59.4	1.9998	64.1	143.8
EF 29-	2	32.3	60.1	1.9840	59.7	112.6
EF 28-	2	325.2	66.1	1.8831	65.3	230.4
EF 27-	3	23.8	54.6	2.9948	56.8	128.7
EF 26-	2	351.3	53.1	1.9911	58.1	179.5
EF 25-	2	328.9	67.4	1.9964	68.0	228.0
EF 24-	2	77.9	74.4	1.9963	56.6	45.9
EF 23-	2	305.4	40.3	1.7116	35.3	232.8
EF 22-	2	350.5	56.2	1.9965	61.1	181.7
EF 21-	2	330.7	79.6	1.9985	78.0	291.5
EF 20A	2	312.2	85.1	1.9993	70.4	323.7
EF 20-	2	12.0	73.4	1.9999	81.9	116.7
EF 19-	2	341.6	59.3	1.9957	62.9	197.8
EF 18-	2	341.5	73.1	1.9998	79.2	227.8
EF 17-	2	0.7	62.2	1.9996	68.3	164.4
EF 16-	2	48.9	70.1	1.9999	63.7	77.0
EF 15A	2	20.4	83.3	1.9915	76.8	6.3
EF 15-	2	314.1	84.9	1.9946	70.8	323.0
EF 14-	2	224.4	79.0	1.9944	47.4	323.7
EF 13-	3	344.6	78.8	2.9987	83.1	291.1
EF 12B	2	237.8	41.7	1.2971	9.4	294.2
EF 12A	2	50.6	2.1	0.3747	16.5	112.1
EF 12-	2	4.9	70.2	1.9997	78.9	150.8
EF 11-	2	28.1	75.5	1.9963	77.5	74.1
EF 10-	2	12.3	80.2	1.9997	82.6	18.8
EF 9-	2	3.1	66.8	1.9982	74.2	158.3
EF 8-	2	19.9	68.0	1.9900	72.6	120.0
EF 7-	2	64.8	69.6	2.0000	56.6	64.5
EF 6-	2	352.0	59.7	1.9991	65.1	180.4
EF 5-	2	358.5	74.3	1.9895	85.5	174.9
EF 4A	2	19.4	85.3	2.0000	73.7	356.9
EF 4-	2	27.5	81.9	1.9995	77.1	20.2
EF 3-	2	10.0	83.9	1.9972	76.9	355.1
EF 2-	2	25.4	62.4	1.9988	64.4	119.9
EF 1-	2	56.9	73.6	1.9992	63.9	61.0

F SKAGAFELL
VGP LATITUDE

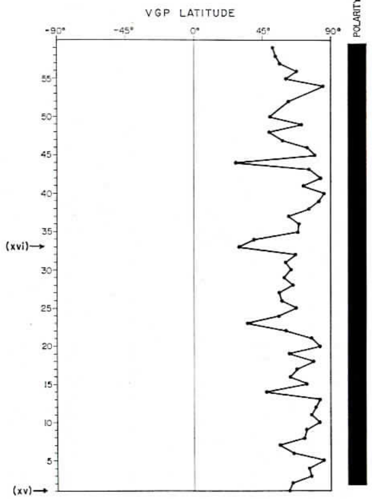

PROFILE J
MELRAKKANES

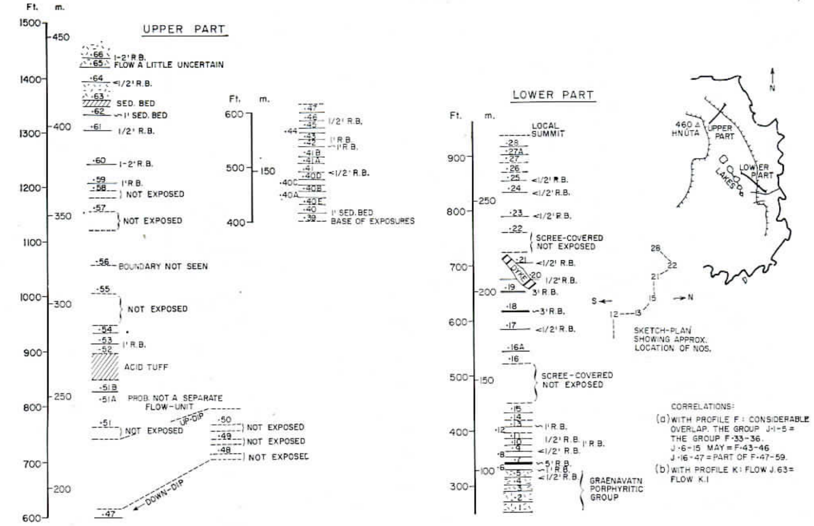

J MELRAKKANES

NO	N	D	I	R	θ'	φ'
EJ 66-	2	186.0	-78.8	1.9911	-85.4	193.9
EJ 65-	2	196.1	-74.4	2.0000	-81.7	275.0
EJ 64-	2	105.0	-39.1	1.9952	-26.3	72.0
EJ 63-	2	212.5	-62.6	1.9991	-62.6	288.2
EJ 61-	2	162.5	-70.1	1.9998	-76.4	34.2
EJ 60-	2	192.1	-62.3	1.9907	-68.0	321.6
EJ 59-	2	252.4	45.7	1.9994	17.2	282.8
EJ 58-	2	218.4	64.9	1.8493	25.3	317.5
EJ 57-	2	244.6	33.8	2.0000	6.4	285.9
EJ 56-	2	58.0	-30.2	1.5027	-1.9	110.9
EJ 55-	2	164.1	-64.1	1.9982	-69.4	18.2
EJ 54-	2	349.9	50.9	1.9953	56.5	181.2
EJ 53-	2	313.9	70.3	1.9991	65.2	253.5
EJ 52-	2	244.4	71.7	1.9994	40.5	304.6
EJ 51B	2	10.6	73.5	1.9806	82.8	116.9
EJ 51A	2	348.9	60.5	1.9926	66.1	186.3
EJ 51-	2	334.2	61.7	1.9973	64.0	212.0
EJ 50-	2	313.7	73.5	1.9973	68.2	263.8
EJ 49-	2	313.5	73.5	1.9968	68.0	263.7
EJ 48-	2	340.0	80.1	1.9996	80.3	303.6
EJ 47-	2	4.7	69.9	1.9996	79.0	150.9
EJ 46-	2	16.0	66.4	1.9924	72.2	129.0
EJ 45-	2	1.8	74.4	1.9999	86.2	151.7
EJ 44-	2	3.3	70.6	1.9994	80.2	154.3
EJ 43-	2	2.4	66.3	1.9970	74.2	159.7
EJ 42-	2	33.8	62.8	1.9955	62.4	106.2
EJ 41B	2	21.9	60.6	1.9970	63.9	126.2
EJ 41A	2	25.7	63.0	1.9999	65.3	117.5
EJ 41-	2	12.8	65.3	1.9953	71.5	137.2
EJ 40E	2	349.9	64.3	1.9970	70.8	187.1
EJ 40D	2	56.2	69.8	1.9897	60.4	69.7
EJ 40C	2	8.5	66.4	1.9949	73.7	145.0
EJ 40B	2	9.4	64.9	1.9999	71.6	144.8
EJ 40A	2	38.6	49.1	1.9999	48.0	111.7
EJ 40-	2	320.5	69.2	1.9917	66.9	244.0
EJ 39-	2	316.2	69.4	1.9999	65.2	249.0
EJ 28-	2	20.6	66.6	1.9998	71.1	120.2
EJ 27A	2	24.6	66.9	1.9990	70.2	112.7
EJ 27-	2	24.0	69.6	1.9981	73.5	106.6
EJ 26-	2	15.8	69.0	1.9969	75.5	124.0
EJ 25-	2	113.4	87.2	1.9992	61.8	356.4
EJ 24-	2	45.2	34.9	1.9708	35.7	109.9
EJ 23-	2	3.0	53.5	1.9961	59.5	160.6
EJ 22-	2	331.4	67.3	1.9986	69.2	225.5
EJ 21-	2	162.9	85.4	1.9889	55.7	350.2
EJ 20-	2	345.5	53.5	1.9951	58.3	188.8
EJ 19-		29.2	76.9		77.7	59.8
EJ 18-	2	98.7	72.0	1.9122	46.2	36.5
EJ 17-	2	223.9	55.9	1.8470	16.6	309.8
EJ 16A	2	325.4	74.7	1.9891	74.1	260.1
EJ 16-	2	276.1	62.5	1.9716	41.1	273.1
EJ 15-	2	54.1	-22.6	0.0990	3.6	112.8
EJ 14-	2	27.8	56.0	1.9989	57.5	121.2
EJ 13-	2	315.8	72.1	1.9791	67.7	256.9
EJ 12-	2	7.9	68.2	1.9961	76.2	144.3
EJ 11-	2	21.6	69.9	1.9930	74.7	109.7
EJ 10-	2	257.8	71.9	1.9968	44.8	296.4
EJ 9-	2	325.0	62.7	1.9967	61.8	226.1
EJ 8-	2	30.3	70.7	1.9840	72.3	93.5
EJ 7-	2	37.9	64.3	1.9706	62.4	98.8
EJ 6-	2	152.7	11.0	1.9967	-17.1	13.9
EJ 5-	2	180.5	80.7	1.9998	46.4	345.2
EJ 4-	2	23.1	81.5	1.9979	78.0	18.2
EJ 3-	2	46.4	79.2	1.9968	71.6	40.3
EJ 2-	2	92.3	86.9	1.9942	63.5	359.6
EJ 1-	2	77.0	86.5	1.9916	65.2	1.8

J MELRAKKANES
VGP LATITUDE

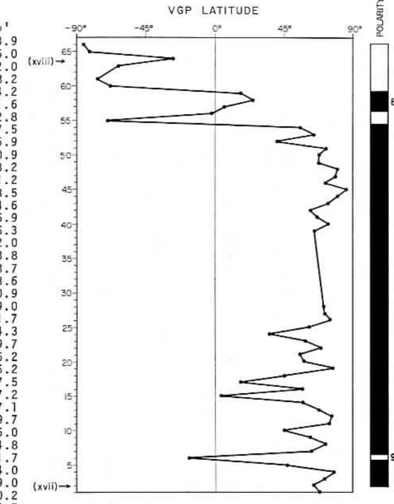

PROFILE K

HENGILL

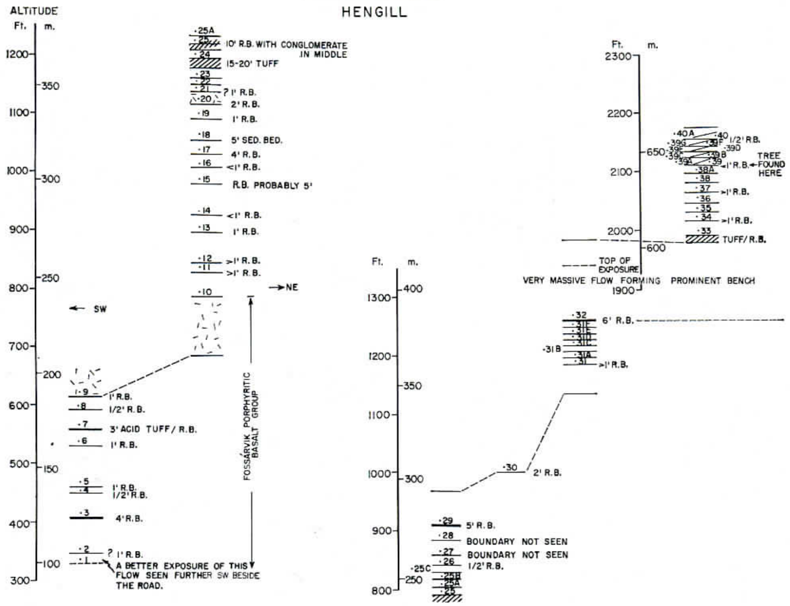

K HENGILL

NO	N	D	I	R	θ'	φ'
EK 40A	2	357.5	81.3	1.9985	81.4	340.3
EK 40-	2	18.7	80.7	1.9990	80.0	20.4
EK 39G	2	355.4	74.6	1.9874	86.0	199.4
EK 39F	2	317.8	87.5	1.9990	67.9	336.4
EK 39E	2	13.8	83.8	1.9998	76.2	357.6
EK 39C	2	334.1	79.8	1.9991	78.6	296.4
EK 39B	2	318.4	85.7	1.9999	70.1	328.5
EK 39-	2	4.1	86.3	1.9993	71.8	347.0
EK 38A	2	349.8	40.7	1.9996	48.2	179.4
EK 38-	2	332.6	64.4	1.9965	66.3	217.9
EK 37-	2	342.7	63.5	1.9994	68.3	199.9
EK 36A	2	341.3	67.6	1.9958	73.0	209.3
EK 36-	2	338.8	72.3	1.9989	77.6	230.6
EK 35-	2	282.3	8.0	0.9444	8.9	245.8
EK 34-	2	343.8	70.5	1.9970	77.3	212.3
EK 33-	2	13.7	72.4	1.9998	80.4	115.3
EK 32-	2	97.1	-56.9	1.3201	-36.3	87.6
EK 31F	2	196.0	12.8	1.1612	-17.9	327.5
EK 31E	2	138.2	18.0	1.9950	-9.9	27.2
EK 31D	2	17.1	74.6	1.9726	81.6	90.3
EK 31C	2	4.1	-23.2	1.9350	13.3	161.2
EK 31B	2	234.7	47.6	1.8200	12.4	298.1
EK 31A	2	246.9	37.5	1.9965	9.5	284.7
EK 31-	2	271.3	43.2	1.9997	23.1	265.5
EK 30-	2	319.6	69.9	1.9883	67.3	246.7
EK 29-	2	201.7	-78.6	1.9999	-80.6	223.5
EK 28-	2	103.6	-66.3	1.9876	-48.1	91.2
EK 27-	2	216.6	-50.9	1.8782	-50.1	292.8
EK 26-	2	231.3	-68.3	1.9998	-60.9	256.9
EK 25C	2	227.8	-69.0	1.9962	-63.2	258.7
EK 25B	4	209.6	-70.9	3.9807	-72.8	273.4
EK 25A	7	221.9	-72.5	6.9769	-69.1	254.4
EK 25-	4	212.6	-72.8	3.9987	-73.4	262.2
EK 24-	2	45.7	-85.0	1.9871	-56.9	152.3
EK 23-	2	327.7	-65.3	1.9993	-24.7	188.7
EK 22-	2	329.2	-66.1	1.9959	-25.5	187.4
EK 21-	2	304.4	-74.6	1.9800	-42.4	197.8
EK 20-	2	169.9	-65.3	1.9976	-72.1	7.9
EK 19-	2	161.8	-70.1	1.9994	-76.2	35.1
EK 18-	2	249.9	-67.9	1.9999	-52.5	242.1
EK 17-	2	224.2	-66.2	1.9999	-61.8	268.1
EK 16-	2	217.3	-73.0	1.9968	-71.6	256.4
EK 15-	2	218.9	-67.4	1.9982	-65.2	271.7
EK 14-	2	225.9	-69.2	1.9854	-64.2	260.1
EK 13-	2	154.6	-22.9	1.4968	-34.5	15.9
EK 12-	2	216.6	-59.5	1.9991	-58.0	286.3
EK 11-	2	210.8	-67.8	1.9987	-69.0	281.1
EK 10-	2	206.9	-55.6	1.9969	-57.5	302.6
EK 9-	2	193.3	-77.7	2.0000	-84.2	230.6
EK 8-	2	231.4	-76.8	1.9981	-68.7	230.7
EK 7-	2	237.2	-67.9	1.9982	-57.9	252.5
EK 6-	2	191.7	-84.8	1.9902	-74.5	173.2
EK 5-	2	137.8	-85.9	2.0000	-69.8	149.3
EK 4-	2	170.2	-77.5	1.9981	-85.6	101.7
EK 3-	2	233.7	-78.3	1.9977	-68.6	223.4
EK 2-	2	215.2	-67.8	1.9997	-67.2	275.2
EK 1-	2	204.7	-14.9	1.1971	-30.5	316.6

K HENGILL

VGP LATITUDE

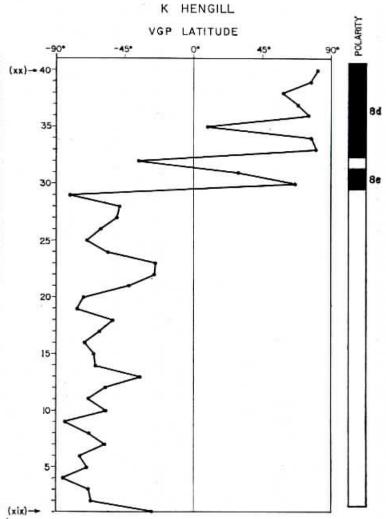

PROFILE L

LANGAGIL

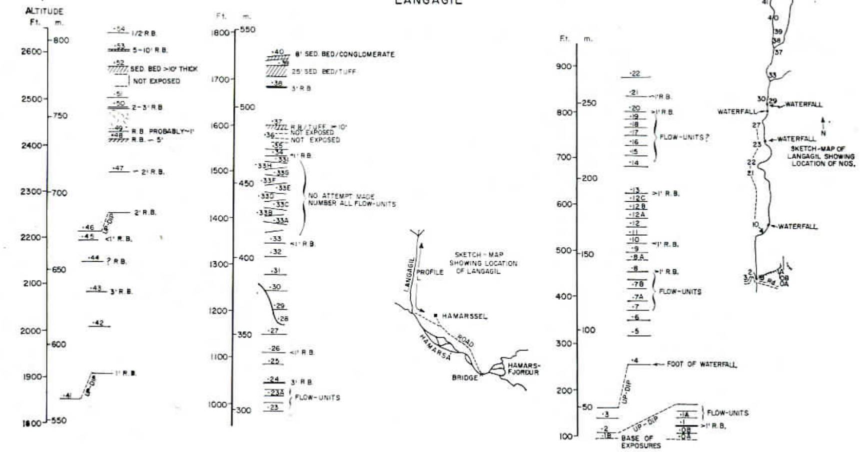

L LANGAGIL

NO	N	D	I	R	θ'	φ'
EL 54-	2	275.2	34.6	1.9999	19.3	259.1
EL 53-	2	233.8	3.4	2.0000	-13.1	289.5
EL 52-	2	132.8	-75.4	1.9987	-69.4	91.4
EL 51-	2	250.6	-31.7	1.9540	-23.8	265.4
EL 50-	2	4.6	37.5	1.6845	46.3	159.2
EL 49-	2	223.4	-75.0	1.9994	-70.7	243.5
EL 48-	2	246.8	-72.4	1.9954	-58.5	236.2
EL 47-	2	243.8	-81.3	1.9955	-66.8	207.0
EL 46-	2	154.6	-67.1	1.9993	-70.1	39.7
EL 45-	2	266.1	-52.1	1.9991	-30.9	243.3
EL 44-	2	8.1	56.1	1.9545	61.6	151.6
EL 43-	2	219.5	6.4	1.9856	-16.3	304.0
EL 42-	2	303.7	51.5	1.9929	43.0	239.8
EL 41-	2	216.3	-77.4	1.9712	-75.0	233.9
EL 40-	2	319.7	-46.5	1.9756	-7.6	200.6
EL 39-	2	223.8	-72.1	1.9926	-67.9	254.4
EL 38-	2	169.5	-57.2	1.9989	-62.5	3.6
EL 37-	2	246.7	-79.1	2.0000	-64.7	215.9
EL 36-	2	238.2	-40.8	1.9982	-34.4	274.3
EL 35-	2	219.7	-69.6	1.9930	-67.2	265.8
EL 34-	2	163.5	-65.1	1.9686	-70.4	20.6
EL 33I	2	203.2	-74.6	1.9982	-79.0	262.5
EL 33H	3	236.7	-73.3	2.9925	-63.6	240.6
EL 33G	2	236.1	-71.8	1.9997	-62.4	245.2
EL 33F	2	238.7	-72.6	1.9994	-62.1	241.3
EL 33E	2	210.5	-70.5	2.0000	-72.0	274.1
EL 33D	2	217.1	-62.4	1.9955	-60.6	282.6
EL 33C	2	209.9	-67.6	1.9994	-69.0	283.2
EL 33B	2	205.1	-69.8	1.9997	-73.3	284.4
EL 33A	2	340.8	-76.8	1.9958	-40.1	175.9
EL 33-	2	159.5	-56.3	1.9998	-59.7	19.1
EL 32-	2	155.2	-64.9	1.9956	-67.8	34.5
EL 31-	2	160.7	-49.7	1.9996	-53.8	14.2
EL 30-	2	177.6	-74.5	1.9990	-86.2	3.4
EL 29-	2	154.2	-70.2	1.9883	-73.5	48.7
EL 27-	2	179.1	-75.4	2.0000	-87.8	356.5
EL 26-	2	199.0	-69.4	1.9990	-75.0	296.3
EL 25-	2	218.1	-66.1	1.9839	-64.1	275.5
EL 24-	2	202.8	-68.7	1.9984	-72.8	291.5
EL 23A	2	230.8	-62.3	1.9999	-55.0	267.2
EL 23-	2	216.9	-66.7	1.9963	-65.3	275.8
EL 22-	2	226.6	-70.1	1.9979	-64.7	257.6
EL 21-		206.0	-74.8		-77.9	258.3
EL 20-	2	194.6	-73.1	1.9985	-80.9	289.3
EL 19-	2	113.6	45.9	1.9618	15.2	42.9
EL 18-	2	66.4	73.4	1.9767	59.7	54.1
EL 17-	2	109.3	70.0	1.9997	40.3	32.1
EL 16-	2	307.9	-6.9	1.9942	12.1	219.0
EL 15-	2	150.7	-42.1	1.9612	-45.4	24.8
EL 14-	2	173.6	-23.8	1.9007	-37.7	353.3
EL 13-	2	227.0	-57.6	1.9927	-52.1	276.1
EL 12C	2	349.5	54.4	1.9996	59.6	182.6
EL 12B	2	349.7	56.9	1.9999	62.2	183.1
EL 12A	2	354.8	59.9	1.9988	66.0	175.0
EL 12-	2	357.6	55.9	1.9995	61.8	169.5
EL 11-	2	3.2	58.8	1.9964	64.8	159.6
EL 10-	2	344.6	52.9	1.9996	57.5	189.6
EL 9-	2	348.5	66.6	1.9972	73.4	192.5
EL 8A	2	18.2	76.6	1.9972	82.2	67.8
EL 8-	2	35.9	65.6	1.9781	64.5	99.1
EL 7B	2	51.1	62.6	1.9999	55.2	86.6
EL 7A	2	47.4	71.6	1.9999	65.9	72.8
EL 7-	2	47.4	69.2	1.9998	63.5	79.0
EL 6-	2	16.9	33.2	1.9981	42.2	143.4
EL 5-	2	15.7	26.3	1.9987	38.2	145.9
EL 4-	2	12.0	24.0	1.9985	37.3	150.5
EL 3-	2	13.1	69.7	1.9919	77.0	128.3
EL 2-	2	349.2	72.6	1.9989	81.6	208.4
EL 1B	2	20.5	72.7	1.9980	78.3	99.3
EL 1A	2	38.4	59.1	1.9976	56.9	104.7
EL 1-	2	29.6	72.3	1.9991	74.2	88.1
EL 0B	2	313.3	86.0	1.9977	69.2	328.9
EL 0A	2	258.4	73.3	1.9989	46.8	297.7

L LANGAGIL

VGP LATITUDE

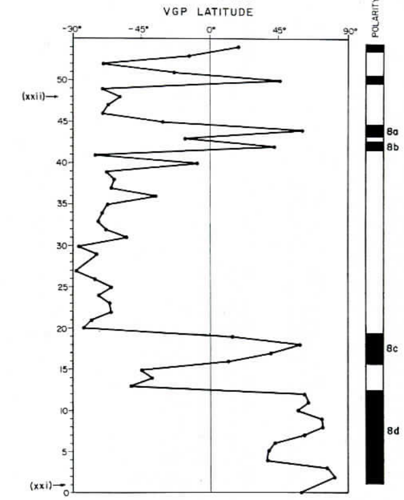

PROFILE M

KARFAGIL

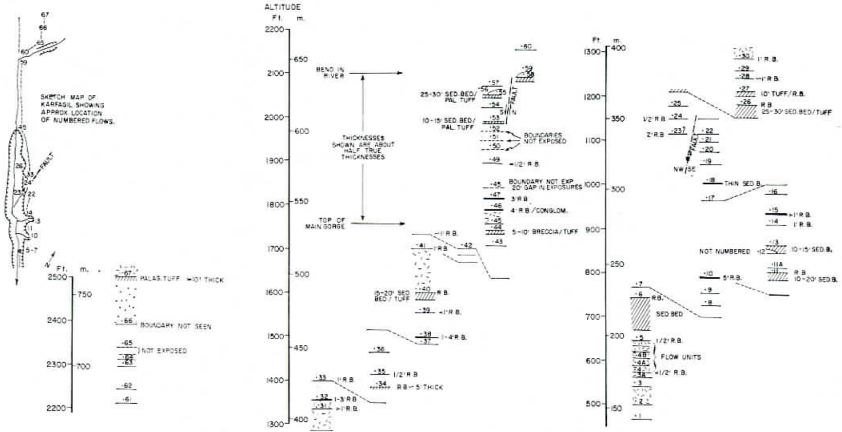

M KARFAGIL

NO	N	D	I	R	θ'	φ'
EM 67-	2	0.2	78.6	1.9966	86.5	346.5
EM 66-	2	358.1	64.9	1.9972	72.3	169.5
EM 65-	2	328.0	41.2	1.9995	44.1	207.7
EM 64-	2	308.8	89.3	1.9424	65.5	342.6
EM 63-	2	32.2	76.2	1.9955	76.1	63.5
EM 62-	2	19.2	62.4	2.0000	66.4	128.6
EM 61-	2	1.0	58.8	1.9983	65.0	163.4
EM 60-	2	6.8	42.9	1.9877	50.1	155.6
EM 59-	2	12.4	72.8	1.9981	81.3	116.8
EM 58-	2	93.6	75.1	1.9998	51.7	34.4
EM 57-	2	96.9	79.0	1.9997	55.5	24.5
EM 56-	2	350.2	72.0	1.9982	81.0	201.7
EM 55-	2	63.3	73.5	1.9994	61.2	55.5
EM 54-	2	94.5	82.5	1.9996	59.8	15.8
EM 53-	2	164.3	70.6	1.9961	30.1	355.6
EM 52-	2	43.7	80.7	1.9706	72.7	31.9
EM 51-	2	80.5	62.3	1.7209	42.4	60.5
EM 50-	2	56.7	76.4	1.9948	66.3	50.4
EM 49-	2	338.9	80.8	1.9961	79.3	308.7
EM 48-	2	16.3	74.0	1.9999	81.3	97.9
EM 47-	2	349.2	83.8	1.9994	76.4	335.5
EM 46-	2	340.3	81.7	1.9971	78.6	316.6
EM 45-	2	18.4	72.8	1.9996	79.2	102.7
EM 44-	2	48.3	70.0	1.9974	63.9	76.2
EM 43-		58.2	66.6		56.2	74.0
EM 42-	2	19.8	72.7	1.9864	78.5	100.7
EM 41-	2	37.2	62.4	1.9996	60.6	102.3
EM 40-	2	23.3	21.3	1.9985	34.0	137.3
EM 39-	2	29.1	62.0	1.9929	63.1	113.7
EM 36-	2	351.5	66.0	1.9969	73.1	185.1
EM 35-	2	353.0	76.0	1.9950	86.8	238.9
EM 34-	2	11.7	74.2	1.9979	83.2	107.3
EM 33-	2	132.2	70.2	1.9999	34.4	16.9
EM 32-	2	47.4	83.6	1.9996	70.9	14.8
EM 31-	2	127.4	74.6	1.9977	41.7	16.2
EM 30-	2	228.3	85.4	1.9996	57.8	332.4
EM 29-		12.1	40.5		47.8	148.6
EM 28-	2	342.9	73.9	1.9994	80.8	232.7
EM 27-	2	47.7	79.6	1.9999	71.3	38.0
EM 26-	2	341.3	81.5	1.9992	79.1	316.2
EM 25-	3	33.1	66.5	2.9883	66.6	100.9
EM 24-	2	47.8	60.3	2.0000	54.3	92.5
EM 23-	2	48.6	73.6	1.9984	67.3	65.5
EM 22-	2	45.8	77.0	1.9788	71.0	52.7
EM 21-	2	59.1	81.3	1.9974	68.1	27.7
EM 20-	2	56.7	75.7	1.9976	65.7	52.9
EM 19-	2	52.6	72.5	1.9832	64.5	65.9
EM 18-	2	340.9	73.0	1.9972	79.1	230.1
EM 17-	2	343.8	52.6	1.9997	57.0	190.7
EM 16-	2	348.7	64.0	1.9862	70.1	189.1
EM 15-	2	334.7	64.9	1.9977	67.6	215.2
EM 14-	2	1.7	73.7	1.9994	85.0	155.4
EM 13-	2	5.0	76.1	1.9986	87.6	97.4
EM 11A	2	66.9	4.1	1.9986	11.6	95.5
EM 11-	2	59.8	37.0	1.9936	31.3	93.9
EM 10-	2	286.9	20.7	1.9982	16.9	244.6
EM 9-	2	88.1	-59.1	1.9904	-34.7	96.5
EM 8-	2	65.5	-69.7	1.9963	-38.3	121.5
EM 7-	2	98.3	-82.3	1.9933	-62.6	131.1
EM 6-	2	13.1	-64.3	1.9842	-21.1	155.5
EM 5-	2	342.1	-76.5	1.9990	-39.5	175.2
EM 4B	2	228.3	-75.4	1.9998	-68.9	238.6
EM 4A	2	5.1	-85.3	2.0000	-55.3	163.8
EM 4-	2	26.6	-77.6	1.9991	-42.2	151.2
EM 3A	2	288.9	-50.7	1.9863	-20.6	224.9
EM 3-	2	300.4	-47.3	1.9980	-13.9	216.6
EM 2-	2	257.9	-58.8	1.9994	-40.1	245.7
EM 1-	2	161.4	-61.7	1.7917	-65.8	20.0

M KARFAGIL

VGP LATITUDE

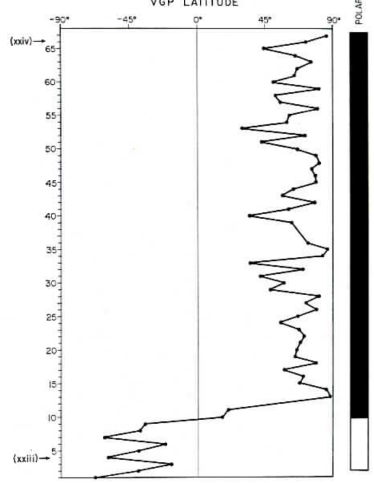

PROFILE N

THRANDARGIL

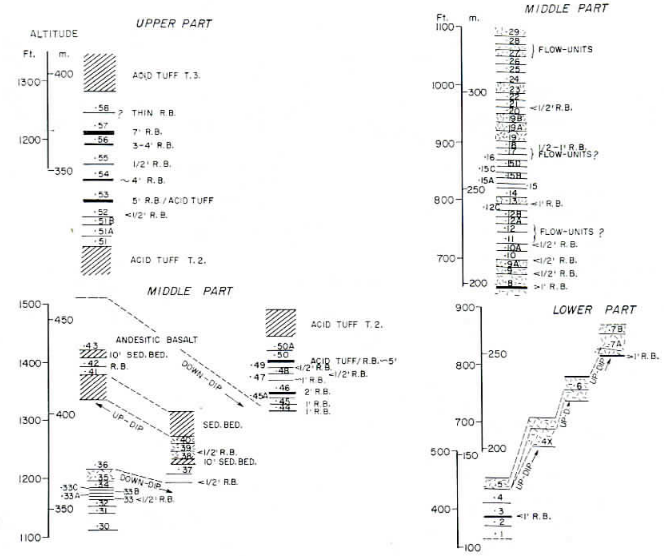

N THRÁNDARGIL

NO	N	D	I	R	θ'	φ'
EN 58-	2	207.0	-48.0	1.9999	-50.6	306.5
EN 57-	2	198.7	-47.9	1.9996	-52.5	317.8
EN 56-	2	35.5	64.3	1.9981	63.3	101.6
EN 55-	2	152.0	50.5	1.9942	8.3	9.1
EN 54-	2	30.6	24.2	1.9992	33.9	128.4
EN 53-	2	61.8	-71.3	1.9851	-39.3	125.4
EN 52-	2	53.6	56.2	1.9981	48.1	90.1
EN 51B	2	317.7	44.9	1.9999	43.4	221.2
EN 51A	2	50.1	45.0	1.9725	40.5	100.6
EN 51-	2	46.6	39.2	1.9864	37.9	106.7
EN 50A	2	285.8	70.0	1.9994	53.1	274.9
EN 50-	2	280.7	80.2	1.9957	61.6	302.8
EN 49-	2	40.1	70.8	1.9921	68.3	81.7
EN 48-	2	30.8	60.4	1.9998	60.8	113.0
EN 47-	2	47.2	61.8	1.9996	56.0	91.4
EN 46-	2	43.5	58.9	1.9999	54.7	98.7
EN 45A	2	51.6	69.7	1.9997	62.1	73.9
EN 45-	2	74.0	49.6	1.9998	34.0	75.0
EN 44-	2	15.9	66.7	1.9997	72.6	128.6
EN 43-	2	69.6	22.5	1.9442	19.2	88.7
EN 42-	2	10.6	72.3	1.9987	81.2	124.8
EN 41-	2	334.5	77.0	1.9999	79.2	270.0
EN 40-	2	32.0	65.2	1.9986	65.5	104.8
EN 39-	2	24.6	67.1	1.9979	70.4	112.0
EN 38-	2	36.5	61.8	1.9953	60.2	103.9
EN 37-	2	78.8	84.9	1.9994	64.7	8.8
EN 36-	2	24.0	83.1	1.9994	76.0	8.4
EN 35-	2	56.6	75.1	1.9964	65.3	54.9
EN 34-	2	36.5	49.8	1.9968	49.2	113.6
EN 33C	2	42.5	45.7	2.0000	43.9	108.7
EN 33B	2	45.0	40.2	1.9992	39.1	108.0
EN 33A	2	39.9	43.3	1.9932	43.1	112.6
EN 33-	2	36.8	42.2	1.9984	43.3	116.6
EN 32-	2	34.4	41.5	1.9965	43.6	119.7
EN 31-	2	24.4	49.3	2.0000	52.4	129.4
EN 30-	2	23.7	45.8	1.9996	49.7	131.6
EN 29-	2	21.1	52.0	1.9945	55.5	132.8
EN 28-	2	24.2	55.9	1.9993	58.4	126.3
EN 27-	2	26.9	52.1	1.9990	54.1	124.7
EN 26-	2	6.8	64.9	2.0000	72.0	150.0
EN 25-	2	345.9	66.1	2.0000	72.2	196.9
EN 24-	2	1.9	62.5	1.9983	69.2	161.3
EN 23-	2	3.4	71.2	1.9997	81.0	153.0
EN 22-	2	342.6	76.7	1.9984	82.6	264.3
EN 21-	2	327.6	77.8	1.9969	76.6	278.4
EN 20-	2	332.7	62.7	1.9980	64.4	215.0
EN 19B	2	334.2	56.3	1.9989	58.3	206.7
EN 19A	2	335.6	46.1	1.9960	49.8	199.7
EN 19-	2	336.1	53.1	1.9999	55.8	202.0
EN 18-	2	341.4	32.5	1.9931	41.4	189.1
EN 17-	2	331.4	62.8	1.9924	64.2	217.1
EN 16-	2	336.2	65.9	1.9964	69.2	214.4
EN 15D	2	332.3	66.3	1.9968	68.4	221.4
EN 15C	2	316.4	62.4	1.9986	58.1	235.7
EN 15B	2	302.7	63.9	1.9988	53.8	251.7
EN 15A	2	303.7	66.7	1.9998	57.1	255.0
EN 15-	2	317.1	63.0	1.9988	58.9	235.7
EN 14-	2	304.6	64.7	1.9999	55.4	251.0
EN 13-	2	18.6	72.2	1.9998	78.5	105.6
EN 12C	2	50.2	71.8	1.9998	64.9	69.6
EN 12B	2	47.9	79.2	1.9981	71.2	40.1
EN 12A	2	48.4	76.1	1.9978	69.4	55.6
EN 12-	2	58.3	73.0	1.9884	62.6	60.3
EN 11-	2	29.7	70.4	1.9971	72.2	95.3
EN 10A	2	30.4	70.3	1.9932	71.8	94.8
EN 10-	2	10.1	76.6	1.9998	85.7	72.1
EN 9A	2	115.4	82.3	1.9875	55.4	9.8
EN 9-	2	119.8	81.9	1.9999	54.1	9.1
EN 8-	2	313.1	77.9	1.9993	71.0	283.0
EN 7B	2	52.2	79.3	2.0000	69.7	38.7
EN 7A	2	34.6	81.0	1.9976	75.4	28.1
EN 7-	2	51.8	76.2	1.9991	68.1	53.3
EN 6-	2	317.6	46.9	1.9993	44.8	222.1
EN 5-	2	321.5	49.1	1.9982	47.9	218.7
EN 4X	2	312.7	47.2	1.9950	43.3	227.8
EN 4-	2	336.5	70.7	1.9998	75.0	226.7
EN 3-	2	338.6	77.4	1.9998	81.0	272.7
EN 2-	2	58.8	70.6	1.9982	60.0	65.8
EN 1-	2	12.0	65.1	1.9966	71.4	138.8

N THRÁNDARGIL

VGP LATITUDE

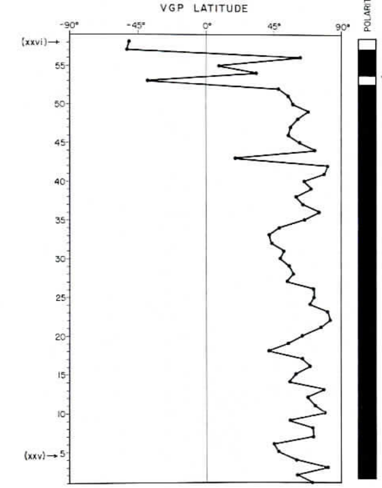

PROFILE O

HVAMMABRUNIR

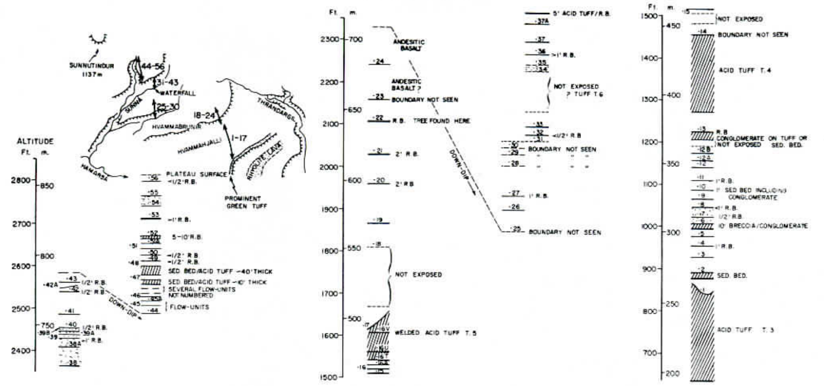

O HVAMMABRÚNIR

NO	N	D	I	R	θ'	φ'
EO 56-	2	335.2	77.8	1.9990	79.6	277.1
EO 55-	2	332.5	55.7	1.9995	57.3	208.6
EO 54-	2	330.9	54.6	1.9999	55.7	210.0
EO 53-	2	333.0	20.0	1.9994	32.5	197.2
EO 52-	2	135.1	69.8	1.9996	33.2	15.2
EO 51-	2	195.5	-45.6	1.9533	-51.2	322.9
EO 50-	2	201.3	-45.9	1.9871	-50.3	314.8
EO 49-	3	175.3	-56.6	2.9975	-62.4	353.3
EO 48-	2	268.2	-75.3	1.9981	-53.7	216.9
EO 47-	2	274.0	44.3	1.9807	25.0	263.5
EO 46-	2	116.6	-75.2	1.9973	-62.6	99.7
EO 45-	2	185.9	-76.6	1.9996	-87.5	253.5
EO 44-	2	280.4	-68.7	1.9770	-41.6	219.2
EO 43-	2	168.0	-57.4	1.9966	-62.5	5.9
EO 42-	2	134.0	-19.8	1.4399	-26.9	37.8
EO 41-	2	229.3	-73.0	1.9922	-66.4	246.7
EO 40-	2	244.7	-76.5	1.9998	-63.3	226.0
EO 39B	2	176.9	-75.8	1.9615	-88.0	30.7
EO 39A	2	232.5	-81.8	1.9994	-70.1	205.5
EO 39-	2	226.4	-81.1	1.9975	-71.9	209.4
EO 38-	2	16.2	78.6	1.9990	82.7	40.3
EO 37-	2	102.9	60.3	1.9844	31.5	44.5
EO 36-	2	123.3	61.9	1.9963	26.5	28.1
EO 35-	2	352.2	70.3	1.9947	79.1	189.9
EO 34-	2	204.9	-59.5	1.9911	-61.8	302.4
EO 33-	2	29.8	57.4	1.9875	58.2	117.1
EO 32-	2	0.4	81.4	1.9999	81.4	345.9
EO 31-	2	323.7	77.6	1.9946	75.0	277.7
EO 30-	2	309.1	67.7	1.9988	60.5	251.7
EO 29-	2	313.3	70.8	1.9987	65.4	254.8
EO 28-	2	317.9	69.9	1.9995	66.5	248.0
EO 27-	2	16.2	47.8	1.9996	52.8	141.3
EO 26-	2	24.0	72.8	1.9999	77.0	93.4
EO 25-	2	72.2	57.9	2.0000	41.7	71.2
EO 24-	2	44.9	76.6	1.9915	71.1	54.7
EO 23-	2	316.9	75.4	1.9705	71.0	268.6
EO 22-	2	314.6	62.6	1.9983	57.6	238.0
EO 21-	2	35.9	69.2	1.9809	68.4	90.9
EO 20-	2	339.1	60.4	2.0000	63.9	202.6
EO 19-	2	123.2	80.6	1.9943	51.5	10.3
EO 18-	2	181.3	69.9	1.9727	28.4	344.3
EO 17-	2	174.0	-62.6	1.9977	-69.1	357.4
EO 16V	2	187.6	-54.6	1.9995	-60.2	332.5
EO 16U	2	174.0	-51.0	1.9999	-56.9	354.5
EO 16T	2	184.7	-58.6	1.9995	-64.6	336.7
EO 16A	2	88.1	-71.9	1.9996	-48.4	109.6
EO 16-	2	61.3	-72.7	1.9972	-41.1	127.1
EO 15-	2	78.5	-81.6	1.9992	-57.3	134.1
EO 14-	2	291.7	-67.4	1.9913	-36.4	212.7
EO 13-	2	330.5	-77.4	1.9990	-42.2	180.9
EO 12B	2	167.9	-71.7	1.9958	-80.0	27.1
EO 12A	2	188.1	-61.5	1.9999	-67.6	329.5
EO 12-	2	186.3	-64.6	1.9982	-71.5	331.5
EO 11-	2	198.8	77.0	1.9925	40.6	334.9
EO 10-	2	215.8	-74.9	1.9984	-73.8	249.3
EO 9-	2	210.0	47.5	1.9866	6.2	318.9
EO 8-	2	240.3	-58.5	1.9503	-47.3	261.6
EO 7-	2	329.3	-84.6	1.9993	-55.0	174.6
EO 6-	2	341.6	67.2	1.9015	72.5	207.5
EO 5-	2	19.0	56.2	1.9998	59.9	133.7
EO 4-	2	14.2	49.0	1.9758	54.2	143.9
EO 3-	2	24.8	53.0	1.9920	55.5	127.1
EO 2-	2	13.1	54.7	1.9968	59.6	143.7
EO 1-	2	324.7	66.3	2.0000	65.5	231.8

O HVAMMABRÚNIR

VGP LATITUDE

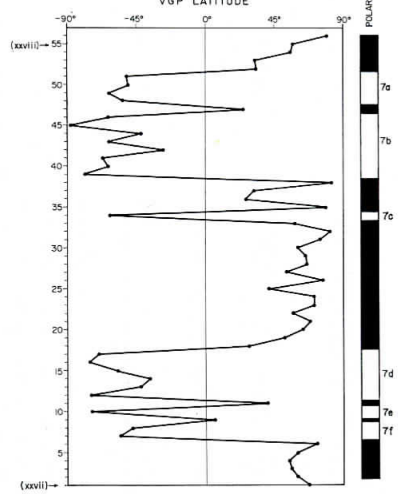

PROFILE P

UPPER GEITHELLNADALUR

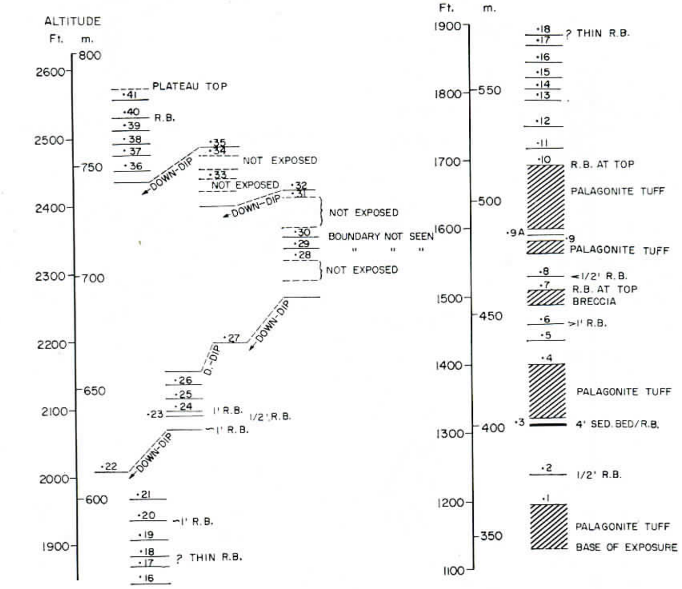

P GEITHELLNADALUR

NO	N	D	I	R	θ'	φ'
EP 35-	2	159.3	-61.8	1.9995	-65.4	23.5
EP 34-	2	168.3	-63.9	1.9739	-70.0	9.4
EP 33-	2	200.4	-22.3	1.9965	-35.1	320.3
EP 32-	2	245.4	-66.9	1.9949	-53.4	247.0
EP 31-	2	244.8	-57.6	1.9999	-44.6	258.0
EP 30-	2	167.2	-75.6	2.0000	-84.1	64.1
EP 29-	2	251.1	-82.0	1.9980	-65.1	202.3
EP 28-	2	317.2	56.1	1.9361	52.3	228.1
EP 27-	2	66.4	6.9	1.9998	13.1	95.1
EP 26-	2	63.1	-34.1	1.6319	-6.1	106.8
EP 25-	2	286.9	-83.8	1.9986	-58.9	188.2
EP 24-	2	182.9	-78.8	1.9957	-86.0	180.1
EP 23-	2	182.0	-56.2	1.9999	-62.1	341.6
EP 22-	2	186.1	-80.1	1.9999	-83.5	182.9
EP 21-	2	214.0	-77.0	1.9970	-75.8	236.9
EP 20-	2	220.7	-64.0	1.9933	-60.9	275.5
EP 19-	2	221.4	-47.2	1.9492	-45.5	288.9
EP 18-	2	171.4	-60.4	1.9903	-66.2	1.2
EP 17-	2	180.8	-72.5	1.9942	-83.2	341.3
EP 16-	2	88.1	-72.5	1.9283	-49.2	110.4
EP 15-	2	351.3	-65.8	1.8217	-22.8	171.3
EP 14-	2	191.5	-87.2	1.9973	-70.0	168.2
EP 13-	2	148.4	-77.8	1.9941	-77.0	98.0
EP 12-	2	162.7	-63.4	1.9994	-68.1	19.4
EP 11-	2	311.7	71.8	1.9829	65.8	259.0
EP 10-	2	280.6	31.4	1.9979	19.8	253.0
EP 9A	2	318.7	64.5	1.9999	61.2	235.9
EP 9-	2	324.6	63.6	1.9999	62.5	227.3
EP 8-	2	278.6	56.1	1.9646	36.2	265.5
EP 7-	2	312.8	86.1	1.9982	69.1	328.9
EP 6-	2	290.4	84.8	1.9940	66.3	320.5
EP 5-	2	161.7	63.7	1.9998	20.9	358.6
EP 4-	2	20.5	67.3	1.9997	71.9	118.4
EP 3-	2	51.2	65.9	1.9999	58.4	81.4
EP 2-	2	358.7	72.8	2.0000	83.5	171.1
EP 1-	2	234.9	72.3	1.9961	38.9	310.5

P GEITHELLNADALUR

VGP LATITUDE

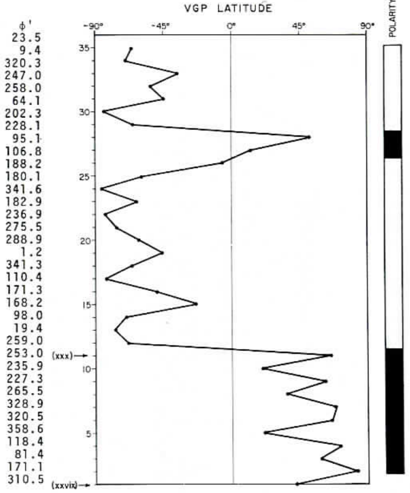

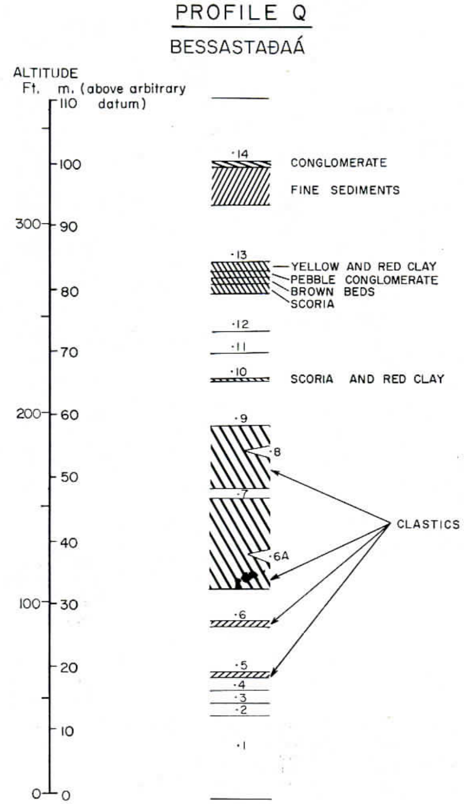

Q BESSASTAÐAÁ

NO	N	D	I	R	θ'	φ'
EQ 14-	2	45.7	83.9	1.9999	71.5	13.2
EQ 13-	2	341.9	70.5	1.9998	76.4	214.5
EQ 12-	2	250.4	-63.0	1.9964	-47.4	248.3
EQ 11-	2	36.4	-86.6	1.9907	-59.2	157.0
EQ 10-	2	25.3	-81.8	1.9942	-50.0	154.4
EQ 9-	2	237.8	-52.5	1.9999	-43.1	268.8
EQ 8-	2	68.1	55.1	1.9996	41.0	77.2
EQ 7-	2	88.1	62.4	1.9941	39.5	54.5
EQ 6-	2	174.8	-66.9	1.9997	-74.2	357.6
EQ 5-	2	213.4	-64.1	1.9969	-63.7	285.3
EQ 4-	2	164.0	-84.9	1.9993	-74.6	154.4
EQ 3-	2	187.7	-80.9	1.9999	-82.3	182.8
EQ 2-	2	87.8	-83.6	1.9999	-61.7	137.3
EQ 1-	2	117.5	-84.1	1.9999	-68.0	136.2

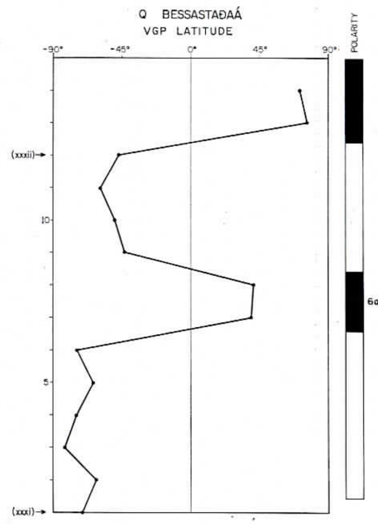

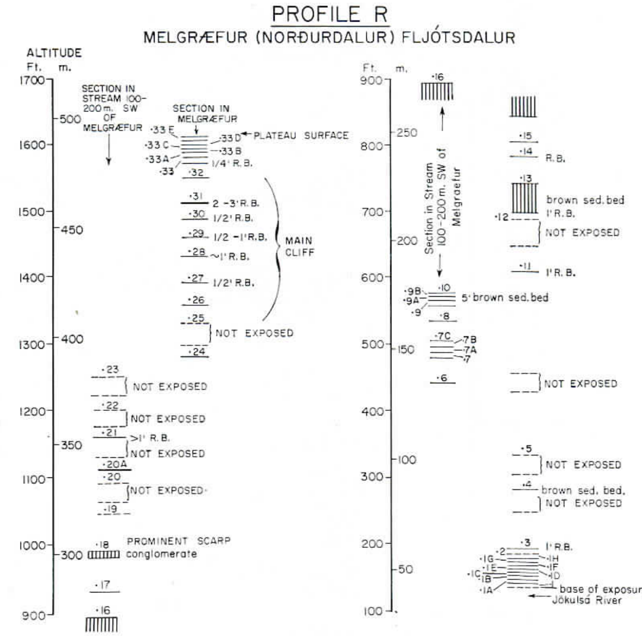

R MELGRAEFUR

NO	N	D	I	R	θ'	φ'
ER 33E	2	165.8	84.1	1.9997	53.4	349.8
ER 33D	2	176.6	76.3	1.9998	39.0	346.9
ER 33C	2	166.9	75.5	1.9994	37.9	352.6
ER 33B	2	171.9	79.1	2.0000	44.0	349.0
ER 33A	2	179.8	74.3	1.9997	35.6	345.1
ER 33-	2	201.9	75.3	1.9998	38.3	332.3
ER 32-	2	262.4	42.0	1.9987	18.7	272.4
ER 31-	2	17.9	64.4	1.9980	68.9	128.8
ER 30-	2	28.7	71.5	1.9999	73.6	93.6
ER 29-	2	38.1	59.5	1.9930	57.2	104.7
ER 28-	2	47.5	49.1	1.9993	44.5	101.4
ER 27-	2	3.4	67.3	1.9998	75.0	156.6
ER 26-	2	22.0	72.4	1.9998	77.3	99.5
ER 25-	2	342.4	72.5	1.9980	79.0	222.7
ER 24-	2	61.3	-80.4	1.9990	-52.4	137.5
ER 23-	2	28.1	-86.3	1.9981	-58.3	158.4
ER 22-	2	213.2	-82.9	1.9999	-74.7	195.0
ER 21-	2	11.7	-74.9	1.9998	-36.8	158.0
ER 20A	2	222.7	-75.5	1.9991	-71.4	242.1
ER 20-	2	219.5	-82.0	1.9997	-73.8	203.0
ER 19-	2	261.0	-75.5	1.9990	-56.5	220.6
ER 18-	2	237.0	-71.9	1.9936	-62.2	244.5
ER 17-	2	217.0	-82.2	1.9997	-74.4	201.4
ER 16-	2	240.9	-59.1	1.9996	-47.6	260.6
ER 15-	2	38.5	-77.6	1.9999	-44.0	144.5
ER 14-	2	35.6	-82.6	1.9891	-52.1	151.1
ER 13-	2	221.6	-77.2	1.9980	-72.9	233.6
ER 12-	2	219.1	-77.2	2.0000	-73.9	234.8
ER 11-	2	355.4	68.3	1.9994	76.4	177.2
ER 10-	2	230.6	41.9	1.9855	7.2	299.7
ER 9B	2	233.0	26.8	1.9999	-1.5	294.2
ER 9A	2	261.3	78.5	1.9995	54.5	305.0
ER 9-	2	238.3	46.1	1.9912	12.7	294.3
ER 8-	2	295.7	59.0	1.9789	46.1	252.4
ER 7B	2	306.0	73.9	1.9916	65.3	268.9
ER 7A	2	247.6	67.2	1.9998	36.0	297.5
ER 7-	2	230.8	62.5	1.9999	25.6	306.6
ER 6-	2	335.8	72.5	1.9999	76.5	234.3
ER 5-	2	331.3	78.5	1.9998	78.2	282.1
ER 4-	2	41.7	80.0	1.9981	73.6	36.9
ER 3-	2	195.5	-79.3	1.9997	-82.6	211.8
ER 2-	2	236.9	-61.2	1.9621	-51.3	262.3
ER 1H	2	119.0	-79.6	1.9999	-67.0	114.1
ER 1G	2	144.8	-75.6	1.9965	-74.5	83.2
ER 1F	2	147.9	-78.1	1.9996	-76.9	99.2
ER 1E	2	134.1	-80.1	1.9997	-72.2	114.2
ER 1D	2	167.1	-81.2	1.9992	-80.9	140.0
ER 1C	2	154.5	-78.9	1.9999	-79.4	106.5
ER 1B	2	139.9	-76.8	2.0000	-73.3	93.2
ER 1A	2	130.7	-79.2	1.9971	-70.8	109.7
ER 1-	2	147.4	-80.0	1.9999	-76.5	114.3

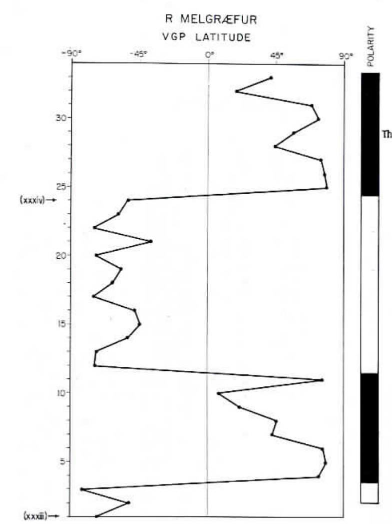

PROFILE S

GRUNDARLÆKUR STREAM

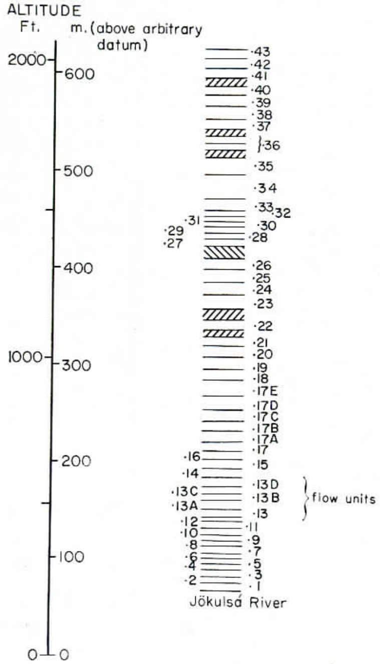

S GRUNDARLAEKUR

NO	N	D	I	R	θ'	φ'
ES 43-	2	81.4	28.9	1.9996	17.5	75.9
ES 42-	2	185.8	-79.8	1.9997	-84.2	184.8
ES 41-	2	218.7	-59.2	1.9908	-56.7	284.2
ES 40-	2	145.2	-58.6	1.9994	-57.5	40.1
ES 39-	2	191.2	-83.5	1.9937	-77.2	176.0
ES 38-	2	170.4	-76.4	2.0000	-85.8	68.3
ES 37-	2	206.0	-69.9	1.9998	-72.9	283.2
ES 36-	2	161.0	-77.2	1.9999	-82.0	87.8
ES 35-	2	350.3	-77.0	1.9950	-40.3	170.2
ES 34-	2	242.9	-83.0	1.9999	-67.7	199.1
ES 33-	2	243.7	-87.8	1.9960	-66.5	174.7
ES 32-	2	129.5	-53.6	1.9985	-47.0	54.4
ES 31-	2	320.4	77.4	1.9978	73.8	276.1
ES 30-	2	47.0	67.6	2.0000	62.0	82.9
ES 29-	2	44.5	73.3	1.9999	68.8	69.8
ES 28-	2	115.5	49.3	1.9999	17.2	39.7
ES 27-	2	59.1	73.1	1.9980	62.4	59.8
ES 26-		201.0	-63.6		-67.2	304.3
ES 25-	2	250.0	-65.6	1.9998	-50.2	245.4
ES 24-	2	253.9	-65.6	1.9984	-48.5	242.2
ES 23-	2	205.8	-70.3	1.9997	-73.5	282.0
ES 22-	2	329.6	72.4	1.9997	73.9	242.4
ES 21-	2	319.0	-65.5	1.9995	-26.9	194.6
ES 20-	2	170.2	-67.9	1.9999	-75.1	9.6
ES 19-	2	152.6	-66.4	2.0000	-68.4	40.2
ES 18-	2	150.4	-66.2	1.9997	-67.4	43.2
ES 17E	2	11.4	76.1	2.0000	84.9	84.4
ES 17D	2	4.6	77.5	1.9998	87.7	40.5
ES 17C	2	1.6	75.1	1.9999	87.0	150.3
ES 17B	2	39.6	83.7	1.9753	72.7	12.3
ES 17A	2	357.9	78.8	1.9990	86.4	332.2
ES 16-	2	21.5	73.3	1.9972	78.4	95.0
ES 15-	2	216.0	81.1	1.9974	49.7	329.2
ES 14-	2	178.1	77.1	1.9999	40.2	345.9
ES 13D	2	195.0	69.5	2.0000	28.7	334.7
ES 13C	2	18.8	75.8	1.9998	81.6	78.7
ES 13B	2	34.6	71.2	1.9996	70.9	87.0
ES 13A	2	26.0	74.7	2.0000	77.8	79.8
ES 13-	2	30.2	74.0	2.0000	75.5	79.7
ES 12-	2	256.9	40.3	1.9896	15.4	276.4
ES 11-	2	16.0	60.7	1.9999	65.0	135.7
ES 10-	2	349.7	74.8	2.0000	84.2	222.7
ES 9-	2	281.1	78.6	1.9994	60.5	296.8
ES 8-	2	351.1	75.5	1.9998	85.5	229.6
ES 7-	2	241.6	79.4	1.9839	51.0	315.6
ES 6-	2	297.2	78.8	2.0000	65.9	291.1
ES 5-	2	352.3	65.9	1.9999	72.8	182.4
ES 4-	2	191.7	86.2	1.9997	57.4	342.0
ES 3-	2	18.9	86.7	1.9973	71.0	351.4
ES 2-	2	68.6	80.5	1.9970	65.2	29.7
ES 1-	2	318.6	68.5	1.9996	65.3	243.0

S GRUNDARLÆKUR VGP LATITUDE

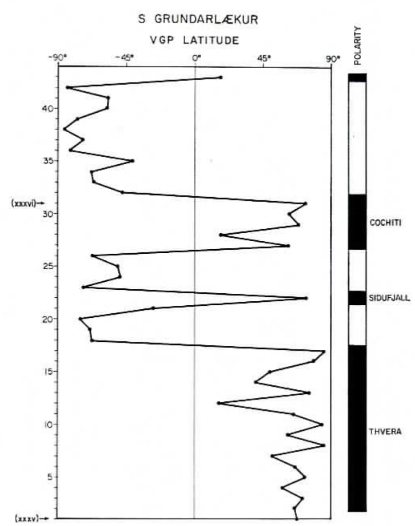

PROFILE T - KLEIFARÁ

NORÐURDALUR-FLJÓTSDALUR

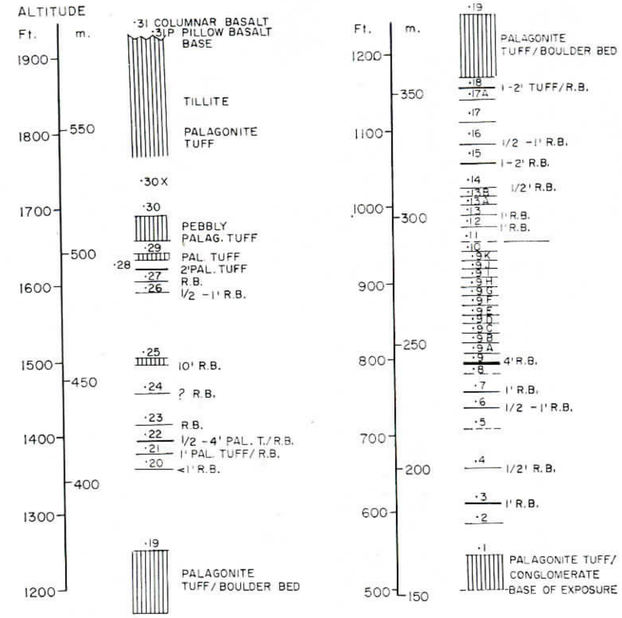

T KLEIFARÁ

NO	N	D	I	R	θ'	φ'
ET 30X	2	23.0	72.8	1.9997	77.3	95.4
ET 30-	2	322.9	79.7	1.9997	75.1	291.1
ET 29-	2	22.2	69.2	1.9981	73.4	111.2
ET 28-	2	63.8	81.0	1.9988	66.9	28.5
ET 27-	2	308.3	55.8	1.9980	48.5	237.1
ET 26-	2	344.5	75.6	1.9848	82.9	245.1
ET 25-	2	300.4	65.7	1.9999	54.6	255.4
ET 24-	2	55.7	80.3	1.9910	69.1	33.0
ET 23-	2	255.0	65.8	2.0000	36.9	290.9
ET 22-	2	249.5	-74.0	2.0000	-59.2	230.5
ET 21-	2	242.6	-72.0	1.9981	-60.0	239.7
ET 20-	2	192.7	-80.6	1.9999	-81.8	193.4
ET 19-	2	164.5	-48.6	1.9997	-53.3	7.6
ET 18-	2	152.1	-60.5	1.9932	-61.8	32.4
ET 17A	2	107.7	-76.2	1.9995	-60.4	106.4
ET 17-	2	145.7	-87.6	1.9996	-68.6	157.4
ET 16-	2	230.9	-75.7	2.0000	-68.1	236.3
ET 15-	2	249.7	-74.3	1.9998	-59.5	229.5
ET 14-	2	129.9	-84.2	1.9997	-70.3	137.5
ET 13B	2	79.9	-84.9	1.9996	-61.4	143.3
ET 13A	2	83.1	-76.6	1.9992	-52.7	119.9
ET 13-	2	93.4	-80.7	1.9996	-60.2	125.8
ET 12-	2	164.9	-69.3	2.0000	-75.8	24.4
ET 11-	2	147.6	-75.4	1.9992	-75.6	80.0
ET 10-	2	139.0	-80.7	1.9996	-73.8	117.6
ET 9K	2	145.4	-73.4	2.0000	-73.0	71.1
ET 9J	2	143.4	-70.3	1.9999	-69.1	61.8
ET 9I	2	72.4	-65.1	2.0000	-35.1	112.1
ET 9H	2	33.7	-80.0	1.9985	-47.5	148.9
ET 9G	2	242.7	-83.4	1.9997	-67.8	196.6
ET 9F	2	210.7	-77.0	1.9993	-77.2	239.0
ET 9E	2	203.1	-77.9	1.9999	-80.4	232.7
ET 9D	2	207.7	-75.6	1.9982	-77.7	251.9
ET 9C	2	211.3	-81.5	1.9997	-76.2	203.2
ET 9B	2	220.8	-83.8	2.0000	-72.4	192.0
ET 9A	2	211.0	-81.9	1.9999	-76.1	200.4
ET 9-	2	146.5	-15.7	0.6848	-28.5	23.1
ET 8-	2	141.0	-29.9	1.7311	-34.5	31.9
ET 7-	2	339.9	68.4	1.9981	73.2	212.3
ET 6-	2	290.3	84.7	1.9999	66.5	319.5
ET 5-	2	46.0	71.3	1.9936	66.2	74.8
ET 4-	2	31.8	74.2	1.9999	74.9	77.1
ET 3-	2	184.5	-67.6	1.9947	-75.4	333.3
ET 2-	2	126.1	39.8	1.9985	6.8	33.4
ET 1-	2	122.1	23.7	2.0000	-1.5	40.5

T KLEIFARÁ VGP LATITUDE

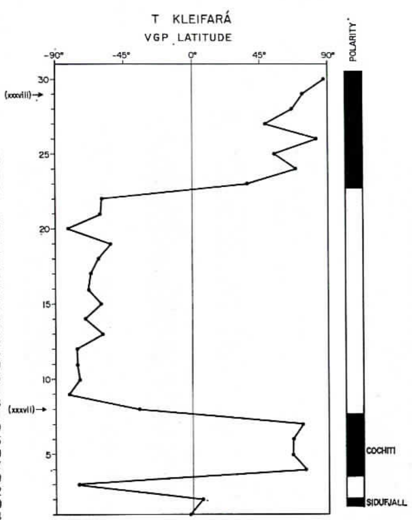

PROFILE U
NORÐURDALUR

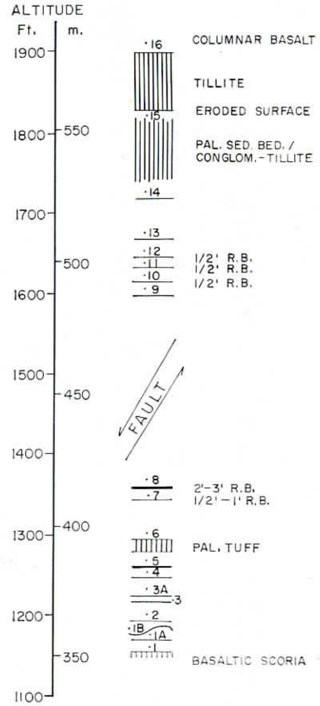

U NORÐURDALUR

NO	N	D	I	R	θ'	φ'
EU 16-	2	326.6	81.8	2.0000	75.5	307.1
EU 15-	2	19.7	-59.7	1.9999	-16.5	149.1
EU 14-	2	311.1	75.7	1.9993	69.0	272.2
EU 13-	2	333.8	77.2	1.9995	79.1	270.3
EU 12-	2	333.9	80.1	2.0000	78.6	297.4
EU 11-	2	349.8	82.9	1.9999	78.4	332.3
EU 10-	2	13.0	83.7	1.9982	76.8	356.9
EU 9-	2	351.0	82.8	1.9999	78.8	333.1
EU 8-	2	34.8	72.7	1.9986	72.3	80.7
EU 7-	2	36.2	15.3	0.8497	27.5	123.3
EU 6-	2	13.9	76.7	2.0000	84.1	69.4
EU 5-	2	26.1	73.5	1.9999	76.7	87.4
EU 4-	2	354.5	71.3	1.9999	80.5	183.7
EU 3A	2	359.0	73.6	1.9992	84.6	170.0
EU 3-	2	3.1	23.7	1.1839	37.4	160.7
EU 2-	2	23.5	71.2	2.0000	75.4	102.1

U NORÐURDALUR

VGP LATITUDE

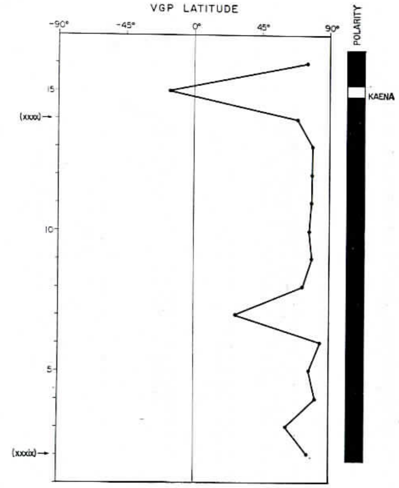

PROFILE V
LAUGARÁ-FLJÓTSDALUR

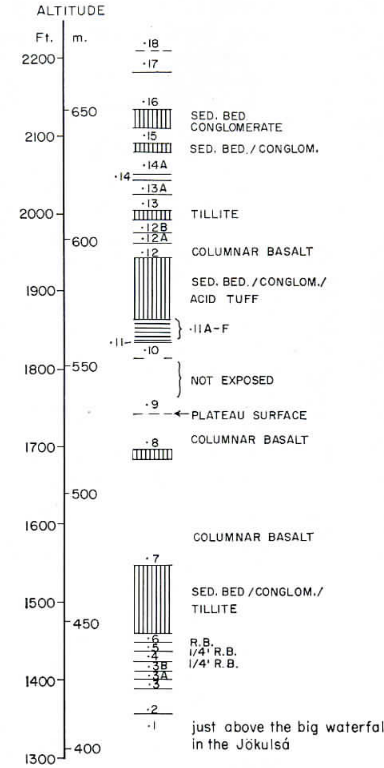

V LAUGARÁ

NO	N	D	I	R	θ'	φ'
EV 18-	2	219.2	-69.4	1.9991	-67.1	266.5
EV 17-	2	230.2	-72.7	1.9996	-65.8	246.6
EV 16-	2	211.6	-60.5	1.9992	-60.5	291.3
EV 15-	2	213.0	-83.6	1.9992	-74.0	190.2
EV 14A	2	193.8	-74.6	1.9993	-82.8	278.2
EV 14-	2	190.9	-80.4	1.9985	-82.4	191.8
EV 13A	2	187.0	-77.2	1.9939	-87.0	235.8
EV 13-	2	325.6	-84.1	1.9876	-54.7	175.7
EV 12B	2	147.5	-74.1	1.9869	-74.6	72.8
EV 12A	2	208.2	-78.8	1.9998	-78.4	223.9
EV 12-	2	223.9	-73.7	1.9998	-69.4	248.3
EV 11G	2	193.2	86.1	1.9998	57.2	341.1
EV 11F	2	213.6	81.5	1.9993	49.9	330.1
EV 11E	2	155.6	42.7	1.3801	1.6	6.4
EV 11D	2	216.2	79.6	1.9956	46.9	327.0
EV 11C	2	148.7	70.6	1.7986	32.0	5.1
EV 11B	2	216.3	82.2	1.9999	51.4	329.8
EV 11A	2	212.0	79.5	1.9996	46.3	328.9
EV 11-	2	28.0	74.5	1.9974	76.8	78.2
EV 10-	2	359.0	82.4	1.9803	79.7	342.9
EV 9-	2	43.1	-62.8	1.8902	-24.0	131.9
EV 8-	3	311.0	-55.5	1.2461	-17.9	204.2
EV 7-	2	6.4	70.9	1.9985	79.9	142.9
EV 5-	2	17.3	81.9	1.9994	79.0	9.6
EV 4-	2	350.2	75.0	2.0000	84.7	225.4
EV 3B	2	9.8	71.1	1.9966	79.6	132.2
EV 3A	2	3.1	75.9	1.9999	88.0	119.8
EV 3-	2	356.2	78.2	2.0000	87.1	214.0
EV 2-	2	277.9	80.6	2.0000	61.3	304.0
EV 1-	2	344.0	79.9	1.9991	81.7	304.3

V LAUGARÁ

VGP LATITUDE

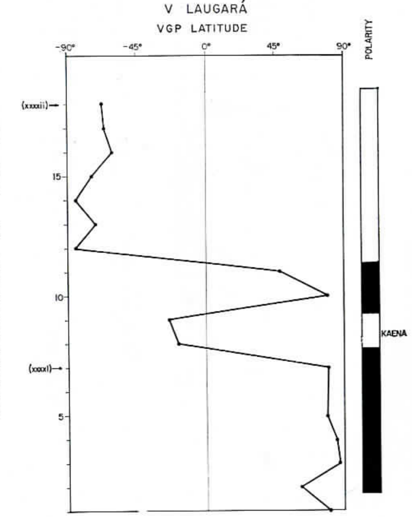

Appendix II

Paleomagnetic data for lavas following demagnetization treatment of all samples in an alternating magnetic field of 250 oersteds

See app I for explanation of tables, which exclude results for: (A) lavas that stratigraphically overlap those in other sections; (B) lavas from which only one specimen was available; and (C) lavas in which only one of the two specimens was demagnetized at a peak alternating magnetic field of 250 oersteds, which was the single field value applied to most (but not all) of the specimens.

G GERPIR

NO	N	D	I	R	θ'	φ'
EG 30-	2	345.2	62.6	1.9425	67.5	194.1
EG 29-	2	189.5	11.4	0.3412	-19.0	335.3
EG 28-	2	181.6	15.7	1.0619	-17.1	343.7
EG 27-	2	169.1	-66.2	1.9892	-72.6	10.2
EG 26-	2	189.6	-76.0	1.9948	-85.6	270.5
EG 25-	2	336.9	-26.0	1.3516	9.5	188.1
EG 24-	2	336.4	-75.2	1.9899	-38.2	179.2
EG 23-	2	295.5	-81.2	1.8479	-54.2	192.4
EG 22-	2	25.8	74.8	1.9238	78.0	80.1
EG 21-	2	159.0	59.3	1.2943	16.3	2.0
EG 20-	2	26.7	61.2	1.9443	62.8	118.7
EG 19-	2	125.1	77.8	1.5222	47.2	14.0
EG 18A	2	24.1	70.6	1.9820	74.4	104.1
EG 18-	2	296.9	72.1	1.6057	59.9	270.8
EG 17-	2	43.9	43.5	1.9865	41.6	108.4
EG 16-	2	41.0	71.6	1.9928	68.7	79.4
EG 14-	2	341.7	54.0	1.9981	57.7	194.3
EG 13-	2	13.1	77.7	1.9956	84.4	52.8
EG 12-	2	354.2	53.8	1.9935	59.2	174.7
EG 11-	2	88.1	77.8	1.9543	56.8	31.7
EG 10-	2	253.3	75.2	1.9957	48.0	303.4
EG 9-	2	53.4	63.0	1.9987	54.6	84.1
EG 8-	2	55.2	75.9	1.9993	66.6	53.8
EG 7-	2	30.1	77.4	1.9985	77.6	57.2
EG 6-	2	37.8	73.7	1.9997	72.0	74.5
EG 5-	2	270.8	84.5	1.9367	62.9	320.8
EG 4-	2	43.7	62.2	1.9948	57.7	95.5
EG 3-	2	279.1	39.4	1.8536	24.0	257.2
EG 2A	2	46.8	67.1	1.9980	61.5	84.6
EG 2-	2	24.6	41.6	1.7902	46.1	132.1
EG 1-	2	343.8	71.1	1.9984	77.8	213.5

H VAÐLAVÍK

NO	N	D	I	R	θ'	φ'
EH 24-	2	4.6	49.7	1.9164	55.5	158.4
EH 23-	2	343.9	47.3	1.9991	52.2	188.8
EH 22-	2	340.6	48.7	1.9998	52.7	193.8
EH 21-	2	286.4	57.6	1.9842	40.9	260.0
EH 20-	2	94.4	62.4	1.9915	37.0	49.9
EH 19-	2	337.4	69.3	1.9987	73.4	219.8
EH 18-	2	306.6	60.4	1.9305	52.0	243.7
EH 17-	2	15.3	70.4	1.9122	77.1	121.8
EH 16-	2	90.3	60.7	1.9942	37.0	54.4
EH 15-	2	172.3	80.0	1.7714	45.6	349.0
EH 14-	2	117.6	49.0	1.7953	16.3	38.6
EH 12-	2	154.1	64.8	1.7196	23.4	4.4
EH 11-	2	65.2	-11.0	1.9682	5.1	100.3
EH 10-	2	45.5	47.8	1.9727	44.3	104.7
EH 9-	2	348.6	60.5	1.9859	65.7	186.4
EH 8-	2	92.1	20.3	0.3547	8.6	69.0
EH 7-	2	8.6	54.0	1.9073	59.2	151.4
EH 6-	2	71.9	79.8	1.9893	63.7	32.2

A HUNDSVÍK

NO	N	D	I	R	θ'	φ'
EA 42A	2	151.0	-55.4	1.9974	-56.3	30.4
EA 42-	2	268.7	18.7	0.9945	8.2	260.7
EA 38-	2	149.6	82.9	0.9520	52.3	356.9
EA 37-	2	11.5	25.4	1.9996	37.8	151.2
EA 35-	2	328.2	4.8	1.9510	23.5	200.4
EA 33-	3	255.5	-57.4	2.8030	-39.9	249.3
EA 32-	2	243.1	-24.6	1.9904	-22.9	274.7
EA 31B	2	250.9	-17.3	1.7623	-16.1	269.1
EA 31A	2	232.5	-65.9	1.8541	-57.9	260.9
EA 30A	2	56.2	25.1	1.9961	25.9	101.3
EA 27A	2	307.2	-78.1	1.9943	-47.3	192.5
EA 24B	2	200.9	-75.5	1.9946	-80.5	259.7
EA 24-	2	211.0	-34.2	1.9983	-39.5	306.2
EA 23-	2	213.5	-48.6	1.8775	-49.0	298.4
EA 22-	2	207.5	-47.2	1.9987	-49.6	306.6
EA 21-	2	34.1	-66.7	1.9871	-27.1	141.1
EA 20-	2	136.8	-83.4	1.9993	-72.2	135.2
EA 19-	2	127.9	-74.4	1.9985	-66.6	89.9
EA 18-	2	256.6	-80.5	1.9987	-62.8	208.1
EA 17-	2	306.8	-77.8	1.9859	-46.9	193.1
EA 16A	2	118.1	-61.6	1.6809	-49.6	73.1
EA 16-	2	149.4	-80.9	1.9926	-76.8	122.6
EA 15A	2	164.8	-82.6	1.9921	-78.3	146.5
EA 15-	2	281.0	-67.4	1.9986	-40.1	220.6
EA 14-	3	246.4	-77.8	2.9888	-64.0	221.4
EA 13-	3	158.1	-82.8	2.9905	-77.0	141.2
EA 12-	2	203.9	-85.1	1.9977	-73.4	179.4
EA 11-	2	225.3	-84.5	1.9714	-71.0	189.8
EA 10-	2	183.3	-61.6	1.9795	-67.8	339.0
EA 9-	2	183.7	-55.7	1.9960	-61.2	339.1

B NESKAUPSTAÐUR

NO	N	D	I	R	θ'	φ'
EB 23-	2	39.6	-12.5	1.9662	13.0	124.8
EB 22-	2	353.4	83.2	1.9996	78.1	338.0
EB 21-	2	309.5	77.7	1.9994	69.7	282.6
EB 20-	2	37.5	70.5	1.9976	69.0	86.3
EB 19-	2	64.9	68.3	1.9963	55.1	66.1
EB 17-	2	333.7	76.0	1.9998	78.6	260.5
EB 16-	2	344.3	69.6	1.9958	76.0	207.2
EB 15-	2	149.7	74.1	1.8206	37.3	3.6
EB 14-	2	102.4	82.0	1.9426	57.9	15.2
EB 13-	2	352.6	44.0	1.9962	50.6	175.9
EB 12-	2	27.6	83.9	1.6136	74.5	6.5
EB 11-	2	325.5	18.4	1.9117	29.6	205.3
EB 10-	2	324.3	23.6	1.9980	32.0	207.6
EB 9-	2	192.5	-34.1	1.4363	-43.1	329.0
EB 8-	2	172.7	27.8	1.9406	-10.2	352.5
EB 7-	2	49.0	-0.3	0.9449	16.0	113.7
EB 6C	2	211.6	-64.3	1.9990	-64.6	287.6
EB 6B	2	210.2	-56.1	1.9965	-56.6	298.2
EB 6-	2	220.6	0.7	0.9892	-18.5	302.1
EB 5-	2	265.2	-71.6	1.9835	-50.7	226.0
EB 4-	2	273.6	-67.2	1.9813	-42.5	226.0
EB 2-	3	174.2	-69.4	2.9992	-77.8	2.1
EB 1-	2	153.6	-59.3	1.9927	-61.0	29.9

C HJÁLEIGULAEKUR

NO	N	D	I	R	θ'	φ'
EC 59-	2	12.4	76.9	1.9959	84.7	67.3
EC 58-	4	337.1	64.7	3.9947	67.9	210.6
EC 57-	2	195.3	-65.8	1.9955	-71.3	312.0
EC 56B	2	202.3	-76.8	1.9966	-80.6	245.3
EC 56A	2	227.7	-80.2	1.9846	-71.6	215.7
EC 55-	2	226.8	-70.2	1.9987	-64.7	257.7
EC 54-	2	184.5	77.0	0.6613	40.2	342.9
EC 53-	2	25.6	49.8	1.8203	52.2	128.0
EC 52B	2	346.5	70.3	1.9965	77.6	204.6
EC 51-	2	351.3	71.5	1.9989	80.4	195.5
EC 50-	4	294.5	53.2	2.8205	40.5	249.6
EC 49-	2	296.3	68.3	1.9994	55.7	263.7
EC 48A	2	2.0	58.5	1.9944	64.2	161.7
EC 48-	2	5.7	64.7	1.9715	71.4	152.9
EC 47-	2	42.4	58.1	1.9280	54.2	101.2
EC 46-	2	39.8	69.7	1.9956	67.2	86.1
EC 45-	2	39.6	1.0	1.2681	19.6	122.8
EC 44-	2	62.5	85.3	1.9942	67.7	7.5
EC 41-	2	349.2	53.2	1.9991	58.2	182.5
EC 40-	2	342.2	26.9	1.9515	37.9	187.4
EC 38-	2	352.8	68.3	1.9882	76.1	184.4
EC 37-	2	26.2	61.0	1.9950	62.7	119.6
EC 36-	2	21.5	75.4	1.9993	80.2	79.7
EC 35-	2	335.7	59.5	1.9977	61.8	206.9
EC 34-	2	349.8	82.6	1.9991	79.0	331.8
EC 33A	2	346.8	65.8	1.9986	71.8	194.4
EC 33-	2	348.4	67.9	1.9981	74.8	194.3
EC 31-	2	332.2	79.2	1.9860	78.5	288.8
EC 30-	2	324.8	82.2	1.9710	74.8	309.8
EC 29-	2	267.2	51.9	1.6870	28.0	272.9
EC 28A	2	3.6	84.4	1.9760	76.0	348.2
EC 27-	2	15.5	59.5	1.9952	63.9	137.8
EC 26-	2	246.2	-16.9	1.6977	-17.8	273.5
EC 25-	2	213.5	2.8	1.9996	-19.4	309.6
EC 24-	2	210.7	-3.3	1.9031	-23.0	311.7
EC 23A	2	237.7	-34.4	1.9491	-30.5	277.2
EC 23-	2	240.8	-42.9	1.9987	-34.7	271.1
EC 22A	2	273.2	-82.9	1.9970	-60.8	194.9
EC 22-	2	197.4	-81.2	1.9993	-80.0	195.7
EC 21-	2	186.9	-76.9	1.9966	-87.1	249.8
EC 20-	2	201.5	-72.2	1.9844	-77.2	282.0
EC 19-	2	287.9	-74.2	2.0000	-46.4	208.1
EC 18-	2	165.7	-54.6	1.9960	-59.0	8.4
EC 17-	2	169.8	-47.8	1.9099	-53.4	0.5
EC 16A	2	210.8	-56.3	1.9120	-56.5	297.3
EC 16-	2	194.9	-65.9	1.9988	-71.4	312.8
EC 15-	2	127.6	-79.1	1.9973	-69.7	109.9
EC 14-	2	141.1	-77.7	1.9998	-74.1	98.2
EC 13D	2	135.0	-57.9	1.8812	-53.0	52.2
EC 13C	2	113.1	-43.9	1.9650	-32.9	66.1
EC 13B	2	114.8	-21.0	1.9991	-20.2	57.1
EC 13A	2	120.6	-46.6	1.9037	-37.9	60.0
EC 13-	2	114.3	-22.4	1.9982	-20.7	58.0
EC 12-	3	164.6	-72.8	2.9832	-80.2	40.3
EC 11-	2	169.8	-76.2	1.9994	-85.4	65.6
EC 10-	2	200.9	-71.0	1.9899	-76.1	288.1
EC 9-	2	182.1	-75.5	1.9980	-87.5	322.6
EC 8-	2	37.6	-37.2	1.0327	-0.4	130.6
EC 7-	2	218.5	-73.9	1.9999	-71.8	253.1
EC 6-	2	227.1	-79.3	1.9997	-71.6	220.4
EC 5C	2	218.0	-79.9	1.9995	-74.8	217.4
EC 5B	2	226.9	-65.6	1.9989	-60.0	267.0
EC 5A	2	237.2	-70.3	1.9975	-60.4	248.5
EC 5-	2	200.8	-70.7	1.9488	-75.8	289.6
EC 4-	2	238.8	-18.7	1.3359	-21.6	280.2
EC 3-	2	161.5	-80.9	1.9989	-80.1	131.2
EC 2-	2	73.9	-72.9	1.9279	-45.2	119.8
EC 0C	2	354.4	-73.8	1.8963	-34.8	168.8
EC 0B	3	204.4	-70.3	2.9791	-74.0	284.7
EC 0A	3	213.3	-62.5	2.9791	-62.0	287.9

D GAESADALUR

NO	N	D	I	R	θ'	φ'
ED 65-	2	262.7	-49.6	1.8110	-30.3	247.6
ED 64-	2	201.5	-41.1	1.9915	-46.4	316.2
ED 63A	2	72.1	-86.8	2.0000	-62.2	152.0
ED 63-	2	345.1	-78.4	1.9700	-42.9	173.1
ED 62-	2	237.8	-71.9	1.9998	-61.8	244.3
ED 61-	2	137.1	-15.9	1.9998	-25.8	33.8
ED 60A	2	45.0	75.8	1.9965	70.6	59.8
ED 60-	2	48.7	67.5	1.9956	61.2	81.8
ED 59A	2	2.7	57.9	1.9965	63.6	160.5
ED 59-	2	11.0	61.8	1.9942	67.2	144.2
ED 58-	2	228.4	-51.9	1.9965	-46.4	279.2
ED 57-	2	173.9	-50.9	1.9993	-56.5	354.9
ED 56-	2	163.8	-68.1	1.9960	-73.9	24.5
ED 55-	2	213.6	-59.4	1.9969	-58.7	290.9
ED 54-	2	169.4	-59.1	1.9855	-64.2	4.3
ED 52-	4	108.1	-71.1	3.9791	-55.3	95.0
ED 51-	4	236.1	-38.0	3.9247	-33.4	277.6
ED 50-	2	127.5	-58.8	1.9974	-50.9	61.1
ED 49-	2	182.2	-83.4	1.9870	-77.9	167.7
ED 48A	2	192.4	-53.2	1.9895	-58.0	325.7
ED 48-	2	202.6	-58.7	1.9864	-61.4	307.0
ED 47-	2	257.9	-67.1	1.9981	-48.5	237.7
ED 46-	2	169.0	-64.1	1.9931	-70.0	8.2
ED 45-	2	187.9	-57.6	1.9872	-62.9	331.7
ED 43-	2	24.3	51.4	1.9984	54.0	129.0
ED 42-	4	334.6	69.7	3.8779	73.0	225.8
ED 41-	2	260.3	22.3	1.9962	6.4	269.0
ED 40-	2	298.2	-58.2	0.9832	-24.4	214.2
ED 39-	2	302.9	19.6	1.8384	22.7	229.0
ED 38-	2	252.5	-54.0	1.8926	-38.2	254.2
ED 37V	6	230.0	-64.9	5.9326	-57.9	264.8
ED 37C	2	227.8	-68.6	1.9985	-62.7	260.4
ED 37A	6	233.3	-68.7	5.9799	-60.5	255.0
ED 37-	2	220.4	-70.9	1.9962	-68.2	262.1
ED 36-	2	157.8	-72.7	1.9938	-77.5	53.1
ED 35-	2	313.1	-43.6	1.9115	-7.4	207.0
ED 34-	2	216.8	-46.7	1.9924	-46.4	295.2
ED 33-	2	210.2	-68.1	1.9953	-69.4	282.2
ED 32-	2	258.2	-62.0	1.9974	-43.1	243.1
ED 31-	2	248.1	-59.9	1.9955	-45.3	253.6
ED 29A	2	112.7	-84.7	1.9979	-67.0	140.1
ED 29-	3	51.6	-69.9	2.5307	-35.0	130.9
ED 28-	2	272.0	-68.4	1.9713	-44.5	225.8
ED 27-	3	226.0	-66.4	2.9964	-61.1	266.6
ED 25-	2	216.3	-57.1	1.9819	-55.5	289.5
ED 24-	3	208.0	-56.8	2.9986	-58.0	300.7
ED 23-	2	188.0	-55.3	1.9914	-60.5	332.1
ED 22A	2	193.2	-52.3	1.9930	-57.0	324.7
ED 22-	2	209.5	-61.1	1.9888	-61.9	294.7
ED 21-	2	201.6	-60.0	1.9985	-63.0	307.5
ED 20-	2	172.3	-33.9	1.8172	-43.4	355.5
ED 19-	2	171.9	-38.5	1.9796	-46.5	356.3
ED 18-	2	182.3	-47.1	1.9976	-53.4	341.9
ED 17-	2	164.3	-23.4	1.9192	-36.2	4.5
ED 16-	2	190.9	-31.0	1.9990	-41.3	331.4
ED 14-	2	212.9	-59.5	1.9958	-59.1	291.7
ED 13-	2	214.1	-56.1	1.9927	-55.3	293.1
ED 11-	2	185.0	-53.8	1.9962	-59.3	337.3
ED 10-	2	189.6	-67.2	1.9975	-74.3	322.2
ED 9-	2	200.5	-56.8	1.9996	-59.9	311.6
ED 8-	2	125.4	-68.1	1.9778	-59.3	75.7
ED 7-	2	139.0	-68.8	1.9898	-65.7	63.5
ED 6-	2	169.4	-82.1	1.9921	-79.8	149.4
ED 5-	2	255.4	-74.9	1.9996	-58.0	225.3
ED 4-	2	213.7	-70.9	1.9868	-71.0	269.5
ED 3-	2	181.8	-59.4	1.9918	-65.2	342.1
ED 2-	2	215.1	-59.7	1.9559	-58.4	288.7

E SLENJUDALUR

NO	N	D	I	R	θ'	φ'
EE 20-	2	144.0	-71.7	1.9942	-70.8	66.5
EE 19B	2	15.2	75.0	1.9993	82.6	92.4
EE 19A	2	24.9	65.0	1.9954	67.6	116.5
EE 19-	2	20.3	65.7	1.9867	69.9	122.9
EE 18-	2	89.5	85.4	1.8639	63.4	6.3
EE 17-	2	1.4	71.6	1.9947	81.4	160.3
EE 15-	2	19.1	57.7	1.9752	61.2	133.2
EE 14D	2	309.2	73.7	2.0000	66.5	266.4
EE 14-	2	50.5	71.0	1.9982	64.0	72.4
EE 13C	2	334.3	36.1	1.8618	42.0	198.6
EE 13B	2	345.6	50.5	1.9992	55.1	187.3
EE 13A	2	356.3	51.0	1.9806	56.8	171.2
EE 13-	2	347.9	58.9	1.9992	63.8	186.9
EE 12-	2	3.6	71.7	1.9816	81.4	152.0
EE 11-	2	74.8	76.6	1.9947	59.9	41.4
EE 10-	2	202.1	61.6	1.3019	19.0	328.4
EE 9-	2	120.6	71.4	1.9994	39.1	23.7
EE 8-	2	266.2	77.9	1.9913	55.2	301.9
EE 7-	2	10.5	77.6	1.9981	85.4	52.8
EE 6-	2	230.4	73.3	1.7831	39.6	314.4
EE 5-	2	14.1	75.6	1.9983	83.5	86.9
EE 4-	2	50.9	74.5	1.9987	67.2	61.3
EE 3-	2	270.1	50.8	1.1777	28.3-	269.9

F SKAGAFELL

NO	N	D	I	R	θ'	φ'
EF 32-	2	350.7	62.0	1.9982	67.8	183.4
EF 31B	2	359.2	60.8	1.9850	67.0	166.8
EF 31A	2	3.6	57.0	1.9999	62.6	159.2
EF 31-	2	3.9	53.8	1.9994	59.4	159.1
EF 30-	2	39.1	55.5	1.9566	53.0	107.4
EF 29-	2	33.5	60.1	1.9814	59.5	110.3
EF 28-	2	332.4	66.8	1.8482	68.8	221.9
EF 27-	3	23.6	54.3	2.9904	56.8	128.5
EF 26-	2	352.4	51.5	1.9847	57.0	177.2
EF 25-	2	328.9	67.0	1.9959	67.8	227.2
EF 24-	2	73.6	74.8	1.9944	58.5	46.7
EF 23-	2	301.4	49.7	1.6273	40.6	240.9
EF 22-	2	339.6	68.3	1.9627	73.0	213.2
EF 21-	2	338.0	80.2	1.9970	79.9	301.4
EF 20A	2	314.7	86.3	1.9953	69.4	330.4
EF 20-	2	22.3	74.6	1.9967	79.3	85.3
EF 19-	2	340.1	59.8	1.9924	63.2	200.2
EF 18-	2	341.5	73.1	1.9998	79.3	228.4
EF 17-	2	343.7	67.4	1.9761	73.1	203.4
EF 16-	2	47.1	69.8	1.9997	64.2	78.6
EF 15A	2	13.9	84.6	1.9885	75.1	355.4
EF 15-	2	321.8	83.1	1.9892	73.4	314.9
EF 14-	2	226.7	79.7	1.9921	48.6	323.3
EF 13-	3	345.0	78.8	2.9897	83.1	292.6
EF 12B	2	238.3	41.6	1.2948	9.4	293.4
EF 12A	2	79.4	2.8	0.2029	5.7	84.4
EF 12-	2	6.6	71.8	1.9972	81.1	141.1
EF 11-	2	31.5	75.7	1.9946	76.1	68.9
EF 10-	2	13.0	79.8	1.9995	82.7	22.4
EF 9-	2	3.1	66.8	1.9982	74.4	157.9
EF 8-	2	21.5	66.9	1.9876	71.0	118.5
EF 7-	2	64.0	70.4	1.9999	57.7	63.0
EF 6-	2	352.1	60.7	1.9983	66.4	180.2
EF 5-	2	311.3	71.8	1.9506	65.6	259.0
EF 4A	2	347.2	83.3	1.9959	77.4	332.0
EF 4-	2	22.0	79.1	1.9963	80.5	40.5
EF 3-	2	9.3	86.4	1.9909	72.0	349.2
EF 2-	2	25.7	62.4	1.9986	64.5	118.7
EF 1-	2	58.3	74.0	1.9989	63.7	58.2

J MELRAKKANES

NO	N	D	I	R	θ'	φ'
EJ 63-	2	205.6	-49.1	1.9590	-51.6	308.3
EJ 61-	2	168.7	-71.8	1.9991	-80.1	24.3
EJ 60-	2	192.4	-61.5	1.9793	-66.6	321.9
EJ 59-	2	260.4	27.2	1.8646	9.0	270.1
EJ 58-	2	210.5	60.5	1.8432	19.0	321.7
EJ 57-	2	241.1	35.7	1.9960	6.5	289.3
EJ 56-	2	63.2	-28.1	1.0617	-2.8	105.7
EJ 55-	2	164.9	-44.3	1.8205	-50.0	6.6
EJ 54-	2	351.5	43.3	1.9638	50.0	177.4
EJ 53-	2	312.3	70.3	1.9988	64.5	254.0
EJ 52-	2	244.4	71.7	1.9994	40.8	304.2
EJ 51B	2	292.7	68.7	1.7388	54.6	267.3
EJ 51A	2	348.3	59.2	1.9885	64.2	186.3
EJ 51-	2	332.9	54.4	1.9741	55.9	207.2
EJ 50-	2	310.5	71.0	1.9888	64.4	257.5
EJ 49-	2	333.6	77.0	1.9816	78.9	268.7
EJ 48-	2	340.0	80.1	1.9996	80.5	301.9
EJ 47-	2	8.0	71.0	1.9976	79.8	138.8
EJ 46-	2	14.6	67.9	1.9876	74.2	129.9
EJ 45-	2	357.5	76.3	1.9998	88.6	218.7
EJ 44-	2	344.1	62.4	1.9809	67.1	195.8
EJ 43-	2	2.4	66.3	1.9970	73.8	159.7
EJ 42-	2	33.8	73.1	1.9719	73.1	81.1
EJ 41B	2	21.9	60.6	1.9970	63.6	126.6
EJ 41A	2	28.7	62.3	1.9991	63.4	114.5
EJ 41-	2	14.8	63.9	1.9909	69.0	135.4
EJ 40E	2	347.6	63.7	1.9960	69.3	190.7
EJ 40D	2	58.2	70.6	1.9887	60.4	66.9
EJ 40C	2	9.1	68.3	1.9922	75.9	141.7
EJ 40B	2	9.5	65.6	1.9996	72.1	144.2
EJ 40-	2	337.4	65.4	1.9727	68.8	211.3
EJ 28-	2	20.6	66.6	1.9998	70.8	121.0
EJ 27A	2	28.4	66.0	1.9985	67.6	109.2
EJ 27-	2	13.6	66.9	1.9841	73.0	133.9
EJ 26-	2	17.7	68.3	1.9948	73.8	122.7
EJ 25-	2	78.7	88.9	1.9988	65.2	350.6
EJ 24-	2	45.5	37.2	1.9630	36.8	109.0
EJ 23-	2	0.7	57.0	1.9711	62.7	164.1
EJ 22-	2	338.1	60.5	1.9609	63.4	204.1
EJ 21-	2	255.5	86.6	1.9634	62.4	330.9
EJ 20-	2	347.3	54.5	1.9895	59.2	185.9
EJ 17-	2	240.3	16.6	1.4862	-4.3	285.9
EJ 16A	2	29.0	72.8	1.8275	74.8	88.0
EJ 16-	2	270.4	68.0	1.9292	44.9	282.8
EJ 15-	2	67.1	-15.3	0.0953	2.4	99.4
EJ 14-	2	21.0	57.3	1.9826	60.3	130.5
EJ 13-	2	308.6	60.4	1.8996	52.8	241.5
EJ 12-	2	333.3	58.6	1.9342	60.1	209.6
EJ 11-	2	23.2	70.4	1.9912	74.5	106.3
EJ 10-	2	259.6	73.1	1.9937	47.3	296.6
EJ 9-	2	332.2	44.3	1.8894	47.3	203.5
EJ 8-	2	28.8	60.9	1.9446	61.8	115.9
EJ 7-	2	34.3	64.8	1.9614	64.1	103.2
EJ 6-	2	36.9	43.1	1.7696	43.7	116.6
EJ 5-	2	196.8	81.1	1.9980	47.9	337.9
EJ 4-	2	23.8	79.2	1.9917	79.9	40.3
EJ 3-	2	46.1	78.4	1.9949	71.7	45.9
EJ 2-	2	92.3	86.9	1.9942	63.9	359.7

K HENGILL

NO	N	D	I	R	θ'	φ'
EK 40-	2	18.9	81.1	1.9984	79.7	18.3
EK 39-	2	37.1	88.1	1.9991	67.8	351.3
EK 38A	2	352.2	40.9	1.9987	48.2	176.2
EK 38-	2	330.3	66.5	1.9931	67.7	224.3
EK 37-	2	342.6	64.9	1.9966	69.7	201.4
EK 36A	2	338.9	67.4	1.9947	71.7	212.5
EK 36-	2	335.8	71.2	1.9981	75.1	229.1
EK 35-	2	282.2	3.9	0.8219	6.9	245.1
EK 34-	2	343.4	70.0	1.9952	76.3	210.6
EK 33-	2	13.8	72.0	1.9997	79.7	118.7
EK 32-	2	95.4	-49.8	1.3081	-29.7	84.8
EK 31F	2	188.9	19.7	0.8206	-14.7	336.3
EK 31E	2	138.8	10.0	1.9556	-13.8	27.8
EK 31D	2	17.1	74.6	1.9726	81.5	93.0
EK 31C	2	70.8	-17.7	0.8695	-0.3	96.5
EK 31B	2	231.9	46.1	1.8039	10.7	300.1
EK 31A	2	246.4	36.1	1.9932	8.7	284.8
EK 31-	2	265.8	43.8	1.9939	21.3	270.4
EK 30-	2	313.6	74.0	1.9818	68.6	264.4
EK 29-	2	184.9	-78.2	1.9960	-86.9	202.6
EK 28-	2	108.6	-69.4	1.9570	-53.6	91.6
EK 27-	2	214.1	-51.3	1.8692	-51.0	296.2
EK 26-	2	235.5	-68.9	1.9984	-59.7	252.8
EK 25C	2	227.8	-69.0	1.9962	-63.1	259.6
EK 25B	4	209.1	-69.6	3.9717	-71.4	279.7
EK 25A	7	216.9	-72.3	6.9616	-71.1	260.9
EK 25-	4	212.0	-72.4	3.9976	-73.2	266.0
EK 24-	2	81.7	-70.5	1.7655	-44.8	111.8
EK 23-	2	324.7	-66.6	1.9989	-27.2	190.6
EK 22-	2	317.6	-70.6	1.9784	-34.1	193.3
EK 21-	2	306.8	-72.7	1.9744	-39.4	198.5
EK 20-	2	168.6	-63.0	1.9945	-68.6	8.0
EK 19-	2	160.4	-69.8	1.9988	-75.0	35.8
EK 18-	2	220.7	-67.8	1.9657	-64.8	269.7
EK 17-	2	227.8	-63.9	1.9969	-57.8	268.6
EK 16-	2	212.9	-72.8	1.9941	-73.2	263.1
EK 15-	2	222.2	-68.2	1.9946	-64.6	267.1
EK 14-	2	222.4	-69.1	1.9807	-65.4	264.9
EK 13-	2	154.8	-21.7	1.4689	-33.6	15.5
EK 12-	2	217.2	-59.0	1.9975	-57.0	286.7
EK 11-	2	199.2	-67.2	1.9901	-71.9	302.2
EK 10-	2	206.3	-56.7	1.9908	-58.3	303.2
EK 9-	2	217.7	-76.6	1.9981	-74.1	239.6
EK 8-	2	217.9	-74.4	1.9918	-72.5	251.2
EK 7-	2	241.4	-68.9	1.9950	-57.2	247.9
EK 6-	2	207.4	-86.9	1.9858	-70.1	173.7
EK 5-	2	163.9	-85.5	1.9997	-73.4	156.6
EK 4-	2	172.7	-77.9	1.9970	-86.5	110.7
EK 2-	2	223.0	-67.9	1.9990	-63.9	267.0
EK 1-	2	203.3	-14.8	1.0910	-30.3	318.3

L LANGAGIL

NO	N	D	I	R	θ'	φ'
EL 48-	2	249.6	-71.1	1.9910	-56.2	237.4
EL 47-	2	258.3	-81.6	1.9825	-63.3	203.3
EL 46-	2	154.1	-67.6	1.9990	-70.3	40.8
EL 45-	2	271.3	-53.1	1.9988	-29.6	238.5
EL 44-	2	358.2	62.0	1.9111	68.3	168.8
EL 43-	2	252.3	2.5	1.7862	-6.3	272.0
EL 42-	2	303.7	51.5	1.9929	42.9	239.6
EL 41-	2	224.8	-74.0	1.9492	-69.3	247.3
EL 40-	2	303.2	-56.9	1.5487	-21.5	210.9
EL 39-	2	224.5	-71.8	1.9913	-67.3	255.6
EL 38-	2	168.9	-57.7	1.9980	-62.7	4.6
EL 37-	2	250.6	-80.1	1.9992	-64.3	211.4
EL 36-	2	230.6	-41.1	1.9886	-37.5	282.1
EL 35-	2	219.8	-69.0	1.9919	-66.5	267.9
EL 34-	2	163.5	-65.1	1.9686	-70.1	20.1
EL 33I	2	203.0	-73.4	1.9968	-77.9	272.8
EL 33H	3	242.7	-73.2	2.9882	-61.1	237.3
EL 33G	2	234.3	-72.0	1.9994	-63.4	246.6
EL 33F	2	236.6	-72.5	1.9989	-63.0	243.5
EL 33E	2	210.5	-70.5	2.0000	-71.9	275.0
EL 33D	2	217.5	-61.9	1.9943	-59.8	283.1
EL 33C	2	208.1	-67.6	1.9989	-69.5	286.4
EL 33B	2	202.9	-66.9	1.9986	-70.7	296.1
EL 33A	2	309.4	-66.9	1.9668	-30.9	201.1
EL 33-	2	160.1	-55.8	1.9991	-59.1	17.6
EL 32-	2	156.6	-65.7	1.9932	-68.9	33.1
EL 31-	2	161.1	-44.4	1.9987	-49.3	11.9
EL 30-	2	176.1	-74.4	1.9985	-85.6	11.1
EL 29-	2	172.7	-82.8	1.9536	-78.9	156.1
EL 27-	2	177.3	-74.8	1.9998	-86.3	6.2
EL 26-	2	199.0	-69.4	1.9990	-74.8	297.2
EL 25-	2	216.0	-65.5	1.9826	-64.2	279.7
EL 24-	2	199.3	-71.1	1.9952	-76.7	290.9
EL 23-	2	215.0	-67.2	1.9921	-66.4	277.8
EL 22-	2	228.4	-70.5	1.9978	-64.4	255.6
EL 20-	2	189.0	-73.8	1.9953	-83.4	301.9
EL 19-	2	123.2	41.6	1.9178	8.9	36.1
EL 18-	2	173.5	76.3	1.8199	38.9	349.0
EL 17-	2	109.3	70.0	1.9997	40.5	32.3
EL 16-	2	309.3	-0.4	1.9665	15.4	218.8
EL 15-	2	164.7	-39.4	1.8619	-46.3	6.0
EL 14-	2	171.6	-23.0	1.8993	-36.8	355.6
EL 13-	2	218.5	-58.0	1.9897	-55.6	286.0
EL 12C	2	349.5	54.4	1.9996	59.3	182.5
EL 12B	2	348.9	57.1	1.9997	62.0	184.3
EL 12A	2	352.5	59.1	1.9951	64.6	178.9
EL 12-	2	357.6	56.6	1.9984	62.2	169.6
EL 11-	2	2.7	60.1	1.9934	66.0	160.3
EL 10-	2	344.9	53.0	1.9978	57.3	189.1
EL 9-	2	355.1	68.4	1.9911	76.5	178.4
EL 8A	2	23.3	77.6	1.9952	80.3	56.9
EL 8-	2	37.3	65.3	1.9772	63.6	98.5
EL 7A	2	40.8	74.8	1.9952	71.6	67.1
EL 7-	2	49.3	67.6	1.9992	61.0	81.1
EL 6-	2	16.7	33.1	1.9979	41.8	143.9
EL 5-	2	15.7	26.3	1.9987	37.9	146.0
EL 4-	2	9.8	30.5	1.9951	41.1	152.9
EL 3-	2	15.5	69.2	1.9893	75.6	124.8
EL 2-	2	258.1	82.3	1.8770	58.4	316.2
EL 1B	2	19.3	72.8	1.9977	78.7	102.5
EL 1A	2	38.4	59.1	1.9976	56.7	105.2
EL 1-	2	28.8	71.2	1.9984	73.3	94.9

M KARFAGIL

NO	N	D	I	R	θ'	φ'
EM 66-	2	354.3	64.8	1.9941	71.6	177.9
EM 65-	2	346.6	33.9	1.9728	42.8	182.8
EM 64-	2	313.8	85.4	1.9382	70.1	325.7
EM 63-	2	27.6	78.4	1.9932	78.7	48.6
EM 62-	2	18.4	62.7	1.9999	66.8	130.2
EM 61-	2	345.3	60.8	1.9880	65.5	192.4
EM 60-	2	9.1	43.3	1.9782	49.9	152.6
EM 59-	2	12.3	72.9	1.9958	81.2	117.9
EM 58-	2	91.2	76.4	1.9991	54.2	33.5
EM 57-	2	100.9	80.0	1.9987	55.8	20.9
EM 56-	2	353.4	72.1	1.9966	81.6	190.7
EM 55-	2	45.6	70.8	1.9921	65.9	77.2
EM 54-	2	98.0	82.5	1.9995	59.4	15.0
EM 53-	2	193.7	73.2	1.7806	34.2	336.8
EM 52-	2	60.2	79.5	1.8082	67.3	36.6
EM 51-	2	176.8	46.2	1.5011	2.5	348.2
EM 50-	2	179.2	74.0	1.8239	35.1	345.9
EM 49-	2	337.9	80.3	1.9953	79.8	302.2
EM 48-	2	21.4	75.0	1.9993	80.0	83.1
EM 47-	2	5.3	84.2	1.9983	76.2	349.7
EM 46-	2	325.4	81.7	1.9929	75.3	306.6
EM 45-	2	40.5	72.6	1.9874	69.8	76.3
EM 44-	2	52.7	69.5	1.9970	61.5	74.0
EM 42-	2	32.8	76.7	1.9845	76.2	61.4
EM 41-	2	75.4	71.3	1.9527	54.1	52.9
EM 40-	2	29.3	14.6	1.4792	28.9	131.7
EM 39-	2	19.5	58.1	1.9724	61.5	132.3
EM 36-	2	348.7	72.8	1.9657	81.4	209.4
EM 35-	2	351.5	76.4	1.9936	86.3	248.1
EM 34-	2	359.9	75.6	1.9595	87.9	166.1
EM 33-	2	132.2	70.2	1.9999	34.6	17.1
EM 32-	2	70.3	78.9	1.9861	63.5	35.9
EM 31-	2	127.4	74.6	1.9977	41.9	16.4
EM 30-	2	230.9	85.0	1.9995	57.7	330.7
EM 28-	2	340.9	74.2	1.9989	80.3	237.5
EM 27-	2	48.9	80.6	1.9994	71.3	33.0
EM 26-	2	337.9	81.6	1.9988	78.5	312.8
EM 25-	3	35.8	67.2	2.9794	66.1	96.8
EM 24-	2	50.2	61.6	1.9987	54.4	89.1
EM 23-	2	47.2	72.9	1.9962	67.3	69.4
EM 22-	2	23.9	76.7	1.9511	79.9	65.7
EM 21-	2	63.3	82.2	1.9941	67.5	23.2
EM 20-	2	64.4	78.3	1.9942	65.1	40.1
EM 19-	2	43.7	73.7	1.9424	69.5	69.4
EM 18-	2	335.3	74.9	1.9952	78.5	250.5
EM 17-	2	343.4	51.9	1.9991	56.1	190.9
EM 16-	2	3.8	61.9	1.9661	68.2	157.8
EM 15-	2	358.2	55.5	1.9883	61.1	168.4
EM 14-	2	5.3	74.6	1.9990	85.5	130.7
EM 13-	2	6.8	77.6	1.9961	86.9	47.2
EM 11A	2	71.6	7.8	1.9832	11.3	90.5
EM 11-	2	34.3	2.5	1.8908	21.7	128.0
EM 10-	2	289.9	19.9	1.9944	17.6	241.6
EM 9-	2	135.9	-36.9	1.9512	-37.1	40.2
EM 8-	2	68.0	-69.7	1.9962	-39.3	120.0
EM 7-	2	99.9	-82.2	1.9930	-63.2	130.0
EM 6-	2	28.1	-32.5	1.5475	4.7	138.7
EM 5-	2	323.6	-78.7	1.9929	-45.6	183.7
EM 4B	2	230.5	-75.1	1.9997	-67.8	239.3
EM 4A	2	5.1	-85.3	2.0000	-55.6	163.9
EM 4-	2	19.9	-72.9	1.9858	-34.2	152.9

N THRÁNDARGIL

NO	N	D	I	R	θ'	φ'
EN 58-	2	207.6	-50.3	1.9980	-52.1	305.1
EN 57-	2	197.0	-49.4	1.9983	-53.8	320.1
EN 56-	2	35.2	64.1	1.9978	63.0	103.0
EN 55-	2	156.6	55.2	1.9817	12.2	4.6
EN 54-	2	31.7	24.7	1.9978	33.7	127.3
EN 53-	2	55.7	-54.7	1.8925	-19.1	119.8
EN 52-	2	55.7	57.7	1.9955	48.5	87.2
EN 51A	2	70.5	42.6	1.9125	30.4	81.8
EN 51-	2	20.0	25.5	1.6111	36.7	140.8
EN 50A	2	286.3	70.2	1.9992	53.6	274.6
EN 50-	2	276.7	78.9	1.9927	59.4	299.8
EN 49-	2	39.7	72.6	1.9849	70.2	77.0
EN 48-	2	34.7	57.7	1.9954	56.7	111.0
EN 47-	2	47.6	61.5	1.9984	55.5	91.9
EN 46-	2	43.5	58.9	1.9999	54.5	99.3
EN 45A	2	52.2	66.8	1.9925	58.9	79.7
EN 45-	2	70.0	51.7	1.9980	37.4	77.9
EN 44-	2	354.4	68.0	1.9906	75.9	180.0
EN 43-	2	93.7	-6.8	1.6999	-4.6	73.5
EN 42-	2	10.1	71.8	1.9985	80.5	129.9
EN 40-	2	30.7	63.3	1.9874	63.7	110.4
EN 39-	2	25.9	66.7	1.9968	69.2	111.7
EN 38-	2	39.4	53.7	1.9601	51.3	108.3
EN 37-	2	109.4	84.6	1.9993	59.8	5.6
EN 36-	2	1.4	84.1	1.9971	76.5	346.6
EN 35-	2	54.0	75.0	1.9939	66.3	57.7
EN 34-	2	37.9	51.9	1.9925	50.3	111.2
EN 33C	2	42.5	45.7	2.0000	43.7	109.1
EN 33B	2	45.5	38.9	1.9986	37.9	108.4
EN 33A	2	38.1	42.5	1.9908	42.9	115.4
EN 33-	2	36.9	43.7	1.9960	44.1	116.3
EN 32-	2	34.6	41.3	1.9963	43.2	119.9
EN 31-	2	25.4	48.6	2.0000	51.3	128.7
EN 30-	2	23.8	46.2	1.9993	49.7	131.8
EN 29-	2	26.3	50.7	1.9937	52.8	126.7
EN 28-	2	24.3	55.6	1.9990	57.8	126.8
EN 26-	2	6.8	64.9	2.0000	71.7	150.5
EN 25-	2	350.3	65.7	1.9999	72.2	187.1
EN 24-	2	1.9	62.5	1.9983	68.9	161.5
EN 23-	2	4.9	71.4	1.9983	80.9	147.9
EN 22-	2	342.6	76.7	1.9984	82.6	262.2
EN 21-	2	328.4	78.0	1.9952	77.1	278.4
EN 20-	2	332.7	62.7	1.9980	64.2	214.7
EN 19B	2	336.3	57.0	1.9974	59.3	204.1
EN 19A	2	334.5	46.4	1.9939	49.4	201.3
EN 19-	2	335.3	53.5	1.9998	55.7	203.3
EN 15D	2	330.8	66.1	1.9964	67.4	222.8
EN 15C	2	316.4	62.4	1.9986	58.0	235.5
EN 15B	2	302.3	63.1	1.9983	52.9	251.0
EN 15A	2	304.9	67.5	1.9975	58.4	254.9
EN 15-	2	315.2	63.0	1.9980	58.1	237.6
EN 14-	2	304.0	65.1	1.9996	55.6	251.9
EN 13-	2	20.8	72.2	1.9987	77.5	102.8
EN 12C	2	47.8	71.3	1.9994	65.5	73.8
EN 12B	2	45.9	79.0	1.9976	72.0	42.7
EN 12A	2	49.1	76.3	1.9978	69.3	55.2
EN 12-	2	57.9	73.0	1.9883	62.9	61.4
EN 11-	2	29.9	70.5	1.9965	72.1	95.7
EN 10A	2	32.0	70.1	1.9925	70.8	94.2
EN 10-	2	13.2	77.4	1.9997	84.4	58.0
EN 9A	2	106.8	82.3	1.9872	57.4	13.0
EN 9-	2	115.2	82.6	1.9995	56.3	9.4
EN 8-	2	310.4	78.2	1.9978	70.3	284.9
EN 7B	2	53.7	79.6	1.9991	69.5	37.7
EN 7A	2	36.4	79.6	1.9966	75.4	39.5
EN 7-	2	61.9	79.1	1.9946	66.4	38.1
EN 6-	2	318.2	47.5	1.9987	45.4	221.7
EN 5-	2	321.7	48.6	1.9974	47.4	218.2

O HVAMMABRÚNIR

NO	N	D	I	R	θ'	φ'
EO 55-	2	328.1	56.6	1.9992	56.5	215.1
EO 54-	2	331.2	54.9	1.9998	55.8	209.8
EO 53-	2	346.0	28.0	1.9747	39.1	182.9
EO 52-	2	352.8	29.5	1.7673	40.7	174.6
EO 51-	2	193.5	-47.1	1.9409	-52.4	325.6
EO 50-	2	200.1	-46.5	1.9829	-50.8	316.6
EO 49-	3	175.9	-56.6	2.9915	-62.1	352.3
EO 48-	2	185.4	-74.2	1.9412	-85.0	313.3
EO 47-	2	273.1	41.7	1.9788	22.9	263.4
EO 46-	2	110.9	-73.9	1.9964	-59.3	99.1
EO 45-	2	186.4	-77.6	1.9966	-87.1	226.4
EO 44-	2	279.8	-68.6	1.9768	-41.9	220.2
EO 43-	2	170.7	-57.3	1.9934	-62.4	1.4
EO 42-	2	134.2	-19.0	1.4226	-26.5	37.4
EO 41-	2	238.5	-46.8	1.8151	-38.4	271.5
EO 40-	2	241.4	-76.3	1.9993	-64.5	229.0
EO 39B	2	149.2	-68.0	1.8263	-69.0	49.1
EO 39A	2	229.4	-81.7	1.9983	-71.2	206.8
EO 39-	2	222.3	-81.3	1.9962	-73.3	208.8
EO 38-	2	13.8	79.3	1.9978	83.0	29.6
EO 37-	2	87.1	50.2	1.8845	29.0	63.6
EO 36-	2	123.5	62.3	1.9956	27.0	28.0
EO 35-	2	354.0	58.5	1.9293	64.1	176.1
EO 34-	2	212.1	-68.4	1.8763	-69.0	278.7
EO 33-	2	47.9	58.4	1.9236	52.4	94.9
EO 32-	2	356.0	81.1	1.9996	82.1	336.7
EO 31-	2	323.7	77.6	1.9946	75.1	276.8
EO 30-	2	302.5	65.5	1.9911	55.4	253.9
EO 29-	2	313.3	71.4	1.9981	66.0	256.2
EO 28-	2	316.8	69.7	1.9937	65.8	248.2
EO 27-	2	14.5	47.3	1.9985	52.5	144.1
EO 26-	2	24.0	72.8	1.9999	75.9	94.9
EO 25-	2	82.3	56.8	1.9899	36.5	63.8
EO 24-	2	61.6	70.1	1.9528	58.4	65.3
EO 23-	2	344.0	62.5	1.8616	67.1	196.0
EO 22-	2	304.1	70.3	1.9729	61.0	261.1
EO 21-	2	21.1	70.4	1.9229	75.3	109.9
EO 20-	2	359.2	52.8	1.9490	58.5	166.6
EO 19-	2	115.3	81.7	1.9896	54.9	11.6
EO 18-	2	257.0	66.7	1.6188	38.6	290.8
EO 17-	2	181.1	-62.2	1.9913	-68.6	343.3
EO 16V	2	187.7	-54.9	1.9993	-60.2	332.6
EO 16U	2	172.5	-49.6	1.9995	-55.2	356.7
EO 16T	2	186.9	-58.1	1.9984	-63.6	333.2
EO 16A	2	97.6	-74.8	1.9968	-55.3	109.0
EO 16-	2	74.6	-74.6	1.9938	-47.6	121.6
EO 15-	2	96.7	-82.0	1.9984	-62.3	130.2
EO 14-	2	283.1	-72.4	1.9820	-45.5	213.4
EO 13-	2	250.6	-71.4	1.8810	-56.1	236.0
EO 12B	2	169.3	-71.6	1.9942	-80.0	21.9
EO 11-	2	245.0	75.9	1.8139	46.7	308.8
EO 10-	2	219.8	-77.1	1.9961	-73.5	235.8
EO 9-	2	27.8	69.0	1.8622	71.2	103.5
EO 8-	2	248.9	-51.7	1.8441	-37.8	258.9
EO 7-	2	327.7	-85.4	1.9989	-56.9	174.3
EO 6-	2	343.8	66.9	1.8805	72.5	202.3
EO 5-	2	352.2	49.8	1.8877	55.4	177.2
EO 4-	2	19.1	47.7	1.9629	52.0	137.7
EO 3-	2	33.5	52.1	1.9716	51.9	116.5
EO 2-	2	12.7	54.6	1.9967	59.3	144.7
EO 1-	2	324.6	62.3	1.9974	61.0	225.3

P GEITHELLNADALUR

NO	N	D	I	R	θ'	φ'
EP 11-	2	322.5	70.7	1.9621	69.2	244.8
EP 10-	2	291.2	17.2	1.9242	16.9	239.7
EP 9-	2	326.2	61.2	1.9989	60.5	222.0
EP 8-	2	282.1	56.8	1.9474	38.3	263.2
EP 7-	2	333.1	86.2	1.9956	71.3	334.8
EP 6-	2	292.5	83.7	1.9924	66.8	315.1
EP 5-	2	164.1	63.8	1.9996	21.0	357.3
EP 4-	2	20.5	67.3	1.9997	71.7	119.5
EP 3-	2	50.0	66.6	1.9993	59.7	82.2
EP 2-	2	358.7	72.8	2.0000	83.2	171.2
EP 1-	2	252.0	59.2	1.9595	28.8	289.2

Q BESSASTAÐAÁ

NO	N	D	I	R	θ'	φ'
EQ 12-	2	246.2	-62.2	1.9906	-48.3	253.1
EQ 11-	2	40.1	-87.3	1.9833	-60.6	158.3
EQ 10-	2	34.1	-81.0	1.9877	-49.3	150.4
EQ 9-	2	222.4	-48.9	1.9264	-46.3	287.7
EQ 8-	2	68.9	51.7	1.9943	37.8	78.9
EQ 7-	2	80.1	62.1	1.9826	42.4	61.4
EQ 6-	2	176.4	-67.3	1.9993	-75.0	354.3
EQ 5-	2	213.4	-64.1	1.9969	-63.7	285.5
EQ 4-	2	173.6	-85.1	1.9986	-74.5	161.3
EQ 3-	2	177.5	-81.2	1.9983	-82.0	160.1
EQ 2-	2	95.0	-83.3	1.9999	-62.9	135.5
EQ 1-	2	133.4	-81.2	1.9956	-72.0	121.3

R MELGRAEFUR

NO	N	D	I	R	θ'	φ'
ER 24-	2	54.2	-82.8	1.9959	-54.8	145.3
ER 23-	2	10.1	-86.1	1.9964	-57.1	162.8
ER 22-	2	208.8	-82.2	1.9996	-76.4	198.2
ER 21-	2	357.3	-75.5	1.9949	-37.5	166.9
ER 20A	2	218.1	-75.7	1.9977	-73.4	244.6
ER 20-	2	207.4	-83.2	1.9979	-75.5	190.6
ER 19-	2	260.8	-76.6	1.9983	-59.9	218.2
ER 18-	2	235.6	-72.4	1.9921	-63.2	244.7
ER 17-	2	212.7	-81.7	1.9993	-75.7	203.2
ER 16-	2	240.4	-59.7	1.9991	-48.4	260.9
ER 15-	2	34.5	-77.3	1.9990	-42.9	146.8
ER 14-	2	29.5	-81.7	1.9812	-50.0	153.0
ER 13-	2	225.2	-76.3	1.9957	-70.9	237.1
ER 12-	2	218.3	-76.3	1.9999	-73.7	241.2
ER 11-	2	354.1	68.4	1.9883	76.4	181.0
ER 10-	2	276.9	52.5	1.9543	32.5	264.9
ER 9B	2	233.2	25.8	1.9999	-2.0	294.3
ER 9A	2	259.8	78.2	1.9984	53.8	305.4
ER 9-	2	236.7	44.7	1.9847	11.1	295.6
ER 8-	2	189.8	54.9	1.7263	10.6	337.3
ER 7B	2	254.8	68.1	1.8624	39.5	293.7
ER 7A	2	247.6	67.2	1.9998	36.0	297.9
ER 7-	2	229.1	63.4	1.9998	26.2	308.7
ER 6-	2	336.8	74.8	1.9982	79.1	248.1
ER 5-	2	326.0	79.0	1.9989	76.3	287.1
ER 4-	2	46.6	80.6	1.9958	72.0	33.1
ER 3-	2	189.4	-75.4	1.9984	-85.1	281.8
ER 2-	2	228.8	-65.3	1.9164	-58.8	265.5
ER 1H	2	119.0	-79.6	1.9999	-67.0	114.5
ER 1G	2	143.5	-74.6	1.9948	-73.3	79.6
ER 1F	2	151.5	-78.4	1.9988	-78.3	101.8
ER 1E	2	125.2	-79.3	1.9996	-69.0	111.5
ER 1D	2	161.9	-81.2	1.9994	-79.8	134.4
ER 1C	2	154.9	-78.9	1.9999	-79.5	107.0
ER 1B	2	142.1	-76.0	1.9987	-73.7	87.8
ER 1A	2	133.6	-79.1	1.9960	-71.9	109.0
ER 1-	2	146.3	-79.6	1.9999	-76.4	111.4

S GRUNDARLAEKUR

NO	N	D	I	R	θ'	φ'
ES 31-	2	318.9	77.3	1.9974	73.1	276.7
ES 30-	2	41.6	68.1	1.9987	64.8	88.1
ES 29-	2	46.6	73.3	1.9997	67.9	68.6
ES 28-	2	113.8	47.0	1.9997	16.1	42.5
ES 27-	2	52.7	70.6	1.9856	62.7	71.5
ES 25-	2	253.5	-65.7	1.9991	-48.8	243.0
ES 24-	2	253.8	-66.0	1.9978	-49.0	242.2
ES 23-	2	207.3	-71.6	1.9991	-74.3	275.4
ES 22-	2	330.4	76.8	1.9964	77.6	268.9
ES 21-	2	314.8	-66.1	1.9982	-28.6	197.8
ES 20-	2	172.3	-68.2	1.9996	-75.8	5.3
ES 19-	2	146.6	-66.6	1.9983	-66.4	49.5
ES 17D	2	7.6	77.2	1.9996	86.7	58.8
ES 17C	2	359.4	76.1	1.9984	88.7	178.4
ES 17B	2	36.3	84.4	1.9741	72.7	8.0
ES 17A	2	357.9	78.8	1.9990	86.4	332.7
ES 16-	2	19.3	73.7	1.9966	79.7	96.8
ES 15-	2	213.5	79.8	1.9959	47.2	329.5
ES 14-	2	186.2	77.9	1.9981	41.8	342.1
ES 13D	2	195.5	68.8	1.9996	27.6	334.7
ES 13C	2	11.3	76.2	1.9992	85.0	82.7
ES 13B	2	29.4	71.5	1.9995	73.4	92.8
ES 13A	2	25.0	74.8	1.9995	78.3	80.8
ES 13-	2	30.2	74.0	2.0000	75.5	80.2
ES 12-	2	234.7	42.5	1.8767	8.9	296.7
ES 11-	2	16.8	60.8	1.9999	65.0	134.6
ES 10-	2	345.8	75.4	1.9996	83.3	241.3
ES 9-	2	291.1	78.7	1.9952	63.9	293.8
ES 8-	2	357.7	75.3	1.9991	87.2	188.3
ES 7-	2	243.2	79.9	1.9823	52.1	316.2
ES 6-	2	296.6	78.4	2.0000	65.4	290.3
ES 5-	2	353.3	65.3	1.9995	72.1	180.3
ES 4-	2	189.7	86.4	1.9996	57.9	343.1
ES 3-	2	17.7	86.7	1.9971	71.1	351.6
ES 2-	2	66.6	80.0	1.9965	65.5	32.9
ES 1-	2	320.6	64.9	1.9981	62.3	234.2

T KLEIFARÁ

NO	N	D	I	R	θ'	φ'
ET 29-	2	16.3	70.3	1.9957	76.7	120.0
ET 28-	2	68.3	80.7	1.9981	65.4	29.3
ET 27-	2	313.8	59.5	1.9978	54.1	235.1
ET 26-	2	349.1	74.7	1.9778	83.9	224.2
ET 25-	2	298.3	66.5	1.9992	54.6	259.3
ET 24-	2	61.5	79.9	1.9858	67.1	34.5
ET 23-	2	255.0	65.8	2.0000	36.9	291.6
ET 22-	2	249.4	-74.0	1.9999	-59.3	231.3
ET 21-	2	245.1	-72.0	1.9969	-59.0	238.6
ET 20-	2	191.4	-80.8	1.9998	-81.8	190.6
ET 19-	2	164.1	-48.0	1.9992	-52.7	8.6
ET 18-	2	152.1	-60.5	1.9932	-61.8	33.1
ET 17A	2	115.8	-74.8	1.9987	-62.1	98.6
ET 17-	2	167.2	-86.1	1.9996	-72.3	159.8
ET 16-	2	228.2	-75.0	1.9996	-68.7	241.1
ET 15-	2	249.7	-74.3	1.9998	-59.5	230.2
ET 14-	2	134.2	-83.6	1.9994	-71.5	135.7
ET 13B	2	91.7	-83.7	1.9980	-62.5	137.5
ET 13A	2	83.1	-76.6	1.9992	-52.7	120.6
ET 13-	2	97.4	-79.3	1.9992	-60.0	120.7
ET 12-	2	168.1	-70.4	1.9991	-78.1	20.8
ET 11-	2	142.4	-75.1	1.9990	-73.2	82.5
ET 10-	2	144.4	-81.5	1.9991	-75.1	124.6
ET 9K	2	147.4	-73.6	2.0000	-74.1	70.9
ET 9J	2	140.0	-70.5	1.9993	-67.9	66.9
ET 9I	2	69.1	-66.3	1.9991	-35.5	116.1
ET 9H	2	33.7	-80.0	1.9985	-47.5	149.6
ET 9G	2	251.9	-85.2	1.9974	-66.2	188.3
ET 9F	2	205.8	-76.7	1.9978	-79.1	245.1
ET 9E	2	204.0	-77.4	1.9997	-80.0	238.4
ET 9D	2	213.1	-75.8	1.9967	-75.6	247.2
ET 9C	2	218.7	-81.3	1.9987	-74.3	208.1
ET 9B	2	223.5	-84.4	1.9999	-71.4	190.2
ET 9A	2	210.2	-81.3	1.9989	-76.7	205.1
ET 9-	2	150.6	-15.1	0.6715	-29.2	19.3
ET 8-	2	141.0	-29.9	1.7311	-34.5	32.6

U NORÐURDALUR

NO	N	D	I	R	θ'	φ'
EU 14-	2	308.8	75.7	1.9972	68.1	274.2
EU 13-	2	340.4	76.8	1.9977	81.7	263.8
EU 12-	2	338.3	80.1	1.9998	80.0	301.0
EU 11-	2	351.3	83.3	1.9998	77.9	335.8
EU 10-	2	31.6	85.3	1.9957	72.3	1.7
EU 9-	2	351.0	83.6	1.9994	77.2	336.4
EU 8-	2	34.3	72.4	1.9982	72.3	83.3
EU 7-	2	38.4	16.0	0.8180	27.2	121.6
EU 6-	2	13.9	76.7	2.0000	84.1	70.2
EU 5-	2	24.7	73.0	1.9991	76.8	92.4
EU 4-	2	354.5	71.3	1.9999	80.5	184.5
EU 3A	2	356.6	74.0	1.9983	85.0	185.0
EU 3-	2	3.1	23.7	1.1839	37.4	161.5
EU 2-	2	27.5	72.3	1.9971	75.0	92.2

V LAUGARÁ

NO	N	D	I	R	θ'	φ'
EV 18-	2	217.9	-70.7	1.9970	-69.0	265.4
EV 17-	2	223.1	-71.6	1.9938	-67.8	257.4
EV 16-	2	212.5	-62.1	1.9901	-61.8	289.5
EV 15-	2	218.5	-83.6	1.9984	-73.0	192.9
EV 14A	2	196.9	-74.9	1.9983	-81.7	271.2
EV 14-	2	190.8	-80.5	1.9983	-82.3	191.8
EV 13A	2	185.8	-76.7	1.9930	-87.5	256.7
EV 13-	2	319.1	-84.2	1.9854	-55.5	178.6
EV 12B	2	137.1	-78.8	1.9807	-73.0	106.3
EV 12A	2	208.3	-78.4	1.9995	-78.4	228.9
EV 12-	2	223.9	-75.1	1.9987	-70.6	243.5
EV 11G	2	193.2	86.1	1.9998	57.3	342.1
EV 11F	2	225.1	82.9	1.9969	53.7	328.5
EV 11E	2	155.4	42.9	1.3547	1.8	7.6
EV 11D	2	216.2	79.6	1.9956	47.0	328.0
EV 11C	2	151.5	70.1	1.7892	31.0	4.5
EV 11B	2	217.8	82.2	1.9998	51.6	330.2
EV 11A	2	204.2	79.3	1.9989	45.3	333.5
EV 11-	2	23.2	75.7	1.9937	79.7	75.2
EV 10-	2	2.0	82.1	1.9740	80.4	348.6
EV 9-	2	26.6	-54.0	1.7349	-11.5	143.3
EV 8-	3	303.3	-61.9	1.1948	-26.7	208.4
EV 7-	2	4.8	70.1	1.9965	78.9	150.7

References

Ade-Hall, J. M., Dagley, P., Wilson, R. L., Evans, A., Riding, A., Smith, P. J., Skelhorne, R., and Sloan, T., 1972, A paleomagnetic study of the Mull regional dyke swarm: Royal Astron. Soc. Geophys. Jour., v. 27, p. 517-545.

Ade-Hall, J. M., Palmer, H. C., and Hubbard, T. P., 1971, The magnetic and opaque petrological response of basalts to regional hydrothermal alteration: Royal Astron. Soc. Geophys. Jour., v. 24, p. 137-174.

Akimoto, S., and Kushiro, I., 1960, Natural occurrence of titanomaghemite and its relevance to the unstable magnetization of rocks: Jour. Geomagnetic Geoelecture, v. 11, p. 94-110.

Alvarez, W., Arthur, M. A., Fischer, A. G., Lowrie, W., Napoleone, G., Premoli Silva, I., and Roggenthen, W. M., 1977, Upper Cretaceous-Paleocene magnetic stratigraphy at Gubbio, Italy: V Type section for the Late Cretaceous-Paleocene geomagnetic reversal time scale: Geol. Soc. America Bull., v. 88, p. 367-389.

Aziz-Ur-Rahman, and McDougall, I., 1973, Palaeomagnetism and palaeosecular variation on lavas from Norfolk and Philip islands, southwest Pacific Ocean: Royal Astron. Soc. Geophys. Jour., v. 33, p. 141-155.

Banerjee, S. K., 1971, Decay of marine magnetic anomalies by ferrous ion diffusion: Nature Phys. Sci., v. 229, p. 181-183.

Blakely, R. J., 1974, Geomagnetic reversals and crustal spreading rates during the Miocene: Jour. Geophys. Research, v. 79, p. 2974-2985.

Bodvarsson, G., and Walker, G. P. L., 1964, Crustal drift in Iceland: Royal Astron. Soc. Geophys. Jour., v. 8, p. 285-300.

Cande, S. C., and Labreque. J. L., 1974, Behaviour of the earth's palaeomagnetic field from small scale marine magnetic anomalies: Nature, v. 247, p. 26-28.

Cox, A. V., 1968, Lengths of geomagnetic polarity intervals: Jour. Geophys. Research, v. 73, p. 3247-3260.

——— 1969, Geomagnetic reversals: Science, v. 163, p. 237-245.

——— 1975, The frequency of geomagnetic reversals and the symmetry of the non-dipole field: Rev. of Geophysics and Space Physics, v. 13, p. 35-51.

Cox, A. V., and Dalrymple, G. B., 1967, Statistical analysis of geomagnetic reversal data and the precision of potassium-argon dating: Jour. Geophys. Research, v. 72, p. 2603-2614.

Cox, A. V., Doell, R. R., and Dalrymple, G. B., 1964, Reversals of the Earth's magnetic field: Science, v. 144, p. 1534-1543.

Dagley, P., and Lawley, E., 1974, Palaeomagnetic evidence for the transitional behaviour of the geomagnetic field: Royal Astron. Soc. Geophys. Jour., v. 36, p. 577-598.

Dagley, P., and Wilson, R. L, 1971, Geomagnetic field reversals—a link between strength and orientation of a dipole source?: Nature Phys. Sci., v. 232, p. 16-18.

Dagley, P., Wilson, R. L., Ade-Hall, J. M., Walker, G. P. L., Haggerty, S. E., Sigurgeirsson, T., Watkins, N. D., Smith, P. J., Edwards, J., and Grasty, R. L., 1967, Geomagnetic polarity zones for Icelandic lavas: Nature, v. 216, p. 25-29.

Doell, R. R., and Cox, A. V., 1963, The accuracy of the paleomagnetic method as evaluated from historic Hawaiian lava flows: Jour. Geophys. Research, v. 68, p. 1997-2010.

——— 1964, Measurement of the rémanent magnetism of igneous rocks: U.S. Geol. Survey Bull., v. 1203A, 32 p.

Einarsson, Tr., 1957, Magneto-geological mapping in Iceland with the use of a compass: Philos. Mag. Supp. Adv. Physics, v. 6, p. 232-239.

——— 1963, Some chapters of the Tertiary history of Iceland, *in* Love, A., ed., North Atlantic Biota and Their History: London, Pergammon Press, p. 1-9.

Ellwood, B. B., Watkins, N. D., Amerigian, C., and Self, S., 1973, Brunhes epoch geomagnetic secular variation on Terceira Island, Central North Atlantic: Jour. Geophys. Research, v. 78, p. 8699-8710.

Fisher, R. A., 1953, Dispersion on a sphere: Royal Soc. London Proc. A., v. 217, p. 295-305.

Hall, J. M., 1976, Major problems regarding the magnetization of Oceanic Crustal Layer 2: Jour. Geophys. Research, v. 81, p. 4223-4230.

Harrison, C. G. A., 1969, What is the true rate of reversals of the geomagnetic field?: Earth Planetary Sci. Letters, v. 6, p. 186-188.

——— 1976, Magnetization of the ocean crust: Royal Astron. Soc: Geophys. Jour., v. 47, p. 257-283.